

The essential role of RBP7910 with Z-DNA domains in U-indel editing

Najmeh Nikpour
Institute of Parasitology
McGill University
Montreal – Canada

2018

A thesis submitted to McGill University in partial fulfillment of the requirements of the degree of
Doctor of Philosophy.

© Najmeh Nikpour 2018

Abstract

One of the most intriguing features of *Trypanosoma brucei*, a unicellular protozoan parasite, is its unique way of energy production in different life cycle stages. In the mammalian host, trypanosomes generate energy by glycolysis in glycosomes whereas in the insect vector they generate energy by oxidative phosphorylation in mitochondria. Therefore, the control of gene expression during their life cycle is critical to their survival. In mitochondria, mRNAs undergo a unique post-transcriptional editing process by guide RNA-dependent insertion and deletion of uridine nucleotides that requires a multi-protein complex, the editosome. The edited mRNAs translate into the essential protein subunits of the respiratory chain. Interestingly, RNA editing is differentially regulated between the mammalian and insect life cycle stages of the parasite, resulting in differential mechanisms of ATP generation. For example, edited versions of apocytochrome b (a subunit of complex III) and cytochrome oxidase (complex IV) transcripts peak in the insect stage of parasite while NADH ubiquinone oxidoreductase (complex I) subunits 8 and 9 transcripts peak in the mammalian bloodstream form. However, it is unknown how the developmental regulation of editing occurs. My Ph.D. project tested the hypothesis that differential editing may reflect the differential function and/or composition of the components of the editosome and its associated complexes in the different life cycle stages of the parasite. I tackled this intricate question by studying the composition of the mitochondrial protein complexes from the insect stage of parasites using two orthogonal, complementary biochemical approaches and identification of a few novel proteins. Using RNA interference (RNAi)-mediated silencing, I demonstrated the potential function of some of these proteins in the editing process. Down-regulation of one of the proteins, RBP7910 indicated an essential role for the growth and editing of apocytochrome b mRNA levels in the insect form of *T. brucei*. Furthermore,

immunoprecipitation of RBP7910 showed an RNA-dependent interaction of this protein with the members of the guide RNA binding complex (GRBC) and suggested that RBP7910 plays a role in the mitochondrial RNA editing process. The *in vitro* RNA binding and competition assays using recombinant RBP7910 and synthetic mitochondrial RNA substrates showed that RBP7910 interactions with the mitochondrial editing substrates are mainly mediated by the sequence and the secondary structure of these RNAs. Structure-Based analysis of RBP7910 suggested that it resembles a conserved family of Z-DNA binding proteins (ZBPs), sharing two winged helix-turn-helix (WHT) structured Z-DNA binding domains. RNA-binding preferences of purified recombinant wild-type and mutant RBP7910 showed binding to the mitochondrial RNAs by recognizing the RNA substrates through the nucleic acid recognition core of Z-DNA binding domains. Shared nucleic acid interfaces of the Z-DNA binding domains of ZBPs with RBP7910 and the importance of the secondary structure in the RNA-binding activity of RBP7910, implicated that similar to ZBPs, the conformation of the RNA substrates is crucial in recognition of the mitochondrial RNA substrates by RBP7910 during the RNA editing process. Overall, in the insect form of *T. brucei*, RBP7910 with two Z-DNA binding domains binds multiple mitochondrial RNA classes and influences the editing and stability of specific transcripts.

Résumé

L'une des caractéristiques les plus intrigantes du parasite protozoaire *Trypanosoma brucei*, est sa manière distincte de produire de l'énergie lors des différents stades de son cycle de vie. Dans l'hôte mammifère, les trypanosomes génèrent de l'énergie par glycolyse dans les glycosomes, tandis que dans l'insecte vecteur, ils génèrent plutôt leur énergie par phosphorylation oxydative dans les mitochondries. Le control de l'expression génique tout au long de leur cycle de vie s'avère donc crucial à leur survie. L'ARNm mitochondrial subie un processus de modifications post-transcriptionnelles unique grâce à des insertions et des délétions du nucléotide uridine via ARN guide; ce qui est catalysé par un complexe multiprotéique appelé éditosome. Une fois édité, l'ARNm est traduit afin de générer les composants essentiels du complexe respiratoire du parasite. Toutefois, l'édition de l'ARN est régulée différemment dans l'hôte mammifères et dans l'insecte vecteur, entraînant des mécanismes de production ATP distincts. Par exemple, les versions éditées des transcrits d'apocytochrome b (sous unité du complexe III) et du cytochrome oxydase (complexe IV) plafonnent lorsque dans le vecteur, tandis que le nombre de transcrits des sous unités 8 et 9 de NADH ubiquinone oxyreductase (complexe I) culmine lorsque dans le système sanguin de l'hôte vertébré. Cependant, les régulations développementales de l'édition de l'ARN demeurent incomprises. Nous émettons l'hypothèse que l'édition différentielle de l'ARN se reflète dans la variation de fonction et/ou de composition de l'éditosome ainsi que des complexes qui y sont associés lors de différents stades du cycle de vie du parasite. Je me suis attaquée à cette question en étudiant la composition des complexes protéiques mitochondriales du stade vectoriel du parasite, en utilisant deux approches biochimiques orthogonales complémentaires et en identifiant de nouvelles protéines. En inhibant l'expression de certains gènes, à l'aide de la technique d'interférence par ARN, j'ai pu démontrer le rôle potentiel de

certaines de ces protéines lors du procédé d'édition. La caractérisation fonctionnelle de l'une de ces protéines, RBP7910, indique une interaction ARN dépendante de cette protéine avec les composantes du « guide RNA binding complex » (GRBC) et indique que RBP7910 est impliqué dans le procédé d'édition de l'ARN. Les essais *in vitro* de liaison à l'ARN ainsi que par liaison compétitive effectués avec la protéine recombinante RBP7910 et des substrats mitochondriaux synthétiques ont démontrés que les interactions entre RBP7910 et les substrats d'édition mitochondriaux sont principalement attribuables à la séquence ainsi qu'à la structure secondaire de ces ARNs. La structure de RBP7910 est similaire à celle de la famille génétique conservée des protéines qui lient l'ADN Z (ZBPs), ils ont en commun deux domaines de liaisons à l'ADN Z de structure « winged helix-turn-helix » (WHT). Les analyses structurales ont démontré que RBP7910 se lie à l'ARN mitochondrial en reconnaissant les substrats d'ARNs via le site de reconnaissance d'acides nucléiques des domaines de liaisons à l'ADN Z. Les interfaces d'acides aminés qu'ont en commun les domaines de liaisons à l'ADN Z et RBP7910, ainsi que l'importance de la structure secondaire de l'ARN pour que RBP7910 s'y lie, indiquent que, tout comme pour les ZBPs, la conformation des substrats d'ARN mitochondrial est essentielle pour que RBP7910 les reconnaisse lors de l'édition. En somme, les données présentées dans cette thèse désignent RBP7910 comme étant une protéine se liant à plusieurs classes d'ARN mitochondrial et influençant l'édition et la stabilité de certains transcrits.

Table of contents

Abstract	2
Résumé	4
Table of contents	6
List of abbreviations.....	9
List of Figures	13
List of Tables	14
Acknowledgements	15
Contribution of authors	16
Chapter I: Introduction & Literature Review.	17
1.1 Introduction	17
1.2 General introduction	19
1.2.1 <i>Trypanosoma brucei</i> and sleeping sickness.....	20
1.2.2 Chagas disease	21
1.2.3 Leishmaniasis.....	22
1.3 Life cycle.....	23
1.3.1 The life cycle of <i>T. brucei</i> (Figure 1.1).....	23
1.4 Ultrastructure	25
1.5 Mitochondrion.....	26
1.5.1 Fulfilling energy requirements of <i>T. brucei</i>	27
1.6 Kinetoplast	28
1.7 RNA editing	29
1.7.1 The RNA editing core complex (editosome).....	32
1.7.2 Discovery of the MRB1 complex	36
1.7.3 Role of the MRB1 complex in RNA editing process	37
1.7.4. Other MRB1 associated complexes	41
1.7.5 The current model of the MRB1 complex mode of action.....	42

1.8 Developmental regulation of RNA editing	43
1.9 Current and potential methodologies to elucidate the regulatory pathway of RNA editing	44
1.10 Hypothesis and objectives.....	45
Chapter II: Material and methods.	47
2.1 Whole cell protein extract preparation.....	47
2.2 Cytosolic and mitochondrial protein extract preparation	47
2.3 Glycerol gradient (GG) and ion exchange chromatography fractionation, protein identification, and quantification	48
2.4 <i>T. brucei</i> cell culture and RNA interference.....	49
2.4.1 Selection and cloning	50
2.5 Induction of RNAi machinery and monitoring growth curves.....	50
2.6 Quantitative Real-Time PCR	50
2.6.1 RNA isolation	50
2.6.2 DNA removal and DNA preparation	51
2.6.3 Quantitative Real-Time PCR reaction	51
2.7 Generation of C-terminal Myc-tagged cell lines and western-blot analysis	52
2.8 Immunofluorescence assay	53
2.9 Mitochondrial extract preparation of Myc-tagged proteins and IP	55
2.10 Guanylyl transferase assay.....	55
2.11 Cloning of the full length Tb927.10.7910 and point mutations	56
2.12 Purification of the recombinant protein	56
2.13 <i>In vitro</i> transcription and radiolabeling of RNAs	57
2.14 Gel shift assays.....	58
2.15 Database searches and sequence alignment.....	59
Chapter III: Results.	60
3.1 Construction of co-fractionation networks	60
3.2 Identification of novel proteins associated with the RNA editing pathway	62
3.3 Gene expression down-regulation by RNA interference.....	63

3.4 Mitochondrial localization of proteins and immunoprecipitation experiments	71
3.5 Identification of potential ZBDs in Tb927.10.7910	73
3.6 Tb927.10.7910 has a higher affinity for gRNAs than mRNAs	74
3.7 gRNA and mRNAs binding specificity of RBP7910	78
3.8 RBP7910 shows a distinct affinity for the AU sequence	82
3.9 Sequence alignment of the predicted ZBDs of RBP7910 with the corresponding Z α and Z β domains of ZBPs	85
3.10 Functional analysis of RBP7910 RNA-binding activity using structure-based mutagenesis	90
Chapter IV: Discussion.	95
Chapter V: Concluding Remarks & Future Directions.....	103
Chapter VI: Contribution to Knowledge	109
Chapter VII: References.....	111
Appendix	133

List of abbreviations

20s	20Svedberg
A	Adenine
A6	ATPase subunit 6
ADAR1	Adenosine deaminase acting on RNA 1
AP	affinity purification
ATP	Adenosine triphosphate
BF	bloodstream form
BSA	bovine serum albumin
C	Cytosine
CL	cutaneous leishmaniasis
COX	cytochrome oxidase
DAI	DNA-dependent activator of interferon regulatory factors
DAPI	4',6-diamidino-2-phenylindole
EReNTDs	emerging re-emerging neglected tropical diseases
ExoUase	Uridine specific exouridylase
FBS	fetal bovine serum
FC	fold change
G	Guanosine
GAP1,2	guide RNA associated protein1,2
GG	glycerol gradient
GPI	glycosylphosphatidylinositol
GRBC	guide RNA binding complex
gRNA	guide RNA
HAT	human African trypanosomiasis
HTH	helix-turn-helix

I	Inosine
IEX	ion-exchange chromatography
IFA	Immunofluorescence assay
IPTG	Isopropyl β -D-1-thiogalactopyranoside
K _d	equilibrium dissociation constant
kDNA	kinetoplast DNA
KEGG	Kyoto Encyclopedia of Genes and Genomes
KPAF	kinetoplast pentatricopeptide repeat-containing factor
KPAP1	kinetoplastid poly(A) polymerase 1
KREL	Kinetoplastid RNA editing ligase
KREN	Kinetoplastid RNA editing endonuclease
KREPA	Kinetoplastid RNA editing protein A
KREPB	Kinetoplastid RNA editing protein B
KREX	kinetoplastid RNA editing Uridine specific exoribonuclease
KRPPR1	kinetoplastid ribosomal pentatricopeptide repeat 1
ML	mucocutaneous leishmaniasis
MRB	mitochondrial RNA binding
MRB1	mitochondrial RNA binding 1
mRNA	messenger RNA
MRP1,2	mitochondrial RNA binding 1,2
Mrpn1	mitochondrial RNA precursor-processing endonuclease1
MURF	maxicircle unidentified reading frame
NADH	nicotinamide adenine dinucleotide
nt	nucleotide
NTDs	neglected tropical diseases
OB-fold	oligonucleotide/oligosaccharide binding fold
ORF	open reading frame
PAMC	polyadenylation mediator complex

PF	procyclic form
RBP7910	RNA binding protein Tb927.10.7910
RECC	RNA editing core complex
REH	RNA editing helicase
REMC	RNA editing mediator complex
RESC	RNA editing substrate complex
RGG2	glycine-arginine box
RNAi	RNA interference
RPS12	ribosomal protein S12
RRM	RNA recognition motif
RT	room temperature
RT-PCR	real time-polymerase chain reaction
SL	long slender
STRING	Search Tool for the Retrieval of Interacting Genes/Proteins
TAP	tandem affinity purification
TbCFHC net	<i>T. brucei</i> high confidence subset of co-fractionation network
TbCFnet	<i>T. brucei</i> co-fractionation network
Tet	tetracycline
tRNA	transfer RNA
TUTase	terminal uridylyl transferase
U	Uridine
VL	visceral leishmaniasis
VSGs	variable surface glycogens
WHO	world health organization
WHTH	winged helix-turn-helix
WT	wild-type
Y2H	yeast two-hybrid
ZBD	Z-DNA binding domain

ZBP Z-DNA binding protein

Z α Z-alpha

Z β Z-beta

List of Figures

Chapter I: Introduction & Literature Review

Figure 1.1. <i>The lifecycle of Trypanosoma brucei</i>	25
Figure 1.2. <i>Mechanism of U insertion and deletion of RNA editing</i>	32
Figure 1.3. <i>RNA editing core complex (RECC) or editosome</i>	35
Figure 1.4. <i>MRB1 complex organization</i>	40
Figure 1.5. <i>The current model for the contribution of numerous proteins in (U) deletion/insertion RNA editing and mitochondrial RNA processing in T. brucei</i>	42

Chapter II: Results

Figure S2.1. <i>SDS-PAGE analysis of WT RBP7910 and point mutants</i>	135
---	-----

Chapter III: Results

Figure 3.1. <i>Comparison of the fractionation patterns for the proteins involved in the RNA editing between GG and IEX methods</i>	62
Figure 3.2. <i>Growth curves for the candidate gene</i>	64-65
Figure 3.3. <i>Effect of depletion of five candidate genes on the abundance of mitochondrial RNAs</i>	67-69
Figure 3.4. <i>Subcellular localization of three candidate genes</i>	71
Figure 3.5. <i>Tb927.1.1730, Tb927.10.1730 and Tb927.10.7910 proteins possess interactions with TbRGG2 subcomplex</i>	72
Figure 3.6. <i>The protein sequence and domain structure of Tb927.10.7910</i>	73
Figure 3.7. <i>Examination of the RNA-binding activity of Tb927.10.7910 using EMSA</i>	76
Figure 3.8. <i>Competition assays to determine the binding specificity of RBP7910 for CYb pre-edited and edited RNAs and gA6[14] RNA</i>	80
Figure 3.9. <i>Competition assays to determine the affinity binding and specificity of RBP7910 to the labeled poly AU sequence</i>	84
Figure 3.10. <i>Multiple amino acid sequence alignment of predicted N- and C-terminal ZBDs of RBP7910 with Za and Zβ domains of ZBPs, respectively</i>	86
Figure 3.11. <i>Comparison of the protein-DNA interaction in hZαADAR1 and hZαDLM-1</i>	89

Figure 3.12. *gA6[14]* RNA-binding activities of RBP7910 point mutations measured by gel shift mobility analysis.....92-93

List of Tables

Chapter I: Introduction & Literature Review

Table 1.1. *MRB1* complex subunits..... 37

Chapter II: Material and methods

S2.1 Table. *Oligonucleotides used in this study*..... 133-134

Chapter III: Results

Table 3.1. *List of the 50 proteins predicted to be associated with the RNA editing machinery*.....136-137

Acknowledgements

First and foremost, I would like to thank my supervisor, Dr. Reza Salavati, for giving me the opportunity to perform research under his supervision. His support, encouragement and wealth of knowledge have been of great benefit to me and have helped me to grow and improve as a researcher. I would also like to give my special thanks to Dr. T. Geary, the director of Institute of Parasitology and a member of my research committee, for providing me with many valuable insights in my research and being enormously generous for any kind of discussions. I also extend my appreciation to Dr. J. Charron, as another member of my advisory committee for his support in my research and in achieving my academic goals. I would like to express my gratitude to Shirley Mongeau, Serge Dernovici, Kathy Keller, and Mike for their very useful administrative and technical support as well as for their precious kindness. My research was greatly supported by past and present members of the laboratory namely, Dr. H. Najafabadi, Dr. S. Kala, Dr. H. Moshiri, Dr. V. Gazestani, Dr. N. Lopez, and Allen Ma.

I greatly appreciate the contribution of Vaibhav Mehta, who has been a kind and cheerful lab mate and has always supported me in research during complicated situations. I am grateful to M. Haque, F. Baakdah, A. Kottarampatel, M. Kaji, E. Burnet, and M. Dagenais, for their help at the time I needed the most.

I am deeply grateful to my family, my parents, Mostafa and Mina, my siblings, Neda and Naghmeh, and, my son Arvin. Their love, support and encouragement are a constant source of motivation.

Contribution of authors

Being the primary author of the thesis, I designed and executed the experiments and interpreted the result presented here, under the supervision of Dr. Reza Salavati. I generated all the figures and tables.

Parts of Chapter 3 and 4 of this thesis were published as the following manuscript.

V.H. Gazestani*, N. Nikpour*, V. Mehta, H. S. Najafabadi, H. Moshiri, A. Jardim, R. Salavati (2016). “A protein complex map of *Trypanosma brucei*” *PLoS Neglected Tropical Diseases*.10 (1371): e0004533.

I hold co-first authorship with V. H. Gazestani who performed the bioinformatic prediction, and I performed the gene knock-down studies, IFA, IP, and qRT-PCR experiments. V. Mehta shared the GG and IEX-chromatography works with H. Moshiri.H. S. Najafabadi designed part of the experiments and worked on the bioinformatic analysis. A. Jardim contributed with reagents and analysis tools. This work is done under the supervision of R. Salavati.

* Contributed equally to this work

Chapter I: Introduction & Literature Review.

1.1 Introduction

The *Trypanosomatidae* family, which includes the protozoan parasites of the genera *Leishmania* and *Trypanosoma*, causes several neglected tropical diseases (NTD) in humans and animals. The parasites that are responsible for human diseases are *Trypanosoma brucei*, which causes human African trypanosomiasis (HAT) [1], *Trypanosoma cruzi*, which causes Chagas diseases [2], and *Leishmania* spp., which cause leishmaniasis [3]. Approximately, 20 million people worldwide are infected by these parasites with an estimated 95,000 death per year [4]. These infections are severely debilitating and often lead to death if left untreated [5]. The existing treatment options for trypanosomatid diseases are unsatisfactory due to several reasons including, a manifestation of toxic side effects, low therapeutic efficacy, and development of drug resistance [6-8]. Moreover, the development of new drugs is challenging because of the complex life cycles of these parasites and substantial changes in their morphology, cell biology, and biochemistry in different life stages [9-11].

On the other hand, there are some peculiar structural and metabolic features in these pathogens that represent great potentials for new drug targets [12-15]. One example is “mitochondrial RNA editing,” a unique type of insertion-deletion RNA editing that occurs only in the mitochondria of trypanosomatids [16-19]. Insertion and removal of uridines are catalyzed by large, multi-protein complexes known as editosomes, which guides the enzymatic steps of RNA editing (i.e., endonuclease, 3' uridylyl transferase, 3' exouridylylase, and ligase activities) [20, 21]. During the editing process, the open reading frames (ORF) of pre-edited messenger RNAs (mRNAs) are changed based on the information carried on guide RNAs (gRNA) to create mature transcripts that are translated into different components of the mitochondrial oxidative

phosphorylation chain. RNA editing is a crucial process for the survival of parasites [22, 23], especially the procyclic form (PF) insect stage of *T. brucei*, which needs a highly active mitochondrion to produce enough ATP through oxidative phosphorylation [24, 25]. Although bloodstream form (BF) *T. brucei* relies on the substrate-level oxidative phosphorylation using glucose from the mammalian host [26], it still needs an active mitochondrion to maintain other metabolic functions such as calcium homeostasis and fatty acid metabolism [27, 28]. In addition to the editosome as the main catalytic core, there are other complexes also involved in the pathway. These complexes are collectively known as the MRB1 complex [29]. The mitochondrial RNA binding (MRB1) complex also acts as a hub for coordination of editosome activity with the subsequent events such as the addition of long poly adenine-uridine (AU)-tails to the 3' end of fully edited transcripts [30, 31].

Understanding the functional relationship between the enzymatic and non-enzymatic parts of the RNA editing process, global architecture and functionalities of the members of the MRB1 complex, can significantly contribute to the current knowledge of the RNA editing machinery of trypanosomes. Although MRB1 is a less-known complex compared to the well-studied editosome, studies indicated that it has an important role in the initiation and/or progression of the editing [30, 32-34].

RNA editing is differentially regulated during the life cycle of *T. brucei*, through an unknown mechanism [35-41]. The regulation can not be controlled by gRNAs, since there are no differences in the abundance of gRNAs in different life stages of *T. brucei* [42]. However, there may be some unknown mechanisms, by which the different life stages differentially utilize or associate the gRNAs with the editosome during the editing process [32, 43]. The mass spectrometry analysis of the purified editosomes indicates the presence of the same set of

proteins in both life cycle stages [44]. However, recent studies revealed that the function of the components of the editosome could be different during the editing process between BF and PF cells [45].

Hence, the major focus of this study was to gain a more comprehensive insight into the RNA editing process of *T. brucei* by applying a combination of proteomic, genetic, and biochemical approaches to decipher a refined picture of the mitochondrial RNA editing machinery and to characterize potential factors that can developmentally regulate the editing of mitochondrial mRNAs.

1.2 General introduction

NTDs have been overlooked at societal, national, and international levels. These diseases are endemic in developing and resource-poor regions [46-51], in which the majority of populations live in unsanitary conditions with insufficient nutritional intake. Additionally, most affected communities lack access to health care systems for treatment. This makes treatment difficult, even though many of these diseases are preventable or treatable through low-cost interventions [50, 52, 53]. The World Health Organization (WHO) has listed 17 core NTDs, including viral, bacterial, helminth, and protozoan infections [54, 55]. According to WHO, NTDs impact more than one billion people from almost 150 endemic countries [56].

Emerging and re-emerging neglected tropical diseases (EReNTDs) is a sub-category of these diseases that are marked by difficulties associated with prevention, treatment and geographical expansion, and their drawback on economic and social progress [57]. Five EReNRDs have been identified: Chagas disease, HAT, cysticercosis, dengue, and rabies. EReNRDs are described as NTDs of humans that either has rapidly increased in the past two decades and/or “threaten to increase in the near future” [57]. The focus of my study was on *T.*

brucei, a flagellated protozoan that along with *T. cruzi* and different species of *Leishmania* are commonly known as “kinetoplastids” [58]. The kinetoplastid parasites are characterized by the presence of a DNA containing region, called “kinetoplast” in their single large mitochondrion. Despite having similar molecular and cellular biology, kinetoplastid pathogens caused different parasitic diseases in humans. Below, I discuss the characteristics and prevention or treatment options for the disease caused by kinetoplastid pathogens, including HAT, Chagas disease, and leishmaniasis.

1.2.1 *Trypanosoma brucei* and sleeping sickness

HAT also called sleeping sickness, is caused by the protozoan parasite *T. brucei* and is transmitted to humans via tsetse flies (genus *Glossina*). Two sub-species are responsible for HAT in rural areas of sub-Saharan Africa: *T. b. gambiense* and *T. b. rhodesiense* [59, 60]. The majority of infections in West and Central Africa are caused by *T. b. gambiense*, which is endemic in 24 countries, while *T. b. rhodesiense* infects wildlife and domestic animal species in Eastern and Southern Africa [61]. Livestock in rural areas faces a high risk of acquiring nagana, a disease caused by *T. b. brucei* [56, 62].

Due to the geographical distribution of the tsetse vector, approximately 90% of HAT infections occur in sub-Saharan Africa, with some cases reported from regions of the Eastern Mediterranean [56]. Clinical symptoms of HAT can be difficult to diagnose at the initial stage of infection, as the major symptoms can be delayed by months and even years depending on the sub-species; *T. b. rhodesiense* leads to acute infections, whereas *T. b. gambiense* causes chronic infections [63]. HAT symptoms include fever, headaches, and joint pain when the parasites are in the blood and the lymphatic system. Migration of parasites to the central nervous system is characterized by severe neurological disorders which can result in death if left untreated [56].

One important difference between the infections caused by the two sub-species is trypanosomal chancres that can appear after the fly bite. Approximately 26% of infections caused by *T. b. rhodesiense* display chancres, while the symptom is rarely seen in *T. b. gambiense* infections [64, 65].

Few drugs are available for the treatment of HAT (e.g., suramin, eflornithine, melarsoprol, pentamidine, nifurtimox) [66-68]. The efficacy of these interventions depends on the HAT sub-species and the stage of the disease [69, 70]. The most serious drawbacks are poor efficacy, toxicity, hypoglycemia, hypotension, and an inconvenient route of administration causing pain at the injection site. In addition, there are reports of drug resistance in regions where HAT is endemic [7, 60, 67, 70]. Unfortunately, despite increasing partnerships and novel tools for drug discovery, identification of new treatments has been generally unsuccessful [68, 71]. However, fexinidazole which was initially identified and studied in the 1980s, has been shown to have efficacy against advanced-stage *T. b. gambiense* infection in clinical trials [72, 73].

1.2.2 Chagas disease

Chagas disease, also known as American trypanosomiasis, is caused by the protozoan *Trypanosoma cruzi*. It is endemic in 21 countries across Latin America and parts of North America, impacting up to million people, and has an annual mortality rate of approximately 10,000 [74-76]. This parasite can also infect some species of wild and domesticated animals, which serve as a reservoir host. The infection is transmitted to humans through the feces of the hematophagous insects known as Reduviidae kissing bugs. Chagas disease can also be transmitted via blood transfusions, organ transplantation, and congenital transmission. The disease has three characteristic clinical phases: acute, intermediate, and chronic. Chronic stages

are seen in < 10% of infections but can severely damage heart tissue and the gastrointestinal tract, among other tissues.

Chagas disease treatment primarily relies on two antiparasitic drugs, benznidazole, and nifurtimox, which require a long-term course of treatment and careful monitoring and have several toxic side effects [8, 77, 78]. Both drugs target the acute phase, and neither is effective against the chronic stage of infection. Clinical trials conducted in Spain and Argentina to assess a new chemotherapeutic agent, parconazole, alone or in combination with benznidazole [79, 80]. However, new clinical trials using parconazole displayed the limited curative potential of this drug [81]. At this time, no vaccine exists for this infection.

1.2.3 Leishmaniasis

Leishmaniasis is a vector-borne tropical infection caused by protozoan parasites of the genus *Leishmania* and spread by the bite of phlebotomine sandflies. This disease is one of the most significant of NTDs with occurrence in the tropical and subtropical areas and found in 98 countries in Asia, Africa, Latin America, and Europe [10, 82]. Annually, between 0.9 and 1.7 million people are infected by leishmaniasis, but only a small fraction of them will eventually develop the disease and with annual deaths of 20,000 to 30,000 [83]. The *Leishmania* parasite maintains its life cycle by transferring between a sand fly and a mammalian host. The flagellate promastigotes transfer into the skin of a mammalian host by sandfly bite; then promastigotes are phagocytized by macrophages and converted into amastigotes. During proliferation of amastigotes in cells and macrophages of different tissues, the symptoms of the infection become apparent. Depending on the *Leishmania* species, geographic region, and host immune response, three major forms of leishmaniasis are cutaneous (CL), mucocutaneous (ML), and visceral leishmaniasis (VL) [3, 84]. Treatment options include two parenteral agents, amphotericin B, and

pentavalent antimony, and three oral drugs miltefosine and the azoles, fluconazole, and ketoconazole [85]. Unfortunately, none of these drugs are adequate due to high toxicity, long treatment period or inadequate mode of administration, and increasing levels of resistance [6, 86].

1.3 Life cycle

Kinetoplastids have a life cycle alternating between insect vector and mammalian host. Various developmental stages essential for progression of infection occur in both vector and host. Here, I focus on and describe the life cycle and the cell biology of *T. brucei*.

1.3.1 The life cycle of *T. brucei* (Figure 1.1)

T. brucei is transmitted between mammalian hosts by the tsetse fly. After taking up an infected blood meal by the vector, the parasite transforms into the PF, which is the first developmental stage of the parasites in the insect vector. The PF matures into a trypomastigote and establishes in the midgut of the fly, which finally migrates to the salivary gland and converts into an epimastigote. In the last developmental stage in the insect, the epimastigote divides into the non-dividing metacyclic form, and is transferred to a new host upon taking the blood meal by the tsetse fly. The full development of the parasite in the tsetse fly occurs within 20-30 days, to acquiring all the substantial biological changes that make parasite infective to the immune responses by the mammalian host [87].

Injection of metacyclic trypanosomes into dermal connective tissues can cause a local inflammatory reaction and trypanosomal chancre depending on the infecting sub-species. From there, trypomastigotes move via the lymphatic to lymph and then into the bloodstream, where they multiply by binary fission and cause a systematic infection. In contrast to other

trypanosomatids, *T. brucei* has an extracellular life cycle in the mammalian host. *T. brucei* completes its development into long slender forms (LS) in the bloodstream, which evades the host immune system through antigenic variation. This phenomenon is accomplished by presenting antigenically distinct variable surface glycoproteins (VSGs), which are linked to the surface membrane by a glycosylphosphatidylinositol (GPI) anchor [88].

By increasing the number of parasites in the bloodstream, they eventually differentiate into a short stumpy form. The non-proliferative stumpy forms are pre-adapted for transmission to the tsetse flies. The growth of short stumpy parasite is arrested at the G1 phase of the cell cycle till transmission to the midgut of fly, where parasite re-enters to the cell cycle and obtains the morphological changes. Upon up-taking the parasite from the bloodstream, the dense VSG coat is replaced with a less-dense surface coat composed of procyclins, which are also GPI anchored [89].

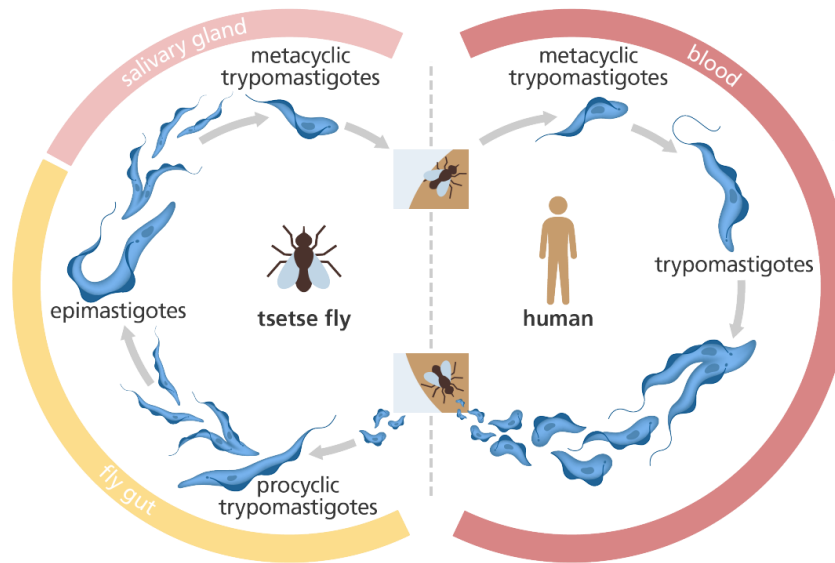


Figure 1.1. *The life cycle of Trypanosoma brucei.* (<https://www.yourgenome.org>)

1.4 Ultrastructure

The *Trypanosomatidae* family consists of protozoan parasites, eukaryotic cells that have the typical ultrastructural organization as their mammalian host cells. However, trypanosomatids have special organelles that are absent from other eukaryotic cells or show some exclusive features only found in trypanosomatids. These structural features are intriguing chemotherapeutic targets with the potential for higher specificity and fewer off-target effects in patients.

Organelles of *T. brucei* include endosomes, Golgi apparatus, lysosomes, nucleus, glycosomes and a large mitochondrion. Despite not having a fixed shape, this organism is mobile and contains a single flagellum for bi-helical motion [90]. The flagellum has an axenomal

structure plus an associated paraflagellar rod [91], and this semi-rigid structure helps parasite motility.

The trypanosome flagellum originates in a basal body that is connected to the mitochondrial membrane and in turn to the mitochondrial genome, the kinetoplast. A tripartite attachment complex links the kinetoplast and basal body and crosses both the cell and the mitochondrial membrane [92]. This complex is composed of a series of filaments that provide guide ropes by which mitochondrial genome segregation is linked to the replication and segregation of the basal body and flagellum.

As the daughter flagellum grows, the nucleus undergoes mitosis. After ending the mitochondrial division, the cytoplasm undergoes cytokinesis to form two identical cells. The single mitochondrion and kinetoplast of *T. brucei* show unique structure and function during the parasite life cycle as explained below.

1.5 Mitochondrion

Mitochondria are double membrane-bound organelles found in all eukaryotic cells, but vary in number, size, and levels of complexity, depending on the organism and cell type [93]. They are responsible for energy production via oxidative phosphorylation and synthesis of key metabolites such as acetyl-CoA, alpha-ketoglutarate, and oxaloacetate.

Five integral enzyme complexes in the inner mitochondrial membrane are involved in mitochondrial respiration via the electron transport chain: *Complex I* – nicotinamide adenine dinucleotide (NADH)-ubiquinone: oxidoreductase, *Complex II* – succinate-ubiquinone dehydrogenase, *Complex III* – ubiquinol: cytochrome *c* oxidoreductase (or cytochrome *bc* 1

complex), *Complex IV* – cytochrome *c* oxidase (COX or cytochrome AA3 complex), and *Complex V* – F₀F₁-ATPase. Three protein complexes in the inner membrane, including complex I, III, and IV, pump protons (H⁺) in the intermembrane space, generating an electrochemical gradient. The protons return to the matrix through complex V while their energy is used to synthesize ATP, and links respiration to the phosphorylation process [94]. In parasitic protists, mitochondrial metabolism varies according to the species and life cycle stage.

1.5.1 Fulfilling energy requirements of *T. brucei*

The BF of the parasite is completely dependent on the unlimited supply of glucose in the bloodstream of the host. Energy generation relies on glycolytic reactions occurring in the a peroxisome-like organelle, called glycosomes.

The first seven enzymes converting glucose into 3-phosphoglycerate exist in the glycosomes while the last three enzymes of the pathway are in the cytosol [95]. The final pyruvate product is excreted into the bloodstream of the host. Pyruvate kinase changes phosphoenol pyruvate to pyruvate and produces ATP in the cytosol. During this process, 2 ATP molecules are used by hexokinase and phosphofructokinase, and phosphofructo kinase produces 1 ATP. Also, NADH production by glycerol-3-phosphate dehydrogenase is oxidized by glycerol-3-phosphate oxidase in the glycosomes, so the consumption and production of ATP and NADH by glycolysis are balanced within the glycosomes.

Although in BF, the mitochondrion has a simple tubular structure devoid of cristae and lacks cytochromes and Krebs-cycle enzymes, it is still essential to maintain other metabolic pathways such as calcium homeostasis and, fatty acid metabolism [96].

In the insect vector, the parasite uses amino acids (including L-proline) as the main energy source and catabolizes them in the mitochondrion, whereas glucose catabolism still takes

place in the glycosomes with some differences from BF: first, 3- phosphoglycerate is produced in the cytosol [97]. Second, phosphoenol pyruvate produced in the cytosol moves to the glycosomes and changes into oxaloacetate by phosphoenolpyruvate carboxykinase and then to malate by glycosomal malate dehydrogenase [98]. Malate is used as a substrate for succinate production, a major-end product exerted by most trypanosomatids [99, 100], and is also shuffled into cytosol to make pyruvate by cytosolic malic enzyme [101] Third, pyruvate is produced from phosphoenol pyruvate and is converted into acetate, lactate, and L-alanine in the mitochondrion and/or the cytosol [102, 103].

The PF of the parasite has a well-developed mitochondrion with abundant crista that is fully functional, and ATP production depends on coupled electron transport machinery and the oxidative phosphorylation system [104].

1.6 Kinetoplast

The mitochondrial genome (KDNA) comprises about 30% of total cellular DNA. This genome is condensed into kinetoplast. The catenated disc-like *T. brucei* mitochondrial DNA contains two different types of circular DNA of varying sizes, maxi- and minicircles. Approximately 50 catenated maxicircles, 20 to 36 Kb in size, and 10,000 catenated minicircles, 0.4 to 2.5 Kb in size, are found in the mitochondrion [105]. Protein-coding genes are polycistronically transcribed in both nucleus and mitochondria by RNA polymerase II from an unknown promoter in trypanosomatids. Most of these genes have no apparent functional relationships [106-108]. These transcripts are further processed via trans-splicing using a

polypyrimidine tract as the signal for a spliced leader site and changed into monocistronic mRNAs [109]. However, the mechanism of how transcripts are processed from the precursor is still unknown.

Topoisomerase, basic proteins, and histone-like proteins have been identified in the kinetoplast structure that help in condensation and replication of KDNA [110, 111].

The maxicircle is structurally and functionally equivalent to the mitochondrial genome in other eukaryotic organisms [112] and encodes ribosomal rRNAs (12s and 9s) and several components of the electron transport chain. A ribosomal protein S12 (RPS12), six subunits of the reduced NADH-dehydrogenase (ND1,4,5,7-9), subunit 6 of the ATP (ATPase: A6), cytochrome b of the bc1-complex (CYb) and subunits I-III of the cytochrome oxidase (COI-III) are ORFs encoded by the maxicircles. Five ORFs with unknown functions, termed maxicircle unidentified reading frames (MURF), may encode additional components of the NADH dehydrogenase complex. Minicircles encode heterogenous sequences called gRNAs that contribute to the creation of maxicircle transcripts [21]. Except for ND4, COI, MURF1, and ND1, most mitochondrial-encoded transcripts are unusual in that they need to be edited to be translated. These cryptogenes are remodeled by using information from the 3' uridylated gRNAs during the process known as RNA editing.

1.7 RNA editing

The term “RNA editing” was initially used to explain an unusual post-transcriptional modification of uridine (U) residues insertion into mitochondrial transcripts of two trypanosomatid protozoans (*T. brucei* and *Crithidia fasciculata*) [39]. Although, the RNA editing does not include post-transcriptional modification processes such as 5' capping, splicing, and 3' poly adenylation of mRNAs, the differences between “modification” and “editing” is still quite

ambiguous. For example, deamination of adenosine (A) and formation of inosine (I) by the deaminase editing enzyme results in (A) to guanosine (G) substitution, since the (I) will be recognized as (G) during translation of mRNA. Hence, editing and modification can be considered a very similar phenomenon.

There are two distinct classes of the RNA editing process: substitution and insertion/deletion. Previous research has established that RNA editing occurs solely in eukaryotes, although cytosine (C)- to- (U) editing of transfer RNAs (tRNA) in Archaea has been recently reported [113]. The hyperthermophilic archaeon uses a C-to-U editing enzyme to deaminates (C) at position 8 of tRNA and creates a (U) at this position, which guarantees a proper tertiary structure and function of tRNAs.

Eukaryotic organelles, namely chloroplasts and especially mitochondria, present the greatest variety of RNA editing systems [114]. The reason for the higher occurrence of editing in these two organelles is not known, although the simpler structure of mitochondrial genomes, which encode few of genes might be the reason. RNA editing systems show a very narrow phylogenetic distribution by restricting into specific organismal groups. For example, the insertion-deletion editing has not been detected outside the Kinetoplastida. C-to-U conversion is specifically seen in land plants and there is no report of this type of editing in of charophyte algae or lineages of green algae [114]. Also, different types of editing can occur in the same organelle of an organism. In the mitochondria of *Leishmania*, both C-to-U editing of tRNA and U deletion-insertion of mRNA occur [115].

In *Kinetoplastids*, RNA editing is a process in which gRNAs direct the insertion, and less frequently deletion, of a defined number of U residues at specific positions of precursor mRNAs to generate mature mRNAs [116] (**Fig. 1.2**).

Editing creates initiation and/or termination codons, corrects frameshifts, and in the case of pan-edited mRNAs (transcripts that undergo large editing directed by multiple overlapping gRNAs), creates an entire reading frame. Three distinct regions are seen in gRNAs: an anchor sequence, a central region and a 3' (U)-tail. The anchor sequence at the 5' end is complementary to the pre-mRNA just downstream of the first editing site (ES). The central region of each gRNA molecule contains guiding nucleotides that interact with the pre-mRNA and guide the insertions and deletions of Us. Finally, gRNAs have (U)-tails at the 3' end that are added post-transcriptionally by a mitochondrial terminal uridylyl transferase (TUTase) [117, 118]. Upon binding to the pre-mRNA, the gRNA 3' (U)-tail interacts with the purine-rich region upstream of the ES. This interaction, which stabilizes the gRNA-pre-mRNA duplex, has been suggested to be one of the functions of gRNA 3' (U)-tail [117, 119].

The RNA editing reaction is initiated by hybridization of the 5' end of a gRNA and precursor mRNA, forming an anchor duplex [120]. The first enzymatic step in the catalytic cascade of RNA editing is an endonucleolytic cleavage at the ES of the precursor mRNA. In insertion editing, uridine residues are added by TUTase to the 3' end of the 5' cleavage product, and in deletion editing, uridine residues are removed by a specific 3' uridine exouridylyase (exoUase). The resulting fragments are joined by an RNA ligase [22, 121].

Based on the number of ESs in the pre-edited transcript, upon editing of the last ES at the most 5' end, the pre-edited transcript is modified into a translatable mRNA with a single initiation and a single termination codon. The editing process is essential for the survival of both developmental stages, although the precise role of this process is not known for the BF [22, 122].

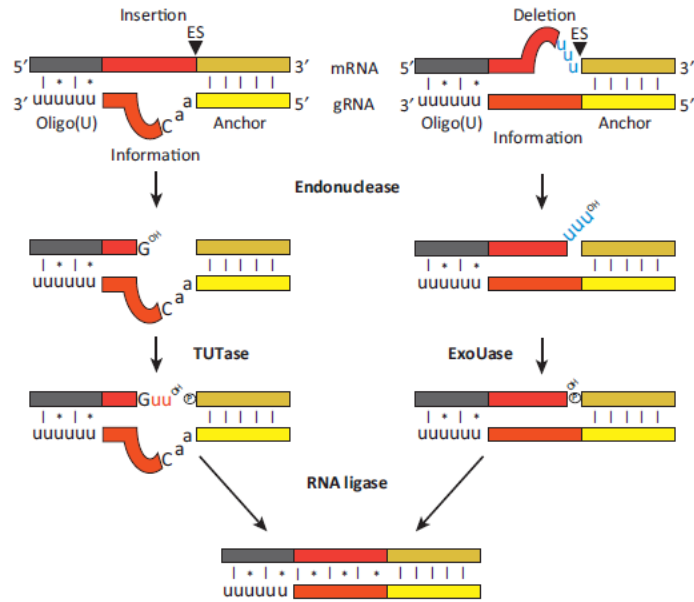


Figure 1.2. Mechanism of U insertion and deletion of RNA editing. Adapted from Hashimi *et al.*,

Trends in Parasitology, Copyright (2012), with permission from Elsevier. gRNA lower strand; domains in solid colors; yellow, anchor; red; information; black Us; 3' oligo (U)-tail and mRNA top strand.

1.7.1 The RNA editing core complex (editosome)

The functional editosome was identified by several methods, including mass spectrometric analysis of the editosome, immunoaffinity chromatography of components of editosome, and tandem affinity purification (TAP) of tagged RNA editing proteins [121, 123-127]. Editosome sediments at approximately 20 Svedberg units (20S) on glycerol gradients, giving this complex the name “20S editosome” [20]. Three distinct RNA editing core complexes (RECC) have been identified with highly dynamic components, that share the same core, composed of 12 proteins.

These core proteins are involved in different steps of RNA editing, including a kinetoplastid RNA editing U specific exoribonuclease (KREX2) [51, 52], 3'TUTase (KRET2) [128, 129], and RNA editing ligases (KREL1 and KREL2) [22, 122, 130, 131]. In addition, six

proteins containing predicted OB-fold kinetoplastid RNA editing protein A1-6 (KREPA1-6) and two proteins with degenerate RNase III motifs (KREPB4 and KREPB5) are present in the core (Fig. 1.3).

Three interacting proteins, KRET2-KREPA1-KREL2, catalyze gRNA-directed U-insertion *in vitro* and KREX2-KREPA2-KREL1 together catalyze gRNA-directed U-deletion *in vitro* [132]. KREPA1 within the insertion subcomplex and KREPA2 from the deletion subcomplex interact and stimulate the function of their respective partners in each subcomplex [133-135]. Also, the direct interactions of KREPA1 and KREPA2 with KREPA3 and KREPA6, create a connecting bridge between insertion and deletion subcomplexes within RECC [136] (Fig. 1.3-A).

The association of the core of the editosome with the three RNase III family endonucleases (KREN1, KREN2, KREN3) and their partner proteins (KREPB8, KREPB7, KREPB6, respectively) creates three variants of RECC [20, 123] (Fig.1.3-B). KREN1/KREPB8 partners and the U-specific exoribonuclease KREX1 are involved in *in vitro* and *in vivo* U deletion functions of the RECC. KREN2/KREPB7 RECC has U insertion activity, and the KREN3/KREPB6 RECC is specific for *cis*-editing of COII transcripts [137]. An *in vitro* full round RNA editing reaction using purified RECC, RNA substrate, and gRNA results in an accurate gRNA-directed U-insertion or deletion editing into one ES [138]. However, the progression of editing or gRNA exchange between ESs has not been achieved by *in vitro* editing assays using purified RECC, which implies the existence of additional factors *in vivo* [43].

Several studies over past decades have revealed another essential multi-protein complex, termed the MRB1 complex or RNA editing substrate complex (RESC) [17]. The main focus of these studies was to address the role of the MRB1 complex in the recruitment of RNA to the

RECC and its function in the progression of editing [17, 43, 139, 140]. The findings suggest that MRB1 complex, a non-enzymatic platform of the RNA editing coordinates the RNA editing and other mitochondrial RNA processing events [141, 142].

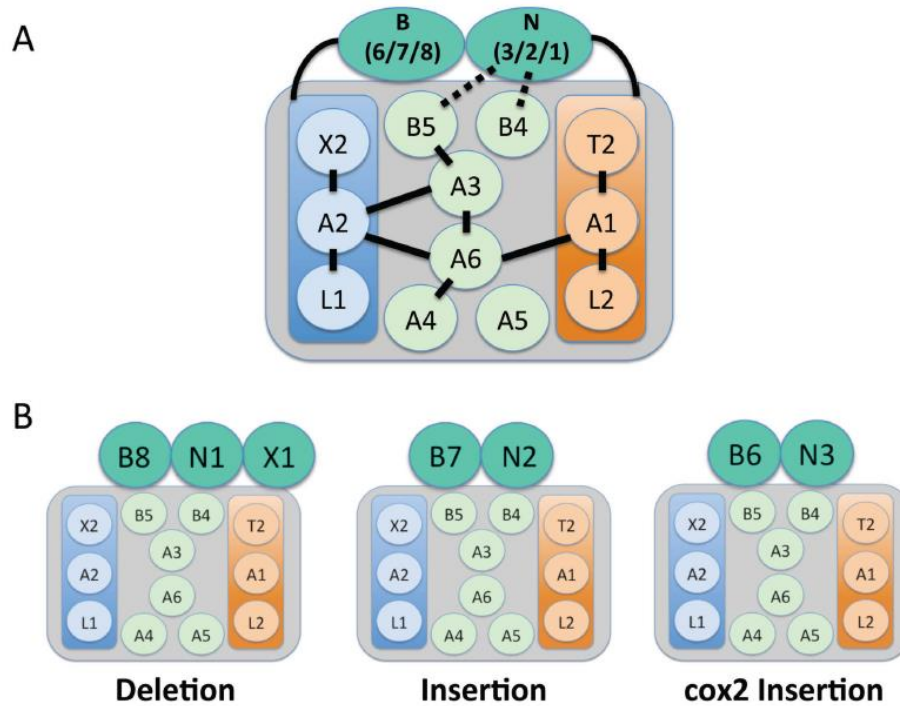


Figure 1.3. RNA editing core complex (RECC) or editosome. Read *et al.*; Wiley Interdisciplinary Reviews: RNA, Copyright (2016), with permission from John Wiley and Sons. Three identified RECC including, deletion complex, insertion complex, and COII insertion complex. A shorthand nomenclature used to identify proteins according to kinetoplastid RNA editing protein (KREP) nomenclature. The core complex shown by light-green circles, deletion sub-complex in light-blue, and insertion sub-complex in orange. Association of the core complex with three different endonucleases defines the function of the complex, N1, N2, and N3 endonucleases are associated with deletion, insertion, and COII insertion complex, respectively.

1.7.2 Discovery of the MRB1 complex

In 2008, using different purification methods, three groups discovered MRB1 complexes with varying compositions [29, 141, 143]. Panigrahi and colleagues immunoprecipitated a complex of 16 proteins including guide RNA associated protein 2 (GAP2), or GRBC1, and a related protein with 31% identity named guide RNA associated protein 1 (GAP1) or guide RNA binding complex 2 (GRBC2) [29] (**Table 1.1**). This list includes proteins with RNA binding affinity, i.e. *T. brucei* RGG2 (TbRGG2) with a glycine-arginine (RGG2) box and an RNA recognition motif (RRM). Using TAP of tagged-TbRGG1, a protein with *in vitro* poly-U RNA binding activity, [144], Hashimi and co-workers [143] detected GAP1 and GAP2 proteins. Finally, Weng *et al.*, purified homologues of GAP1 and GAP2 from *Leishmania tarentolae* by immunoprecipitation of mitochondrial RNA binding protein 1/2 (MRP1/2) proteins [141]. These studies identified a mitochondrial multi-protein complex, with unknown function and composition, now is commonly known as the MRB1 complex [16].

Table 1.1. MRB1 complex subunits. The MRB1 complex also called RESC, MRB1 core as guide RNA binding complex (GRBC), and TbRGG2 subcomplex as RNA editing mediator complex (REMC) [17].

Subcomplex	Name	Alias	TritrypDB#	References
Core	GAP1	GRB2	Tb927.2.3800	[17, 33, 141, 143, 145, 146]
Core	GAP2	GRBC1	Tb927.7.2570	[17, 33, 141, 143, 145, 146]
Core	MRB3010	GRBC6	Tb927.5.3010	[17, 32, 34, 43, 141, 142, 147]
Core	MRB11870	GRBC5	Tb927.10.11870	[30, 34, 142]
Core	MRB5390	GRBC4	Tb11.02.5390	[30, 142, 148]
Core	MRB8620	GRBC3	Tb927.11.16860	[30, 142, 149]
Core	MRB0880	GRBC7	Tb927.11.9140	[17, 142]
TbRGG2	TbRGG2	None	Tb927.10.10.830	[17, 33, 142, 148, 150, 151]
TbRGG2	MRB8170	REMC5A	Tb927.8.8170	[17, 142, 152]
TbRGG2	MRB8180	REMC4	Tb927.8.8180	[17, 142]
TbRGG2	MRB4160	REMC5	Tb927.4.4160	[17, 142, 152]
TbRGG2	MRB1860	REMC2	Tb927.2.1860	[17, 142]
TbRGG2	MRB800	REMC3	Tb927.7.800	[17, 142]
TbRGG2	PhyH	None	Tb927.9.7260	[153]
Unknown	MRB10130	REMC1	Tb927.10.10130	[17, 29, 142]

1.7.3 Role of the MRB1 complex in RNA editing process

Functional analyses of GAP1 and GAP2 showed the gRNA binding and stabilization activity of these proteins, linking the MRB1 complex activity to the RNA editing [141]. GAP1/2 proteins are essential for the parasite viability and are critical for the editing process at both life stages; repression of GAP1 or GAP2 destabilizes the mitochondrial gRNA population and suppresses the editing of all mitochondrial mRNAs, except the *cis*-edited COII transcript [141, 145].

In continuation, a large-scale yeast two-hybrid (Y2H) study of 31 potential members of MRB1 complex identified the core of the MRB1 complex, including GAP1, GAP2, MRB3010, MRB8620, MRB8170, MRB4160, MRB11870, MRB5390, and MRB0880 [142]. The editing initiation of pan-editing transcripts like ATPase 6 (A6) RNA was interrupted by deletion of MRB3010, notably by the accumulation of pre-edited mRNAs and reduction of edited transcripts, mainly at the 3'-most ESs [32].

Similarly, MRB11870 depletion massively affected the initiation of the editing process through the accumulation of pre-edited transcripts [34]. Collectively, functional studies of MRB1 core proteins have highlighted the gRNA binding and stabilizing role of GAP1 and GAP2 proteins, and the contribution of other members of core MRB1 in the initiation of RNA editing.

Another RNA binding protein (RBP) is TbRGG2, having RNA-enhanced interactions with GAP1/2 proteins and other members of the MRB1 core TbRGG2. The RNase treatment of the mitochondrial extract severely diminishes the interaction of TbRGG2 and the members of the core MRB1 [150, 152]. Also, the Y2H experiments verified the association of TbRGG2 with MRB3010 and MRB8620. Down-regulation of TbRGG2 was accompanied by a huge defect on the editing of pan-edited mRNAs in both life stages, while the editing of minimally-edited transcripts remained unaffected. TbRGG2 depletion largely affects 3' to 5' progression of editing in A6 and RPS12 RNAs, with the minimal effects on the editing initiation [33]. Y2H studies also revealed strong interactions of TbRGG2 with MRB4160, MRB8170, and MRB 8180 mostly in an RNA-enhanced manner. Similarly, the pulldown experiments indicated the RNA-enhanced interactions of MRB8170 and the members of the core MRB1 complex. Moreover, finding the association of TbRGG2, MRB8170, and MRB4160 with the mRPN1 endoribonuclease, suggested the involvement of these proteins in gRNA processing of PF parasites [154, 155].

Together these findings propose TbRGG2 as a subcomplex of the MRB1 complex, such way the TbRGG2 interactions with the core MRB1 complex are significantly strengthened by RNA molecules (**Fig. 1.4**) [16].

Aphasizheva and co-workers reconfirmed the earlier reports on the presence of direct protein-protein interactions within the MRB1 core complex, and the RNA-enhanced contacts between the MRB1 core and the TbRGG2 subcomplex(es) [17]. This group used a different nomenclature for the subcomplexes of MRB1 complex; MRB1 complex as RESC, MRB1 core as GRBC, and TbRGG2 subcomplex as REMC. The TbRGG2 role in gRNA utilization during 3' to 5' progression of RNA editing has confirmed using a deep sequencing of TbRGG2, MRB8170, and MRB4160 depleted cells [140]. Also, the results from this study suggested the functions of MRB8170 and MRB4160 in initiation and assembly of RESC. The proposed role of TbRGG2 in progression of editing was in agreement with the earlier report of the RNA unwinding activity of this protein [34].

As mentioned earlier, the role of MRB1 complex components in the RNA editing process has been indicated by knock-down experiments. Most proteins of the MRB1 complex have gRNA [141] or mRNA [17, 43] binding activities, explaining the presence of mainly transient interactions between members of MRB1 complex and RECC. Also, MRB1 members have been detected in RECC purifications and *vice versa* [150, 156]. Nevertheless, many MRB1 members were not represented in these studies. Finally, it is shown that the sedimentation of the 20S RECC is not altered by deletion of MRB1 complex proteins [17, 141, 148].

1.7.4. Other MRB1 associated complexes

One of the post-transcriptional modifications observed in most mitochondrial RNAs is the addition of non-encoded 3' tails, including (A), (U) or a combination of both [40]. Ribosomal RNAs (12S and 9S) are uridylated at the 3' end [157], while most pre-edited transcripts are adenylated prior to editing by kinetoplastid poly (A) polymerase 1 (KPAP1) [158]. Upon completion of the editing process, the short poly A tail (~20-25 nucleotide (nt)) of a fully-edited transcript is extended into a long poly AU-tail (~200-300 nt) by KPAP1 and RET1TUTase [31, 159]. The tail composition is quite transcript-specific, and longer tails generally have a higher number of (U)s. Short A-tails stabilize partially and fully edited mRNAs, and long AU-tails of never-edited and fully edited mRNAs mark transcripts for translation by recognition through the small subunit of the ribosome [31, 160]. In addition to KPAP1 and RET1 TUTase, three kinetoplastid pentatripeptide repeat-containing polyadenylation factors (KPAF1, KPAF2 [31], and KPAF3 [160] are present in the KPAP1 complex. The KPAF1/2 function is necessary for long 3' tail synthesis with the contribution of RET. KPAF3 is more crucial in the selection process of pre-mRNAs for adenylation rather than uridylation, before entering the editing pathway. Interaction of the KPAP1 complex with RECC and the MEB1 complex is transient and RNA-dependent [17, 31].

Another MRB1 protein-mediated interacting complex is the polyadenylation mediator complex (PAMC). Despite not having strong interactions with KPAP1, protein components of the PAMC are involved in the synthesis of both short and long 3' tail of mitochondrial transcripts [17].

1.7.5 The current model of the MRB1 complex mode of action

A recent review [16] summarized our current understanding of the MRB1 role in *T. brucei* mitochondrial RNA metabolism by presenting a model, explaining MRB1 complex function (**Fig. 1.5**). Based on that, the MRB1 core is responsible for initiation of the RNA editing through involvement in the very early events of editing pathway. TbRGG2 subcomplex addresses gRNA utilization and progression of the editing. Other members of this subcomplex facilitate specific gRNA-mRNA annealing via RNA binding activities. This model also highlights the function of KPAP1 complex and PAMC in addition of long AU-tail to the fully-edited transcripts and initiation of translation.

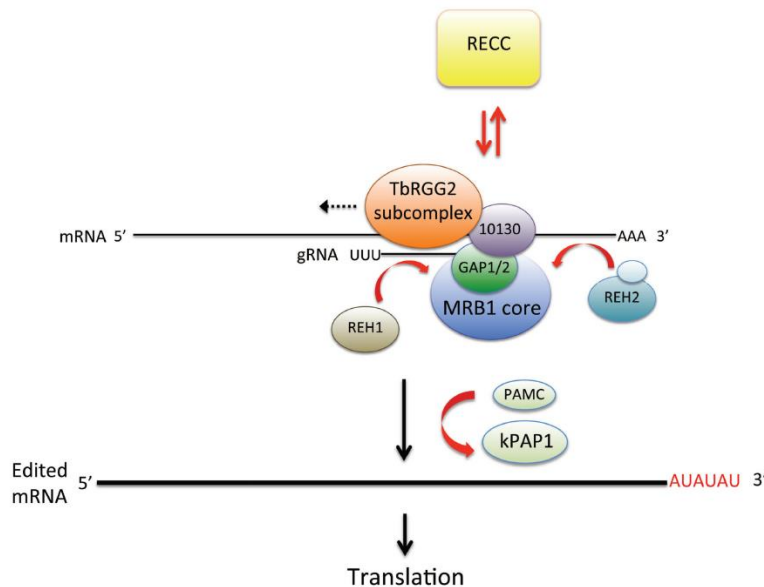


Figure 1.5. *The current model for the contribution of numerous proteins in (U) deletion/insertion RNA editing and mitochondrial RNA processing in T. brucei.* Read *et al.*; Wiley Interdisciplinary Reviews: RNA, Copyright (2016), with permission from John Wiley and Sons. REH1 and REH2 (RNA editing helicase 1 and 2) promote RNA association with MRB1. PAMC and kPAP1 mark the edited transcript for translation by adding long AU-tail to the 3' end of transcripts.

1.8 Developmental regulation of RNA editing

Editing of the mitochondrial RNAs is developmentally regulated in a transcript-specific manner in *T. brucei* [36-38, 161]. For example, edited versions of CYb and COII are not detectable in the BF, while their edited mRNAs are highly abundant in PF parasites. As another example, the abundance of the fully edited NADH dehydrogenase subunit 8 and 9 mRNAs are increased in BF compared to PF [162]. This regulation occurs in coordination with the activities of the trypanosome mitochondrion during the developmental cycles to adapt to the changing environmental conditions.

The molecular basis of this developmental control is unknown. The editosome complexes in PF and BF are similar but not identical, and the BF complexes sediment at >20s fractions compare to PF editing complexes sedimentation at 20s, so it is possible that BF complexes are simpler in composition 20S editosome of PF [163]. Structural differences of the editosome complex during the parasite life cycle can play a role in the developmental regulation of editing. For example, a recent work [45] showed the different functions of KREPA3 and KREPB5 proteins from the RECC between BF and PF stages, which affect cell growth, RECC integrity, and RNA editing. Therefore, KREPA3 and KREPB5 control the differential editing using structurally different RECC between life stages. The gRNA molecules are equally present at both life stages. However, the developmental regulation of editing appears to be at the level of gRNA utilization [35, 42]. The same level of gRNAs and unedited mRNAs of the transcripts with differential editing between BF and PF, like CYb, suggests the presence of some specific factors, which regulate the stability of pre-edited and edited transcripts or facilitate the association of specific gRNAs to the RNA editing machinery.

1.9 Current and potential methodologies to elucidate the regulatory pathway of RNA editing

So far, different methodologies have been employed to uncover the mechanisms of the RNA editing regulatory pathway, including detailed functional studies of editosome proteins at BF and PF life cycle stages or quantitation of BF and PF RNA editing substrates [35]. Moreover, conducting a systematic study of the protein complexes participating in the RNA editing machinery by creating a protein interaction map is another way to elucidate these regulatory pathways. Protein interaction maps contribute considerably to the functional annotation of proteins, which aid in our understanding of the biology of the different organisms [164]. A variety of complementary methodologies is essential to create a comprehensive protein interaction map, and chart protein interactions and complexes [165]. The Y2H system is a well-known approach for capturing pairwise or binary interactions among proteins [166, 167]. Various purification approaches, including Immunoprecipitation (IP) [168], biochemical fractionation [169-171], and affinity purification (AP)-based approaches [172-174], coupled with ultrasensitive mass spectrometric protein identification methods have widely been used for the identification of protein complexes in a specific cellular context. Moreover, computational biology approaches, such as transcriptomics analysis [175] and synthetic lethality [176] have been used to predict the functional association of proteins. There are few examples of large-scale studies for the identification of protein composition of mitochondrial complexes in *T. brucei*. IP of different mitochondrial RNA editing complexes using multiple monoclonal antibodies and parallel TAP tag purification technique identified the composition of protein complexes in the mitochondrial extract of PF parasites [29]. A large-scale Y2H for identification of different subcomplexes of RECC [136] and MRB1 complex [142] and the most recent work on

identifying the subunit organization of purified editosomes using chemical cross-linking and mass spectrometry analysis [177] are another examples. However, different approaches have their limitations, and the results are still compromised by false positives, false negatives, and limited reproducibility. In AP-based approaches, for example, the tagging process may change the binding partners of the tagged protein by inactivation, capping the binding site, or changing the localization of the protein. Highly expressed proteins are also often specifically co-purified with the tagged protein as false positive contaminants. Recovery of transient interactions is less likely if more than one step of purification is used. Although the Y2H system works well at capturing binary, particularly transient interactions, the rate of wrongly identified proteins is relatively high, and the system poorly detects co-complex associations [178]. In biochemical fractionation strategies, fortuitous interactions can arise because confounding protein complexes can still be present in the same fraction regardless of in-depth fractionation [169]. Therefore, the integration of data from different approaches is highly recommended for developing protein maps to improve the precision of interactions and predictions [179].

1.10 Hypothesis and objectives

This research tested the hypothesis that the interaction network of *T. brucei* contains regulatory proteins that function to specify the differential production of the mitochondrial respiratory chain and the RNA substrates that are edited at different life stages of *T. brucei*. Identification of these regulatory proteins and their molecular mechanisms can uncover important targets by which this process can be regulated. Accordingly, two main objectives were pursued in this research.

1. Identification of new proteins with potential involvement in the editing of transcripts, which are preferentially edited at PF life cycle stage.
2. Functional characterization of one of the novel proteins (Tb927.10.7910), identified in the first objective.

Chapter II: Material and methods.

2.1 Whole cell protein extract preparation

Late log phase ($\sim 2 \times 10^7$ cells/ml) *T. brucei* PF IsTaR 1.7 A cells (a derivative of EATRO 164) were grown in 225 cm² flasks to obtain 4×10^9 cells. The cells were harvested by centrifugation at 6,000 x g for 10 min at 4°C and washed once with ice-cold glucose-supplemented PBS (6 mM glucose). The cells were then resuspended in 500 µl lysis buffer [10 mM Tris-HCl pH 7.2, 10 mM MgCl₂, 100 mM KCl, 1 µg/ml pepstatin, 1 Mm Dithiothreitol (DTT), 1% Triton X-100 and 1x EDTA-free protease inhibitor cocktail (Roche Applied Science, ON, CA)] and incubated on a tube rotator for 15 min at 4°C. The lysate was treated with 40 units of RNase-free DNase I (Roche Applied Science, ON, CA) for 1 h on ice and cleared twice by centrifugation at 16,000 x g for 15 min at 4°C.

2.2 Cytosolic and mitochondrial protein extract preparation

Methods for extract preparation were adapted from conventional purification techniques [15, 180, 181]. Cell pellets were washed with ice-cold glucose-supplemented PBS as above, resuspended in 30 ml DTE buffer [1 mM Tris-HCl pH 8.0 and 1 mM EDTA] containing a protease inhibitor cocktail (Roche Applied Science, ON, CA), and lysed using a 40 ml sterile tight-fitting Dounce-homogenizer on ice. The lysate was immediately made isotonic by adding a 2 M sucrose stock solution to a final concentration of 250 mM, and the solution centrifuged at 15,800 x g for 10 min at 4°C. The resulting mitochondrial pellet was resuspended in 0.3 mM CaCl₂ and 40 of RNase free DNase I (Roche Applied Science, ON, CA) in 4.6 ml STM buffer [20 mM Tris-HCl pH 8.0, 250 mM sucrose and 2 mM MgCl₂] for 1 h on ice and precipitated again. The mitochondrial lysate was prepared in 500 µl lysis buffer as described above for whole cells. The supernatant obtained upon collecting mitochondria at 15,800 x g, represents a crude

preparation of the cytosol. The supernatant was centrifuged at 100,000 x g for 1 h at 4°C to eliminate small organelle contamination.

2.3 Glycerol gradient (GG) and ion exchange chromatography fractionation, protein identification, and quantification

Whole cell and mitochondrial extracts were resolved on 10–30% linear glycerol gradients 40mM HEPES pH 7.9, 20 mM Mg(OAc)₂, 100 mM KCl, and 2 mM EDTA at 178,000 x g for 6 hr at 4°C, and fractionated into 46 fractions (250 µl each), as described elsewhere [182]. Protein separation and position on these gradients was standardized with known amounts of BSA (bovine serum albumin), catalase and IgM (Immunoglobulin M), with apparent masses of 66, 230 and 970 kDa, respectively.

Cytosolic and mitochondrial extracts were resolved by liquid chromatography using tandem cationic (S)–anionic (Q) exchange columns (UNOsphere, Bio-Rad Laboratories, QC, Canada), adapted from [169, 183]. The mobile phase consisted of buffer A [10 mM Tris-HCl pH 7.8, 10 mM MgCl₂, 50 mM KCl and 1 mM DTT] and buffer B [buffer A + 950 mM KCl]. Chromatography was performed using a Beckman-Coulter Gold high performance liquid chromatography system. Samples were passed through a 0.22 µm membrane, loaded on the columns and then washed for 15 min with buffer A, followed by 0–50% buffer B (1%/min), a 10 min wash and then 50–100% buffer B (5%/min). The flow-rate was maintained at 400 µl/min, and approximately 40 fractions (800 µl each) were collected.

Identification of proteins and further analysis for protein group determination were done in collaboration with a graduate student in our lab [184]. In addition, construction of primary co-

fractionation network, curation of the high-confidence network, network visualization, and statistical analysis were by the same collaborator [184].

2.4 *T. brucei* cell culture and RNA interference

The RNA interference (RNAi) vector was prepared by amplifying different size fragments (450-500 nt) from the ORF of candidate genes. Amplified fragments were introduced into the p2T7-177 vector [185]. Primers for amplification of targets (**S2.1 Table**) were designed using RNAit software (<http://trypanofan.bioc.cam.ac.uk>), and primers were checked to confirm low-homology with other sequences in the *T. brucei* genome using BLAST. RNAi constructs were linearized by the NotI enzyme within a “targeting sequence” for integration of the plasmid into the genome using homologous recombination of the sequences on either side of the NotI site.

T. brucei 29-13 were used for transfection. This transgenic cell line co-expresses the Tetracycline repressor and T7 RNA polymerase (TetR-T7RNAP), along with neomycin and hygromycin resistance cassettes. Cells were grown in SDM79 media and 2×10^7 parasites used per transfection. Following centrifugation 2,000 x g for 7 min, cells were resuspended in cold Cytomix transfection buffer (120 mM KCl; 0.15 mM CaCl₂; 10 mM K₂HPO₄/KH₂PO₄, pH 7.6; 25 mM HEPES, pH 7.6; 2 mM EGTA, pH 7.6; 5 mM MgCl₂; pH adjusted with KOH). Ten µg linearized DNA were mixed with cells, and transferred to an electroporation cuvette to electroporate using the X100-free programme in a transfection device (Amaxa biotechnology-Nucleofector II). Cells were added to 10 ml SDM-79 with 10% fetal bovine serum (FBS) media (Gibco, Thermo Fisher Scientific, MA, USA), supplemented with 2.5 µg/ml G418, 5 µg/ml hygromycin after electroporation and grown at 28°C. The same procedures were applied for the control flask (but in the absence of any added DNA).

2.4.1 Selection and cloning

P2T7 plasmid [185], has a phleomycin resistance cassette for selection of transfectants. After adding 2.5 µg/ml phleomycin to the transfected flasks and DNA control flasks, cells were serially diluted in 24-well plates. The controls were usually dead after 4 days, and often visible growth appear in transfected cells at around day 8 post-transfection, which varies upon the essentiality level of each gene.

2.5 Induction of RNAi machinery and monitoring growth curves

To induce RNAi, cells were grown to a density of 2×10^6 cells/mL in SDM-79 with 10% FBS media supplemented with 2.5 µg/ml G418, 5 µg/ml hygromycin, 2.5 µg/ml phleomycin and grown at 28°C. For each gene, growth was measured for induced cells (1 mg/mL tetracycline) and uninduced cells, and cells were diluted to the seeding concentration at 2×10^6 cells/mL every 48 h. Cell growth was monitored up to 12 days for all genes and plotted for both uninduced and induced cells.

2.6 Quantitative Real-Time PCR

2.6.1 RNA isolation

Following RNAi induction and cell growth, RNA was collected from induced and uninduced samples for each gene. Days of RNA collection were selected based on the growth curve for each gene; RNA was collected from days without significant differences between Tet-induced and uninduced growth. Whole cell RNA was isolated using TRIzol (Invitrogen-Thermo Fisher Scientific, MA, USA) from almost 10^8 cells by centrifugation at 2,000 x g for 3 min at room temperature (RT). After phenol-chloroform extraction and isopropyl-alcohol precipitation, the RNA pellet was washed with 75% ethanol and air-dried. RNA was dissolved in nuclease-free

water, and the concentration was measured by a nanodrop device (spectrophotometer ND-100). The integrity of each RNA sample was examined by electrophoresis on a 1% agarose gel 100 V for 1h.

2.6.2 DNA removal and DNA preparation

A DNA-free[™] DNA Removal kit (Ambion- Thermo Fisher Scientific, CA, USA)) was used to eliminate genomic DNA from 10 µg total RNA by DNase I treatment. Following the treatment protocol and DNase I deactivation, RNA was precipitated with mg/ml glycogen, 0.1 volumes of 3M NaOAc, and 2.5 volumes of ethanol (100%). The RNA pellet was washed with 75% ethanol, air dried, and resuspended in 10 µl nuclease- free water. The integrity of the RNA was checked again at this step via 1% of agarose gel. Reverse transcription of RNA was done in 25 µl real time-polymerase chain reaction (RT-PCR) reactions, using TagMan reverse transcriptase and random hexamer primers using a TagMan Reverse Transcription Kit (Applied Biosystems- Fisher Scientific, CA, USA). The reaction was carried out in a thermocycler for one cycle at 25°C for 10 min, 42°C for 20 min, and 98°C for 5 min. Minus reverse transcriptase (RT) control samples were prepared at the same time without adding reverse transcriptase to reactions.

2.6.3 Quantitative Real-Time PCR reaction

RT-PCR reactions were carried out in two biological replicates and three technical replicates using SYBR® Green PCR Master Mix (Applied Biosystems- Fisher Scientific, CA, USA) in 25 µl reaction volumes including 12.5 µl 2x SYBER Green master mix, 10 µl 1.5 µM primer mix (forward and reverse primers), and 2.5 µl cDNA template. Primers targeted regions from pre-edited, edited, and never-edited mitochondrial transcripts as previously described [186, 187]. Gene-specific primers were designed to estimate the amount of down-regulation for each

gene (**S2.1 Table**). As an internal control, RT-PCR reactions using 18S rRNA and/or β -tubulin primers were performed, and to reassure RNA purity, the same RT-PCR experiments were done on RNA samples from reactions without reverse transcriptase. Each mRNA target was analyzed using a Rotorgene RG-3000 Real-Time PCR detection system (Corbett Research), under the following conditions: 50°C for 2 min, 95°C for 10 min, followed by 45 cycles at 98°C for 15 sec and 60°C for 1 min. Melting profiles with 0.2°C resolution were used to confirm the generation of the single amplicon, and many of the PCR products were examined using gel electrophoresis. Relative changes in RNA abundance were calculated using $\Delta\Delta C_t$ [188], and the level of each RNA was represented as the mean \pm SEM of six determinations. The arbitrary fold change (FC) cut-offs of >2 and significance p-value of <0.05 was considered for data analysis.

2.7 Generation of C-terminal Myc-tagged cell lines and western-blot analysis

Three genes were chosen for construction of 2xMyc-tagged cell lines. The ORFs of Tb927.1.1730, Tb927.10.1730, Tb927.10.7910 were taken from <http://tritrypdb.org>, (release 24.0) and primers were designed with the addition of either BamHI and HpaI sites (Tb927.1.1730) or BamHI and HindIII sites (Tb927.10.1730 and Tb927.10.7910) for complete ORF amplification (**S2.1 Table**). Amplified fragments were cloned into the pHD-1700 vector [189], and NotI linearized plasmids used for transfection of transgenic trypanosomes lister 427 strain expressing the Tet repressor from pHD1313 cassette integrated into tubulin locus using phleomycin resistance [190].

The day after transfection, 5 μ g/ml of hygromycin was added to the cells for selection of transfected cells and cells were serially diluted by transferring into a 24 well-plate. After obtaining stable clones, cells were grown to a density of 2×10^6 cells/mL in SDM-79 with 10%

FBS media with 5 µg/ml hygromycin and 2.5 µg/ml phleomycin at 28 °C. Tetracycline was added at 0.5 µg/ml to initiate Myc tag expression, and cells were collected after 48 h.

The total number of 10^7 cells were collected from Tet-induced and uninduced samples for each gene and analysed for Myc expression on 10% -12% SDS-polyacrylamide gels at 180 V for 1 h. Proteins were transferred onto nitrocellulose membranes and probed with a monoclonal antibody (1:2000) (Clontech Laboratories, CA, USA) as primary antibody and Goat-AntiMouse HRP Conjugate (1:5000) (Bio-Rad Laboratories, ON, CA) as secondary antibody. Clones having a considerable level of Myc expression in Tet-induced and not in uninduced samples were kept at -80°C for further use. For long-term preservation of c-Myc cell lines, 10^7 cells were spun at for 3 min at 2,000 x g, and the pellet was resuspended in freezing solution (15% glycerol, 20% FBS, 65% SDM-79). Cells were kept at 4°C for 1 h, transferred to -70°C for 2-3 days, and moved to -80°C for long-term storage.

2.8 Immunofluorescence assay

Cellular localization of Tb927.1.1730, Tb927.10.1730, and Tb927.10.7910 Myc-tagged cell lines were examined by Immunofluorescence assay (IFA). To localize the Myc-tagged proteins, parasites were grown to mid-log phase (2×10^7 cells/ml) in SDM-79 with 10% FBS media supplemented with 5 µg/ml hygromycin, 2.5 µg/ml phleomycin, and 0.5 µg/ml tetracycline (induced samples) or without tetracycline (uninduced samples) at 28°C for 48 h. A final concentration of 100 nM MitoTracker™ (Thermo Fisher Scientific, QC, CA) was added to cells to probe mitochondria. After 1 h of MitoTracker treatment, Tet-induced and -uninduced parasites were spun down and resuspended in fresh media. Meanwhile, round coverslips (Thermo Fisher scientific, QC, CAN) were placed into a 24 -well plate and 125 µl 0.01% Poly-L-lysine solution (Sigma-Aldrich, ON, CA) dropped on the top face of the coverslip and incubated

at RT for 1 h. For each slide, 7×10^6 cells were spun down at $1,500 \times g$ for 6 min at 4°C , and resuspended in 1 ml TDB buffer (pH 7.4), [20 mM Na_2HPO_4 , 2 mM Na_2HPO_4 , 5 mM KCl, 80 mM NaCl, 1 mM MgSO_4 , and 10 mM Glucose]. Following 1 h treatment, Poly-L-lysine solution was removed from the coverslips, and each slide was washed two times using 1 ml ddH₂O for 5 min on the shaker. Finally, 1 ml resuspended cells in TDB buffer were placed on each slide and kept at RT. After 1 h incubation, unbound cells were removed, and adherent cells were fixed using 1 ml 4% paraformaldehyde (pH 7.4), (Fisher Scientific, QC, CA) in PBS for 10 min at RT. Slides were washed twice with PBS for 5 min, followed by incubation in 1 ml of PBS overnight at 4°C .

The next day cells were permeabilized on coverslips by exposure to 1 ml 0.2% Triton X-100 for 15 min at RT. After two washes with PBS, coverslips were blocked with 3% BSA for 1 h and then washed with PBS for 5 min. Anti-Myc antibody (1:500) was prepared in PBS and added to coverslips (2 h at RT). After extensive washing with PBS, the secondary Goat Anti Mouse IgG (Alexa Flour®488 (Abcam, CA, USA) (1:500) was prepared in PBS and added to coverslips and incubated for 1 h at RT in the dark. Coverslips were washed four times with PBS before staining nucleic acids with DAPI (4',6-diamidino-2-phenylindole) (100 ng/ml), which strongly binds to A-T rich regions in DNA. After 10-15 min, the slides were washed three times with PBS. A mounting solution, Fluoromount-G® (Southern Biotech, AL, USA) was dropped on a microscope slide (Fisher Scientific, QC, CA), and each coverslip was carefully flipped with parasites down on the slide. After 24 h, slides were imaged in the dark using a Nikon Eclipse E800 upright widefield microscope.

2.9 Mitochondrial extract preparation of Myc-tagged proteins and IP

Mitochondrial extracts from $\sim 5 \times 10^7$ uninduced and Tet-induced (48 h post tetracycline induction) Tb927.1.1730, Tb927.10.1730, and Tb927.10.7910 Myc-tagged cell lines were prepared as described above. The lysis buffer was prepared either with 40 U RNaseOUT (Thermo Fisher Scientific, QC, CA) or 200 $\mu\text{g/ml}$ RNase A from bovine pancreas (Sigma-Aldrich, ON, CA). Anti c-agarose-conjugated beads (Sigma-Aldrich, ON, CA) were washed five times with 1 ml ice-cold PBS at 4°C and subsequently washed once with 1 ml ice-cold IP wash buffer [Tris-HCL, pH 8.0, 10 mM, NaCl 100 mM, NP-40 0.1%, 1X complete EDTA-free protease inhibitor (Roche Applied Science, ON, CA) and 1% BSA]. After the last wash, 50 μl beads were re-suspended for each reaction in 1 ml ice-cold wash buffer and incubated for 1 h at 4°C on a tube rotator. After adding the mitochondrial lysate to the beads, the mixture was rotated for 2 h at 4°C followed by centrifugation for 5 min at 4°C.

Following supernatant removal (unbound proteins), the beads were washed four times with 1 ml IP wash buffer and resuspended in SDS-PAGE loading dye [Tris-HCL, pH 6.8, 50 mM, SDS 2% (W/V), bromophenol blue 0.1% (W/V), glycerol 10%, β -mercapthanol 100 mM). Aliquots of lysate, bound and unbound fractions were loaded on 10% SDS-PAGE gel at 180 v for 1 h. Proteins were transferred onto a nitrocellulose membrane and probed with polyclonal antibodies against MRB 8170 [142], GAP1 [145], MRB 4160 [152], and TbRGG2 [150].

2.10 Guanylyl transferase assay

RNA was isolated from (-Tet) and (+Tet) PF Tb927.10.7910 RNAi cells 2 and 3 days post-Tet induction, and treated with DNase as described above. Eight μg of DNase- treated RNA were labeled with 10 μCi [α - ^{32}P] GTP (3000 Ci/mmol) using ScriptCap™ m7G Capping System kit (CELLSCRIPT™, WI, USA), according to the manufacturer's instructions. Reactions

were phenol: chloroform twice, chloroform extracted once and precipitated. Samples were mixed with 80% formamide loading buffer and resolved on 8% acrylamide-7 M urea gel in 1 X TBE.

2.11 Cloning of the full length Tb927.10.7910 and point mutations

The ORF of Tb927.10.7910 minus N-terminal mitochondrial import signal (the first eight amino acids, (MFSSVLLR), as predicted by Target IP4.1 server) [191] was cloned into the pET30-a vector between NdeI and XhoI restriction sites to generate an N-terminal 6x His-tagged protein. pET30-a/Tb927.10.7910 construct was used as the template to create nine individual alanine substitution point mutations. The point mutations were in the N-terminal of protein including Thr52A, Arg53A, Trp56A in $\alpha 3$ region, and Pro76A, Pro77A, Trp79A in the wing region ($\beta 2$ -strand-loop- $\beta 3$ -strand) and Pro164A, Phe167A, and Trp187A of the C-terminal domain. All mutants were prepared by GenScript Corporation (Piscataway, NJ).

2.12 Purification of the recombinant protein

The pET30-a expression vector was transformed into T7 Express *l*_{ysy}/*l*^q competent *E. coli* strain (New England Biolabs, CA, USA), which was grown into a density of 0.6 OD before induction with 0.5 mM of Isopropyl β -D-1-thiogalactopyranoside (IPTG). Bacterial culture was grown after induction either for 5 h at 30°C or for 8 h at 16°C, which was then collected by centrifugation at 8,000 x g for 15 min at 4°C. The cell pellet from 1L of an induced culture was resuspended in 50 ml of cold PBS (pH 7.2), 10% glycerol, and 1X protease inhibitor mixture (Roche Applied Science, ON, CA), and cells were lysed by sonication on ice for 5 min, followed by centrifugation at 16,000 x g for 15 min at 4°C. The cleared lysate was applied onto a column with 2 mL of IMAC Nickel charged resin (Bio-Rad Laboratories, ON, CA). Proteins were eluted using the increasing gradient of imidazole from 10 mM to 320 mM, prepared in cold PBS

containing 10% glycerol. Eluted fractions were dialyzed in two changes of buffer (PBS with 10% glycerol). The dialyzed recombinant proteins were applied into Amicon centrifugal filter device (Millipore) and concentrated to 1/5 of the starting volume.

The relative sizes of the recombinant proteins were examined by SDS-PAGE (Fig. 2.1) using anti-6x His tag antibody (Clontech Laboratories, CA, USA) and visualized by VersaDoc (Bio-Rad Laboratories, ON, CA) while the concentrations were measured using Quantity One software (Bio-Rad Laboratories).

2.13 *In vitro* transcription and radiolabeling of RNAs

Purified PCR fragments of gA6[14] Δ 16G were amplified from the previously described plasmid encoding gA6[14] Δ 16G, specifying the first ES of the ATPase subunit 6 (A6) pre-mRNA. Riboprobe® System-T7-promega kit was used for *in vitro* transcription of 2 μ g template DNA [192]. The CYb pre-mRNA (102 nt) [193] and CYb-edited mRNA were transcribed from BamHI linearized plasmid and synthetic DNA antisense template with a T7 promoter sequence, respectively using RiboMAX Express-T7-promega kit. Transcripts were either labeled with [α -³²P] UTP (Perkin Elmer, MA, USA) during transcription or were radiolabeled after transcription with [α -³²P] pCp at the 3' end using T4 RNA ligase (New England Biolabs, MA, USA).

Unlabeled RNAs used in competition assays were synthesized from DNA oligonucleotides, listed in **S2.1 Table**, in combination with a T7 promoter oligonucleotide. The 90-nt pBlueScript SK+ (Stratagene, CA, USA) RNA was generated by *in vitro* transcription of the NotI linearized plasmid. The pre-edited A6U5 transcription template was PCR amplified from the plasmid containing its sequence and was used in *in vitro* transcription of the A6U5 pre-mRNA. All RNAs were purified by electrophoresis through 9 % polyacrylamide/7 M urea gels.

2.14 Gel shift assays

The apparent equilibrium dissociation constant (K_d app) was initially calculated for each RNA substrate by performing electrophoretic mobility shift assays (EMSA) [194]. For estimating K_d , increasing concentrations of purified Tb927.10.7910 (wildtype and point mutations) were incubated with fixed concentrations of labeled RNA (gA6[14] Δ 16G substrate, CYb pre-, and edited mRNAs). For gel shift assays, labeled RNAs were heated at 75°C for 3 min followed by a slow cooling period, 1°C/min to 23°C, kept for 30 min at 23°C before transferring the RNAs to the ice. Binding reactions were carried out in RBB50 buffer (20 mM Tris-HCl at pH 7.6, 50 mM KCl, 5 mM MgCl₂, 100 mg/mL BSA, 10% glycerol, and 1 mM DTT), 100 mM KCl, and 20 units RNasin (Promega, CA, USA) in a 20 μ l volume for 30 min at RT. Samples were mixed with gel loading dye (0.25% bromophenol blue, 0.25% xylene cyanol, and 30% glycerol) before loading onto native 10% TBE gels that were pre-run at 110 V for 15 min in 0.5 X TBE at 4°C. After 2 h, gels were fixed in 10% isopropanol plus 7% acetic acid for 30 min and visualized by PhosphorImager (Bio-Rad Laboratories, ON, CA). Free and bound RNA were quantified using the Quantity One software (Bio-Rad Laboratories). The sum of the bound complexes in each lane was considered as the total bound fraction. The data were analyzed by nonlinear curve fitting methods using GraphPad Prism 7 (GraphPad Software, Inc.). The values of K_d app, and active protein concentration, B_{max} , were determined as best fits to the experimental data. The obtained K_d apps were used for calculation of the active protein concentration and the corrected equilibrium dissociation constant, using increasing concentrations of the labeled RNAs over the fixed concentration of protein (wildtype and point mutants proteins). The protein concentration was equivalent to approximate two times of estimated K_d apps.

Competition experiments were carried out as described above using a fixed amount of protein that resulted in approximately 30-50% bound RNA. A saturating concentration of the radiolabeled gA6[14] Δ 16G, CYb pre-mRNA, and CYb edited mRNA, and AU target substrate were used in the separate binding reaction to mix with 1-, 10-, 100-, and 1000-fold molar excess of unlabeled competitor RNA in the RBB50 binding buffer prior to addition of the protein. The percent of competition was estimated as the ratio of bound RNA in the presence of an unlabeled competitor over bound RNA without the competitor.

2.15 Database searches and sequence alignment

Tb927.10.7910 sequence was analyzed for the presence of the recognizable domains using the HHpred program [195], a sensitive software for prediction of the function, structure, and domain compositions of protein through identification of more remotely related proteins or protein families. HHpred predicted two Z-DNA binding domains (ZBD) at the N- and C-terminal regions of Tb927.10.7910. Amino acid sequence of the N-terminal region of Tb927.10.7910 and Z-alpha ($Z\alpha$) domain of adenosine deaminase acting on RNA1 ($Z\alpha$ ADAR1), DNA-dependent activator of interferon regulatory factors (DAI or ZBP1/ $Z\alpha$ DLM-1), virus E3L ($Z\alpha$ E3L), and protein kinases containing Z-domain ($Z\alpha$ PKZ) were aligned using Clustal Omega [196, 197]. The same alignment was done for the C-terminal region of Tb927.10.7910 and Z-beta ($Z\beta$) of $Z\beta$ ADAR1, $Z\beta$ DLM-1, $Z\beta$ PKZ domains.

Chapter III: Results.

3.1 Construction of co-fractionation networks

Possible physical associations among a set of pre-specified proteins in trypanosomatids have been widely investigated using conventional fractionation methods. Biochemical properties of protein complexes can be exploited during these fractionation procedures to separate protein groups. For example, in a GG, proteins are separated according to their density/shape characteristics, while overall protein charges are the determinant for the distribution of protein complexes in ion exchange chromatography (IEX) methods.

Mass spectrometry data for 133 fractions derived from two different biochemical fractionation methods, GG and IEX, on whole-cell, mitochondria, and cytosolic extractions of *T. brucei*, were used for generation of protein groups in four separate fractionation experiments [184]. After applying stringent filtration protocols and employing a computational pipeline, a *T. brucei* co-fractionation network (TbCF net) was created. Orthogonal resources, such as the Kyoto Encyclopedia of Genes and Genomes (KEGG) pathways, the Search Tool for the Retrieval of Interacting Genes/Proteins (STRING) database, and extensive literature searches, generated a high confidence subset of the co-fractionation network (TbCF_{HC} net).

Clustering of the TbCF_{HC} net led to the prediction of 128 protein complexes, many of which were significantly enriched for members of known complexes in *T. brucei*. TbCF_{HC} net predicted the association of 50 proteins within the RNA editing machinery (**S3.1 Table**). Many of these proteins are known subunits of different complexes involved in RNA editing, including 17 proteins of the RECC, 7 proteins of the TbRGG2 subcomplex, 7 members of the core MRB1 subcomplex, 3 proteins of the MRB1 complex, and 1 member of the KPAP1 complex.

Comparison of the fractionation patterns of these 50 proteins between mitochondrial-GG and mitochondrial-IEX experiments revealed that these proteins mainly co-sediment together in GG fractionation while dissociating into different clusters in IEX fractionation (**Fig. 3.1**). Due to technical differences between these two fractionation methods, distribution patterns of proteins confirmed the nature of the interactions for complexes involved in RNA editing. For example, members of the RECC remained clustered in both approaches, which supported the direct protein-protein interactions among RECC members.

However, physical associations among subunits of the MRB1 complex and MRB1 complex with RECC were distinguished by the formation of at least three separate clusters of MRB1 complex proteins. Transient and RNA-dependent interactions underlie the majority of contacts among subunits of the MRB1 and MRB1 complexes with RECC [17, 142]; therefore, increased salt concentrations used in IEX approach dissociate MRB1 complex interactions. These fractionation patterns confirmed previous reports of strong Y2H interactions of MRB8170 and MRB8620 [142], while suggesting an RNA-dependent interaction of MRB6070 and members of core MRB, including MRB3010 and MRB11870.

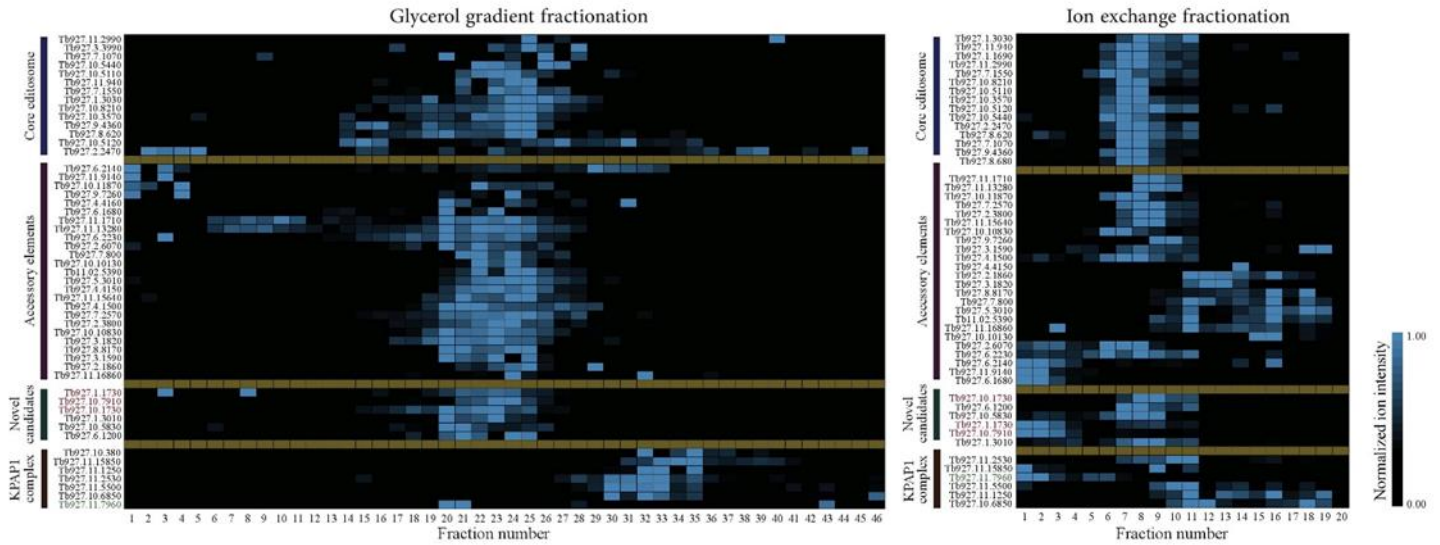


Figure 3.1. Comparison of the fractionation patterns for the proteins involved in the RNA editing between GG and IEX methods. Adopted from Gazestani, Nikpour, et al.; PLoS Neglected Tropical Diseases, 2016. Proteins are categorized in four groups of core editosome (RECC), accessory elements (MRB1 complex), novel proteins, and KPAP1 complex.

3.2 Identification of novel proteins associated with the RNA editing pathway

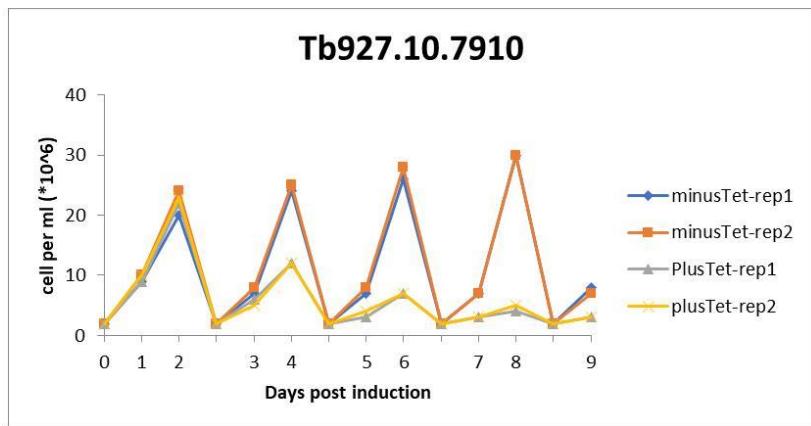
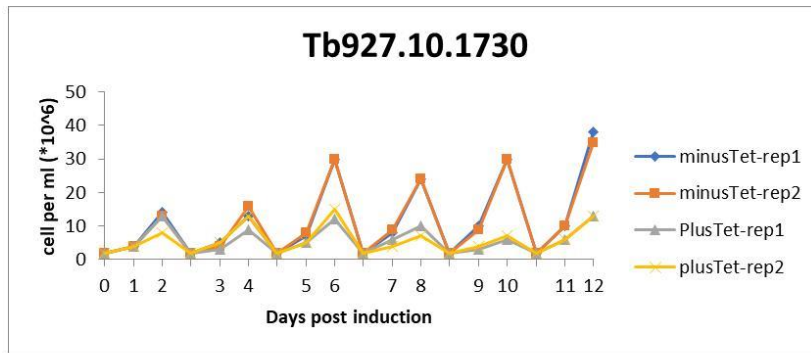
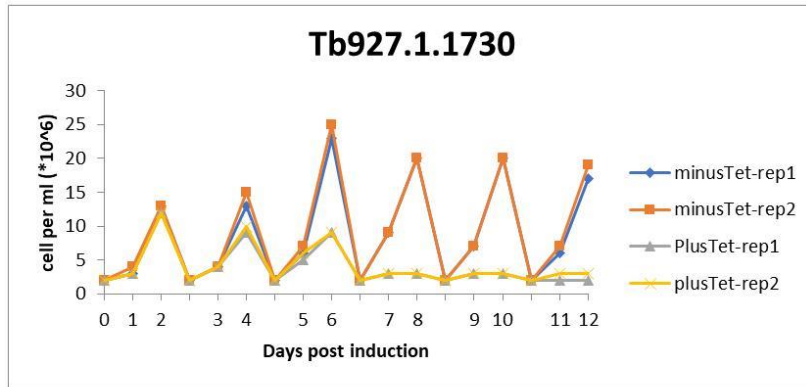
The TbCF_{HC} net also identified six new proteins (Tb927.1.3010, Tb927.10.7910, Tb927.1.1730, Tb927.10.5830, Tb927.6.1200, and Tb927.10.1730) that might be involved in the RNA editing process. The GG experiments showed the co-sedimentation of these proteins with MRB1 complex and RECC and separation from members of KPAP1 complex. Notably, IEX fractionation patterns showed that of Tb927.6.1200 and Tb927.10.1730 remarkably co-fractionated with some members of RECC and MRB1, but the co-elution of the other four

proteins were salt-sensitive to different extents, and Tb927.10.7910 was the most sensitive protein to the presence of salt.

We picked these proteins for further studies by considering that any potential factor(s), controlling PF-specific editing should be essential for parasite survival and the editing of transcripts that are preferentially edited at PF, such as CYb. Therefore, at the very first step of functional studies of candidates, we targeted their essentiality in PF in knock-down studies.

3.3 Down-regulation of gene expression by RNA interference

We used RNAi to check the importance of candidates for the PF stage. Growth rates were compared between plus Tet and minus Tet samples for each candidate up to 12 days post-induction, and RNA was extracted on day 3 post Tet induction to measure the relative expression of mitochondrial-encoded transcripts following RNAi of each gene. All candidates except Tb927.10.5830 were essential for the growth of parasite to variable extents (**Fig. 3.2**).



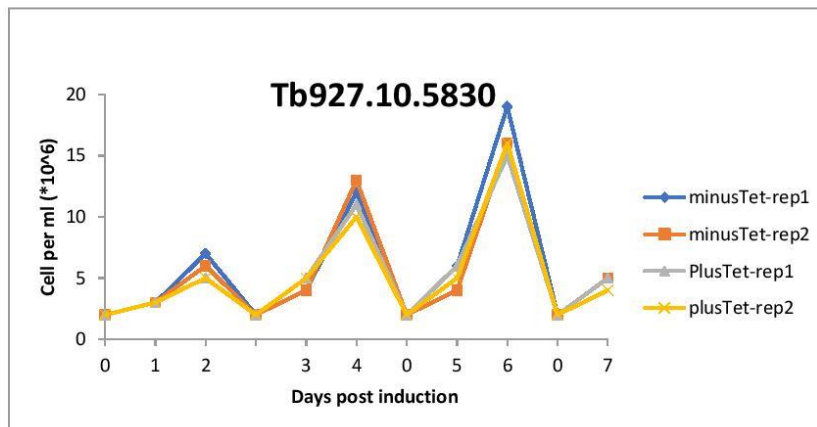
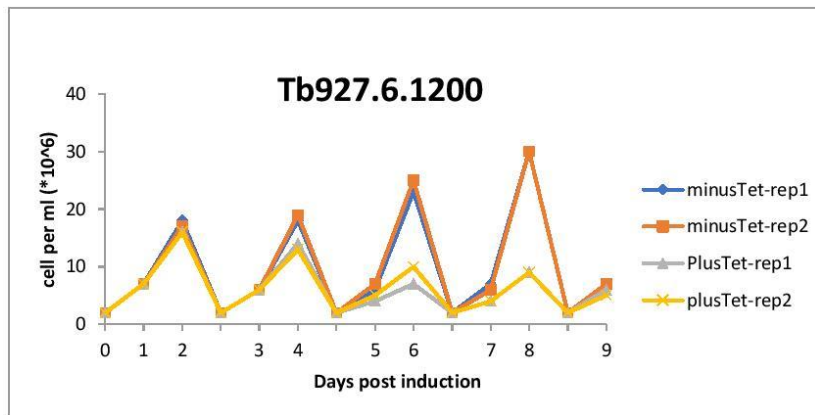
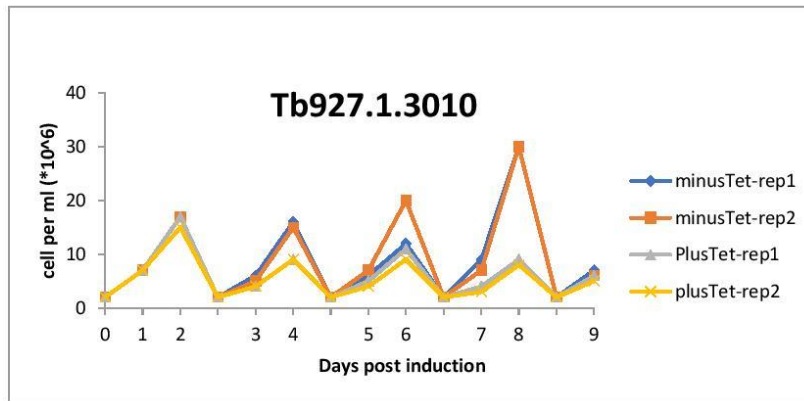


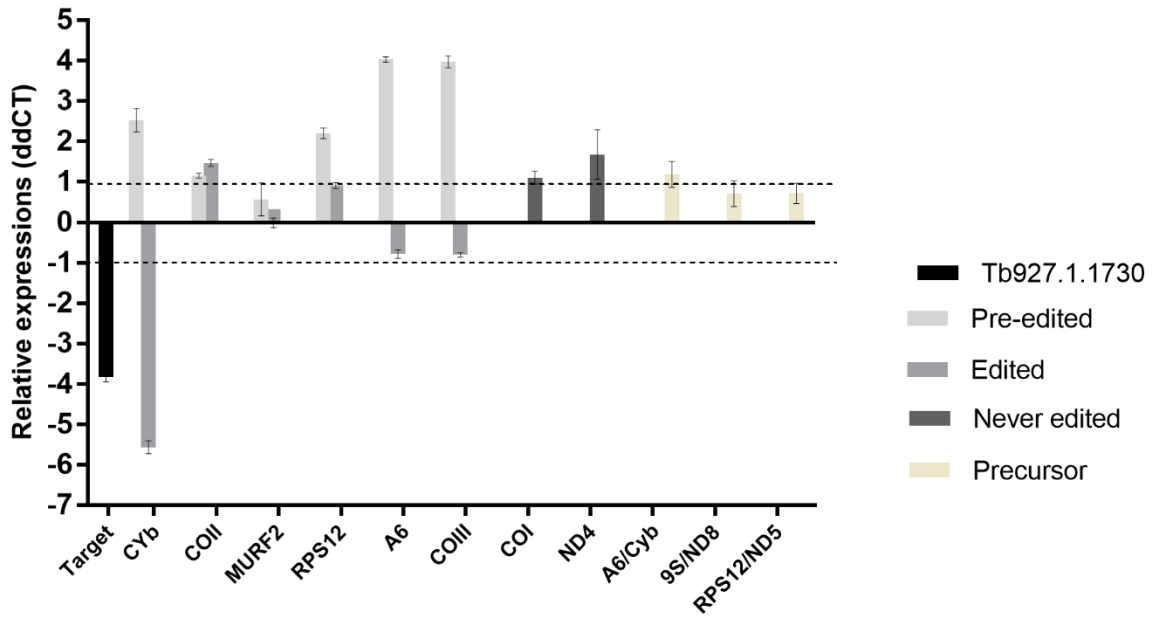
Figure 3.2. Growth curves for the candidate genes. Growth was measured in pf RNAi cell lines of the six candidate genes that were uninduced or induced with 1 $\mu\text{g/ml}$ tet. Cell growth was measured every 24

h and cells were diluted every 48 h to a starting concentration of 3×10^6 cells/ml. Two biological replicates of each candidate gene were used.

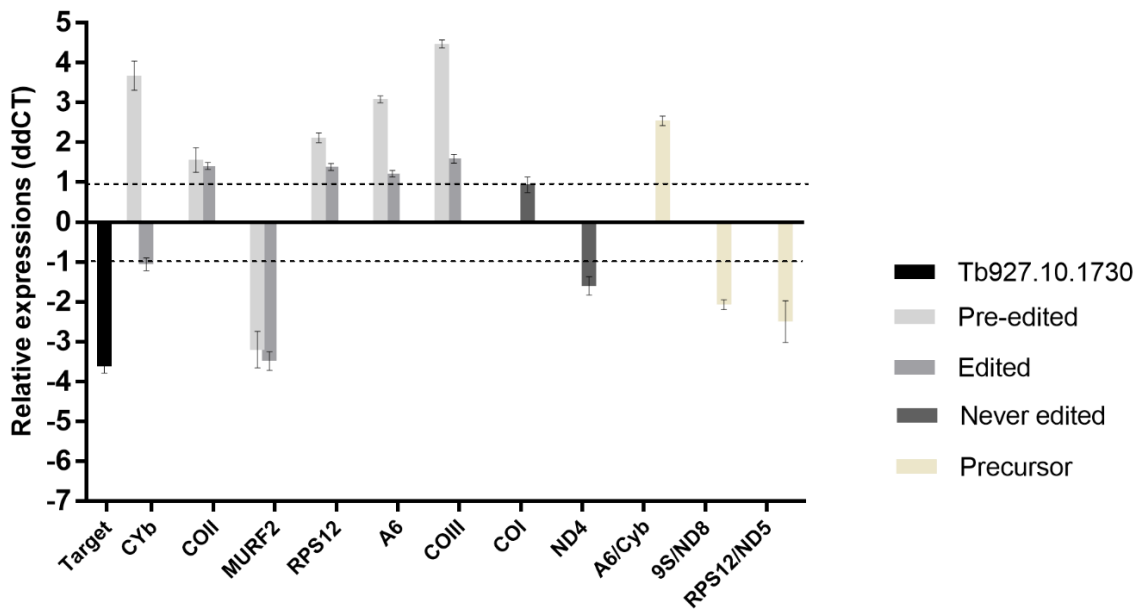
In the next step, we questioned if the editing process was affected following gene ablation. To do so, we performed qRT-PCR reactions using RNA samples from the previous step and primers amplifying pre-edited, edited and never-edited regions of *T. brucei* mitochondrial transcripts. The abundance of three mitochondrial precursor transcripts, A6/CYb, 9S/ND8, and RPS12/ND5, were also examined between induced and uninduced samples (**Fig. 3.3**). qRT-PCR results showed alterations in the mitochondrial mRNA expression patterns following the knock-down of Tb927.1.1730, Tb927.10.1730, Tb927.10.7910, Tb927.6.1200, and Tb927.1.3010. Changes in pan-edited, minimally-edited and never-edited mRNAs varied for each gene depletion.

CYb edited transcripts were decreased following Tb927.1.1730 knock-down, along with the accumulation of pre-edited mRNA. Editing processes of the pan-edited mRNAs A6, RPS12, and COIII were interrupted by the accumulation of the pre-edited transcripts.

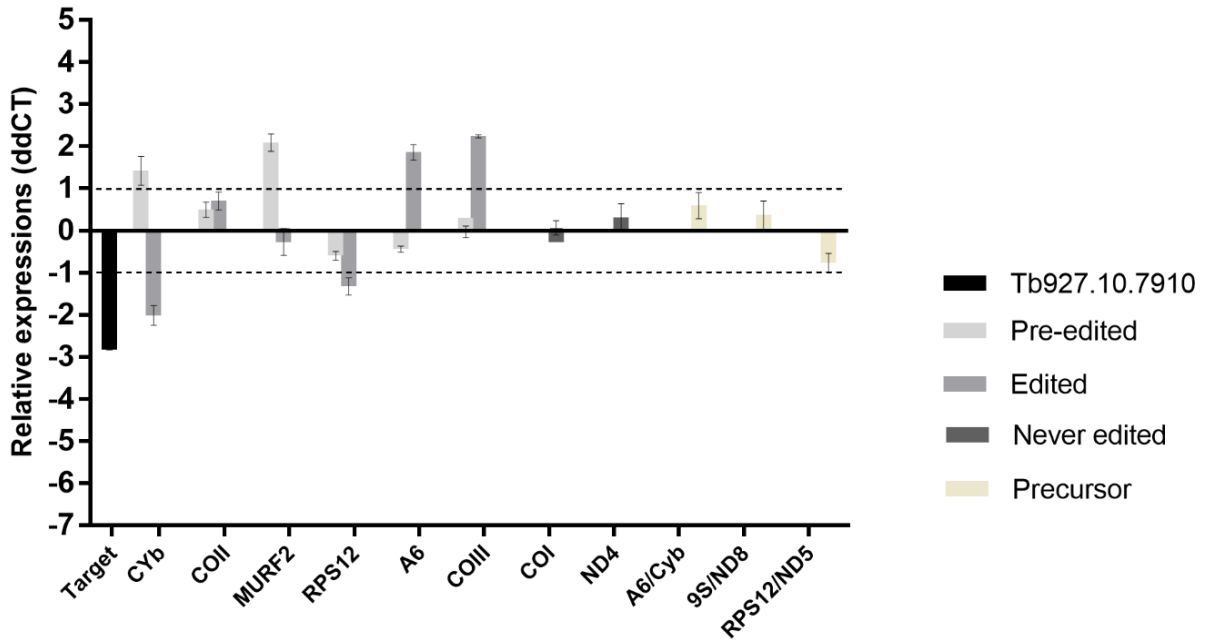
Tb927.1.1730



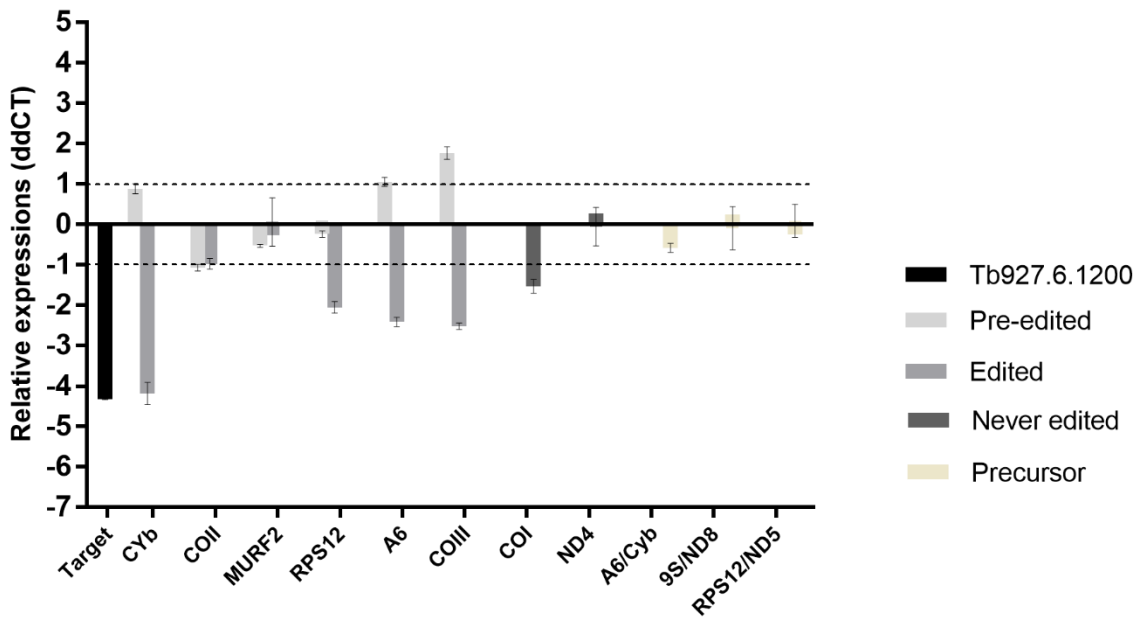
Tb927.10.1730



Tb927.10.7910



Tb927.6.1200



Tb927.1.3010

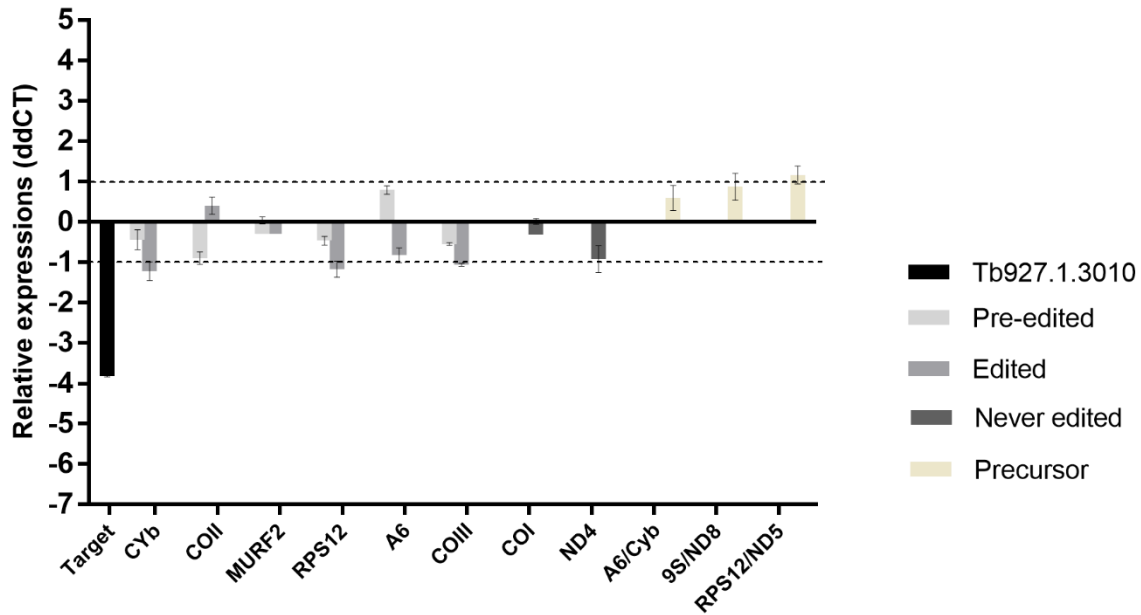


Figure 3.3. *Effect of depletion of five candidate genes on the abundance of mitochondrial RNAs.* qRT-PCR analysis of mitochondrial maxicircle transcripts from PF RNAi cells day 3 post Tet induction. The abundance of RNA in induced cells relative to uninduced cells is plotted. 18S rRNA was used for normalization, and the numbers represent the mean \pm SEM of at least six determinations. The dashed line at “1” reflects no change relative to RNAi induction.

Following Tb927.10.1730 knock down, pre-edited levels of CYb, COII, A6, COIII, and RPS12 increased along with COII, A6, COIII, and PRS12 edited mRNAs. Edited level of MURFII was significantly decreased and never-edited transcript level of ND4 was decreased. Two precursor transcripts, 9S/ND8 and RPS12/ND5, had reduced relative expressions, while the level for A6/Cyb, precursor was increased. Minimally-edited transcript, including the edited level of CYb was decreased along with the accumulation of pre-edited CYb, but only pre-edited MURFII was increased following Tb927.10.7910 knock down. It appears that this protein has a destabilizing effect on edited A6 and COIII, since edited versions of both transcripts were increased following Tb927.10.7910 repression.

Edited levels of CYb and pan-edited transcripts of A6, RPS12, and COIII decreased upon Tb927.6.1200 down-regulation, while only pre-edited COIII was slightly increased. Never-edited transcript, COI stability was decreased upon Tb927.6.1200 deletion. Down-regulation of Tb927.1.3010 had no effect on editing or processing of any transcript.

In conclusion, RNAi-silencing of four candidates caused editing defects to different degrees, but these were not restricted to the specific class of transcripts. Gene silencing effects on relative expression of precursor mRNAs and never-edited transcripts suggested the possible involvement of some genes in the RNA processing pathway prior to editing events, including cleavage of precursor transcripts to monocistronic units or stability of some never-edited transcripts. Our results were not conclusive enough to conclude that each gene function in the editing process. However, more elaborate assays *i.e.*; full gene PCRs and primer extension assays with primers targeting different regions of transcripts, or deep sequencing of different mRNA populations (pre-edited, edited, and partially-edited transcripts) from +Tet and -Tet samples, can be used to determine the mechanism of each encoded protein during RNA editing.

3.4 Mitochondrial localization of proteins and immunoprecipitation experiments

We confirmed the mitochondrial localization of Tb927.1.1730, Tb927.10.1730, Tb927.10.7910 in Myc-tagged cell lines using IFA (Fig. 3.4).

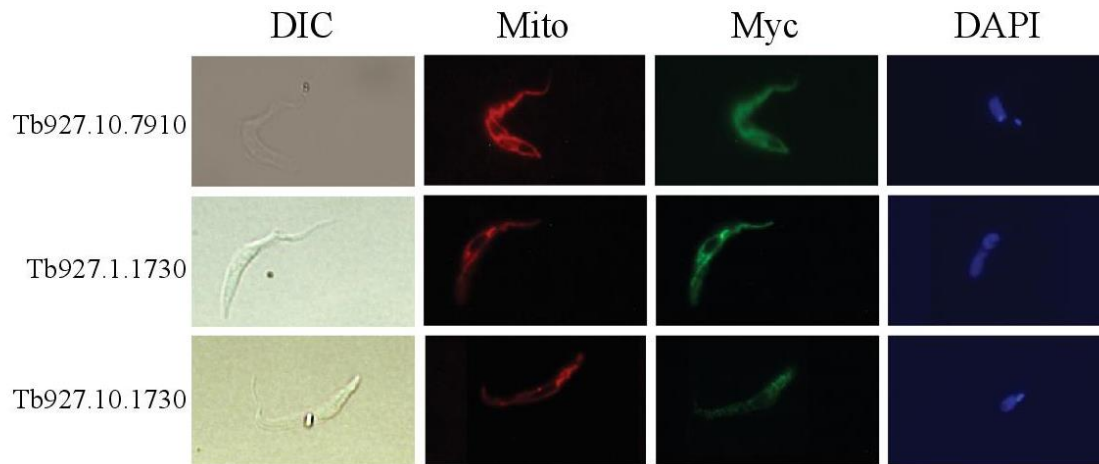


Figure 3.4. Subcellular localization of three candidate genes. Mitochondrial localization for C-terminal 2×mMyc –tagged Tb927.1.1730, Tb927.10.1730, and Tb927.10.7910 proteins. Anti-Myc antibody was used to detect tagged PF. Mitochondrial localization was observed for all three genes upon induction by tetracycline. Mitotracker was used to stain mitochondria and DAPI to stain nuclei.

To confirm interactions of candidate proteins with MRB1 and RECC based on GG and IEX fractionations and to determine if some of the interactions are RNA- dependent, we immunoprecipitated mitochondrial preparations of each protein using anti c-Myc beads and checked for the preserved interacting partners in the presence and absence of RNA (**Fig. 3.5**). Anti c-Myc antibody was used to detect Myc expression in c-Myc Tb927.1.1730, c-Myc Tb927.10.1730, and c-Myc Tb927.10.7910 cells, which shows as input in **Fig. 3.5**. Utilizing antibodies against some members of the core MRB1 (MRB 11870, GAP1, and GAP2) and the TbRGG2 subcomplex (MRB 4160, MRB8170, and TbRGG2) and western blot analysis, we showed MRB 8170 and TbRGG2 interactions with Tb927.1.1730, Tb927.10.1730, and Tb927.10.7910 proteins. Consistent with IEX fractionation patterns in **Figure 3.1**, the interaction of proteins with MRB8170 was largely RNA-mediated, and RNase treatment of inputs abolished the MRB 8170 interaction with all three proteins. Likewise, only Tb927.10.1730 remained bound to TbRGG2, and the other two proteins lost their interactions with TbRGG2 following RNase treatment. Tb927.1.1730, Tb927.10.1730, and Tb927.10.7910 interact with MRB8170 and TbRGG2 from TbRGG2 subcomplex in an RNA-dependent manner, while interaction with MRB8170 is RNA-dependent for all three proteins, only Tb927.1.1730, and Tb927.10.7910 interactions with TbRGG2 relies on RNA molecules.

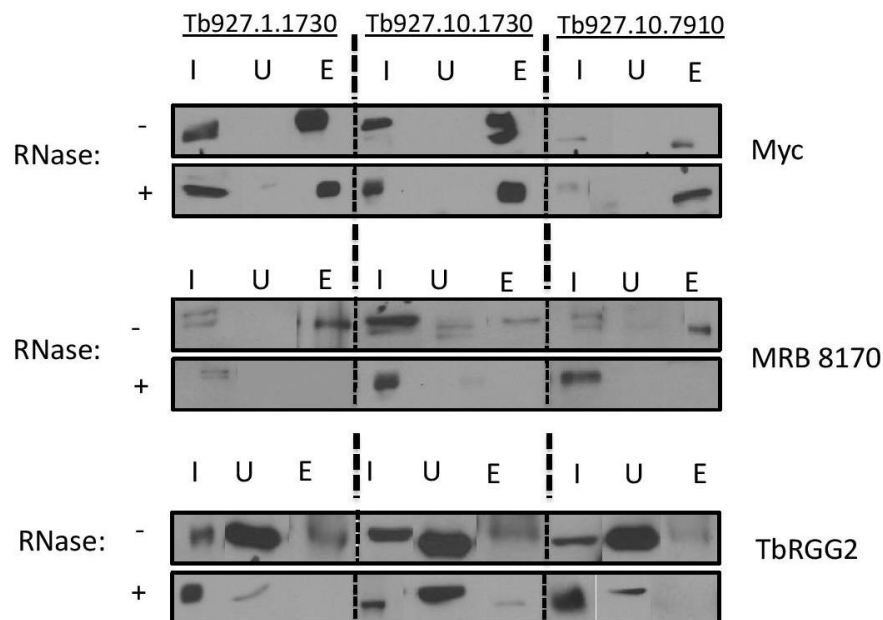


Figure 3.5. *Tb927.1.1730*, *Tb927.10.1730* and *Tb927.10.7910* proteins interact with *TbRGG2* subcomplex. Immunoprecipitation of c-Myc-*Tb927.1.1730*, c-Myc-*Tb927.10.1730*, and c-Myc-*Tb927.10.7910* from mitochondrial extracts was either not treated (-RNase), or treated (+RNase). Proteins from input (I), unbound (U), and eluate (E) were electrophoresed through 10% SDS-polyacrylamide gels and blots probed with antibodies against Myc-tag, MRB8170 and *TbRGG2*.

3.5 Identification of potential ZBDs in *Tb927.10.7910*

Sequence database searching of *Tb927.10.7910* for homology detection using HHpred predicted two potential ZBDs in the N- and C-terminal regions of *Tb927.10.7910*. Secondary structure prediction showed three-helix bundles and three β -sheets with an $\alpha\beta\alpha\alpha\beta$ topology for both domains (**Fig. 3.6**). Similar α/β HTH architecture consisting of three α -helices and three β -strands has been reported in proteins containing ZBDs (ZBPs) [198-200].

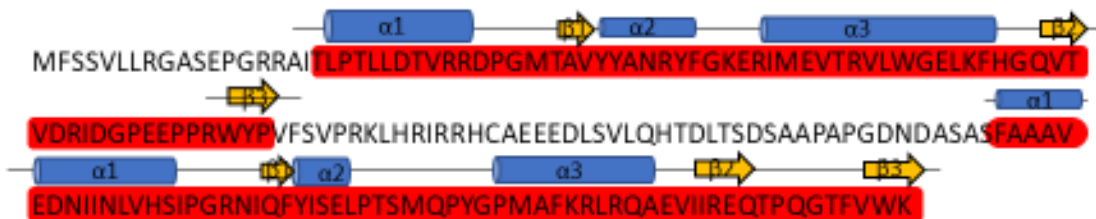


Figure 3.6. The protein sequence and domain structure of *Tb927.10.7910*. Sequence analysis of *Tb927.10.7910* identified two ZBDs, highlighted in red. The predicted secondary structure is indicated above the sequence. α -helices are represented by tubes and β -strands by bold arrows.

3.6 Tb927.10.7910 has a higher affinity for gRNAs than mRNAs

To assess the RNA-binding ability of predicted ZBDs of Tb927.10.7910, we determined the binding affinity of recombinant Tb927.10.7910 to radiolabeled gRNAs and pre-edited and edited mRNAs using EMSA. Different RNA substrates, including (gA6[14]) [42], A6U5 pre-mRNA [119], edited A6U5 (deletion of 3Us), CYb gRNA (gCYb [558] USD-2A-42nt) [201], natural CYb gRNA (gCYb [558]) [202], CYb pre-mRNA [203], and CYb edited-mRNA, were *in vitro* transcribed and labeled with [α -³²P] either during transcription or after transcription at the 3' end of the transcript. Despite detection of a significant protein-RNA complex between recombinant Tb927.10.7910 and gA6 [14], pre-and edited CYb mRNAs, we found no significant binding between the protein and A6 pre-mRNA or any CYb guide RNA variant (data not shown).

Incubation of a fixed amount of the protein with increasing concentrations of radiolabeled substrates (gA6[14] or pre-edited and edited CYb mRNAs) resulted in the formation of a slowly migrating protein-RNA complex (**Fig.3.7-A**). The K_d of the interaction of recombinant Tb927.10.7910 with each labeled RNA substrate was estimated from five individual experiments, and the results were analyzed by non-linear regression. As shown in **Fig. 3.7-A**, the K_d value for the wildtype (WT) protein interacting with the U-tail bearing A6 guide RNA substrate was determined to be 0.2194 ± 0.02 nM, showing a significantly higher affinity than CYb edited mRNA (1.57 ± 0.19) nM and pre-edited CYb mRNA (2.78 ± 0.37) nM substrates.

For further verification of these results, we carried out competition experiments using labeled gA6 [14] RNA, unlabeled CYb gRNA variants and CYb mRNAs as competitors. Natural guide CYb RNA with U-tail competed for binding between the protein and gA6[14] RNA 10 times better than 42-mer CYb gRNA without a U-tail (**Fig. 3.7-B**). The same concentration of

natural gCYb RNA and pre-CYb mRNA (10 times molar excess of unlabeled RNAs) reduced binding to the labeled RNA by 50%. However, edited CYb mRNA, containing almost double the number of Us compared to the pre-edited CYb RNA, competed for binding more efficiently by reducing 30% binding of labeled gA6 [14] RNA to the protein at 10 times molar excess of unlabeled edited CYb mRNA. To examine the specificity of binding for each substrate and define the role of structural features of gRNA in Tb927.10.7910-gA6[14] RNA interaction, we performed competition experiments, discussed in the next section. From here forward, we use the term, RBP7910 (RNA binding protein 7910) for the protein nomenclature.

Figure 3.7. Examination of the RNA-binding activity of Tb927.10.7910 using EMSA. (A) Gel mobility shift assays show the binding of a fixed concentration of the recombinant protein to increasing concentrations of different RNA substrates. The wedges show increasing concentrations of ³²P-labeled RNAs, and shifted bound protein-RNA complexes are marked by the black triangle. Bound and free RNA concentrations from panel A were used to estimate the binding affinity of Tb927.10.7910 for each RNA substrate (left panel). Saturation binding curves were obtained using non-linear regression from five individual experiments for each substrate. Calculated K_d ±SEM value in nanomolar is shown for each labeled RNA substrate. (B) Competition assays verified the higher affinity of the protein to gA6[14] compared to other guides and mRNAs. Competition assays were done by incubating a fixed concentration of purified protein and labeled gA6[14] in the absence and presence of increasing concentrations of unlabeled competitors (gCYb RNA variants, pre-edited, and edited CYb mRNAs). Asterisks indicate the input labeled RNA in the absence of the protein and white stars show the labeled RNA with protein in the absence of the competitor RNA. Numbers above the panels indicate the fold excess of the unlabeled RNA competitors and numbers below each panel are the percentage of shift in the presence of competitor RNAs normalized to the shift in the absence of a competitor (✦). The unlabeled RNA substrate used for each assay is indicated above each panel along with the complete sequence under each panel.

3.7 gRNA and mRNAs binding specificity of RBP7910

Gel shift assays were carried out to examine the specificity of binding of each substrate using radiolabeled substrates in the presence of increasing concentrations of unlabeled RNAs including gA6[14], pre- and edited CYb mRNAs. Unlabeled homologous RNAs effectively reduced the binding at the same molar ratios of labeled RNAs and eliminated the RBP7910-labeled RNA interactions at 10 times molar excess concentration of unlabeled RNAs (**Fig. 3.8-A**, left panel). Also, we examined the competitive binding using a heterologous 92nt pBlueScript RNA up to 1000-fold excess (**Fig. 3.8-A**, right panel), and observed its negligible competitive effect on the interaction of RBP7910 with CYb mRNA and A6gRNA.

Further, we checked the affinity of the protein to the poly (U)-tail of the guide by performing a competition assay using unlabeled gA6[14] RNA minus U-tail in competition with gA6[14] RNA (**Fig. 3.8-B**). While an equimolar ratio of unlabeled gA6[14] RNA with U-tail completely competed away the binding of labeled gA6 [14] RNA to the protein (**Fig. 3.8-A**), 100 times molar excess of the unlabeled gA6[14] RNA minus U-tail as a competitor reduced complex formation only by 25%. This result indicates the importance of the U-tail in the RBP7910-gRNA binding process. We confirmed this using unlabeled poly U as a competitor, which largely competed the bound complex at equimolar ratio of unlabeled poly U and labeled gA6[14] RNA.

To more investigate the contribution of stem-loop elements (secondary structure) and the U-tail in the RBP7910-gRNA interaction, we used a uridylylated non-guide RNA (49 nt) as the competitor (**Fig. 3.8-B**). This RNA has a shorter poly U-tail (15 nt) and only one stem-loop compared to gA6[14] RNA. The non-guide RNA competitor was more efficient in competing the RBP7910-gA6[14] complex than the gA6[14] RNA minus U-tail, but was still 10 times less

efficient than gA6[14] RNA competitor. This result implicates the indispensable roles for the oligo U-tail and the secondary structure of the gRNA in RBP7910-gRNA interaction, although again suggests the oligo U-tail as the main determinant.

In sight of the significant affinity of RBP7910 for gRNA, we asked if RBP79 possesses a general gRNA stabilizing activity during the RNA editing process, similar to other gRNA-binding proteins, such as GAP1 and GAP2 [141]. To determine the necessity of RBP7910 for the stability of the total gRNA population in cell, we examined the total gRNA population between Tet-induced and uninduced RBP7910 RNAi 2 and 3 days post-induction using guanylyl transferase labeling (**Fig 3.8-C**). No prominent changes were observed in the level of gRNAs between induced and uninduced samples. Therefore, the major gRNA-binding activity of RBP7910 is not related to the stability of gRNAs, and gRNA binding of the protein is primarily part of the general RNA recruitment activity of RBP7910 to the RNA editing machinery during RNA editing.

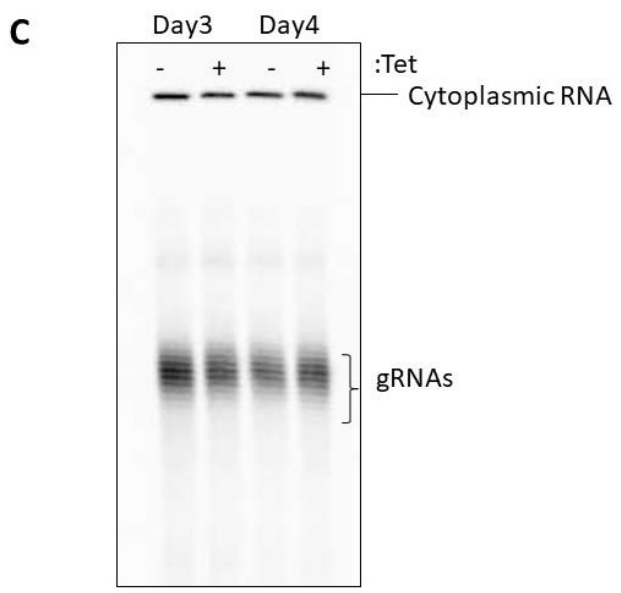
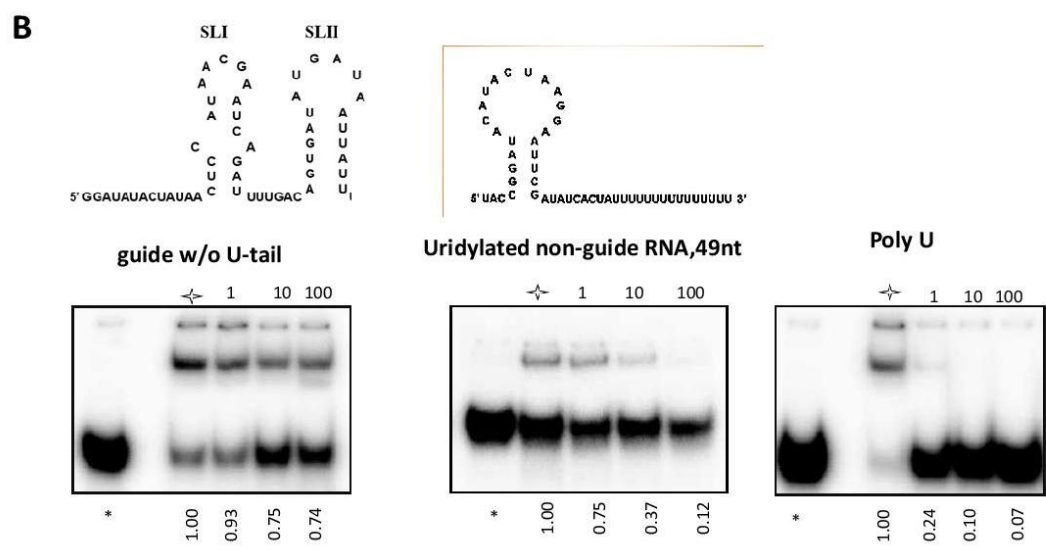
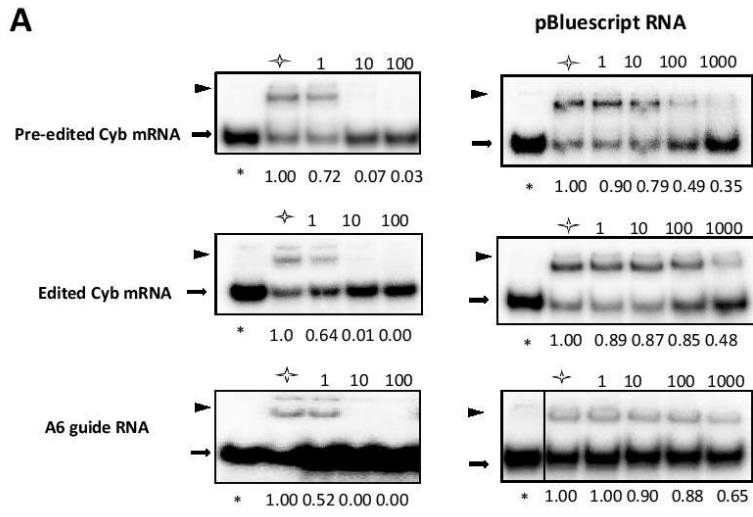


Figure 3.8. Competition assays to determine the binding specificity of RBP7910 for CYb pre-edited and edited RNAs and gA6[14] RNA. (A) RBP7910 protein was individually incubated with labeled pre-edited CYb, edited CYb, and gA6[14] RNAs in the absence and presence of increasing concentrations of each related unlabeled RNAs as a competitor. The asterisks indicate the input labeled RNA in the absence of the protein and the white star shows the labeled RNA with protein in the absence of the competitor RNA. Numbers above the panels indicate the fold excess of the unlabeled RNA competitors and numbers below each panel is the % shift in the presence of competitor RNAs normalized to the shift in the absence of a competitor (✧). Left panel, same as A; except that it uses a different competitor, pBlueScript RNA. (B) Competition assays to determine the role of gRNA oligo (U)-tail and stem-loop structure in gRNA binding. Three different competitors were examined to clarify the role of the oligo (U)-tail and the secondary structure of the gRNA in RBP7910 binding including gA6 RNA without the oligo (U)-tail, uridylated non-guide RNA with one predicted stem-loop and an oligo (U)-tail, and poly-U RNA. A fixed concentration of RBP7910 was incubated with labeled gA6[14] in the absence and presence of increasing concentrations of unlabeled competitors. Asterisks indicate the input labeled RNA in the absence of the protein and white stars show the labeled RNA with protein in the absence of the competitor RNA. Numbers above the panels indicate the fold excess of the unlabeled RNA competitors and numbers below each panel is the % shift in the presence of competitor RNAs normalized to the shift in the absence of a competitor (✧). (C) The effect of RBP7910 RNAi silencing on gRNAs. RNAs from Tet-induced and uninduced RBP7910 RNAi 2d and 3d post-induction were capped with [α - 32 P] GTP by the recombinant guanylyltransferase enzyme. The population of small gRNA molecules was resolved as a ladder of bands on a denaturing 8% acrylamide/7 M urea gel (bottom panel). A cytosolic RNA (top panel) is simultaneously labeled by this reaction and is shown as a loading control.

3.8 RBP7910 shows a distinct affinity for the AU sequence

Mitochondrial mRNAs and gRNAs are AU-rich transcripts with multiple biological functions. Brown and colleagues [204] showed that AU elements function in the pre-edited CYb mRNA as the primary assembly point of the editosome machinery. Following binding of gRNA to the pre-edited CYb mRNA, editing factors are transferred to the AU elements of gRNA. Similarly, another study showed the importance of the AU sequence for formation of the pre-edited/gRNA duplex by using A to C point mutations within the gRNA-binding site, which interfered with the formation of the pre-edited/gRNA duplex [205] and caused of 80% less editing.

Another AU structure of mitochondrial transcripts is the long AU-tail, a post-editing AU extension of the primary short A-tail of pre-edited transcripts. The long AU-tail is a hallmark of the translation process of fully-edited transcripts [31]. In addition to the general factors involved in the synthesis of the long AU-tail, like RET1, KPAP1, and KPAF1, other RBPs can selectively affect stability of AU-tailed mitochondrial mRNAs and activate their translation at the PF life stage [206].

By considering the RNA-binding activity of RBP7910, we next questioned the potential AU sequence-binding affinity of RBP7910. To do so, we labeled a known poly AU motif, a binding target of RBP6 in *T. brucei* [207]. Incubation of increasing concentrations of RBP7910 with a fixed amount of labeled poly AU RNA led to the formation of RNA-protein complexes. The specificity of the protein-RNA interaction was confirmed by a competition assay using unlabeled RNA as a competitor (**Fig.3.9-A**).

Considering the importance of the AU sequence during the editing process and duplex formation of gRNA/pre-edited mRNA [204, 205], we assayed the interaction of RBP7910 with a

modified poly AU sequence containing U to C substitutions. The competition ability of this U to C substituted poly AU RNA was largely abolished compared to the poly AU substrate (**Fig. 3.9-B**).

To determine whether RBP7910 prefers a poly AU or poly U substrate RNA, we tested the competitive abilities of poly U, poly A and poly G RNA on the interaction between RBP7910 and poly AU. The poly U RNA was the most competitive, as it limited complex formation by 50% at an equimolar concentration, while poly A and poly G RNA were similar to the U to C substituted poly AU RNA as seen above.

These results together implicate the ability of RBP7910 to bind to AU-containing RNAs. However, we cannot conclude whether RBP7910 binds to the internal AU sequence of the mitochondrial substrates (gRNAs and mRNAs) or the poly AU-tail of mitochondrial transcripts. Although we have shown the binding ability of RBP7910 to AU sequence, we cannot conclude if this interaction is purely sequence specific or mediated via secondary structures of the sequence. Considering the binding preference of RBP7910 to poly AU sequence, it is likely that the protein is involved in the RNA editing process or in the translation of AU-tailed mRNAs.

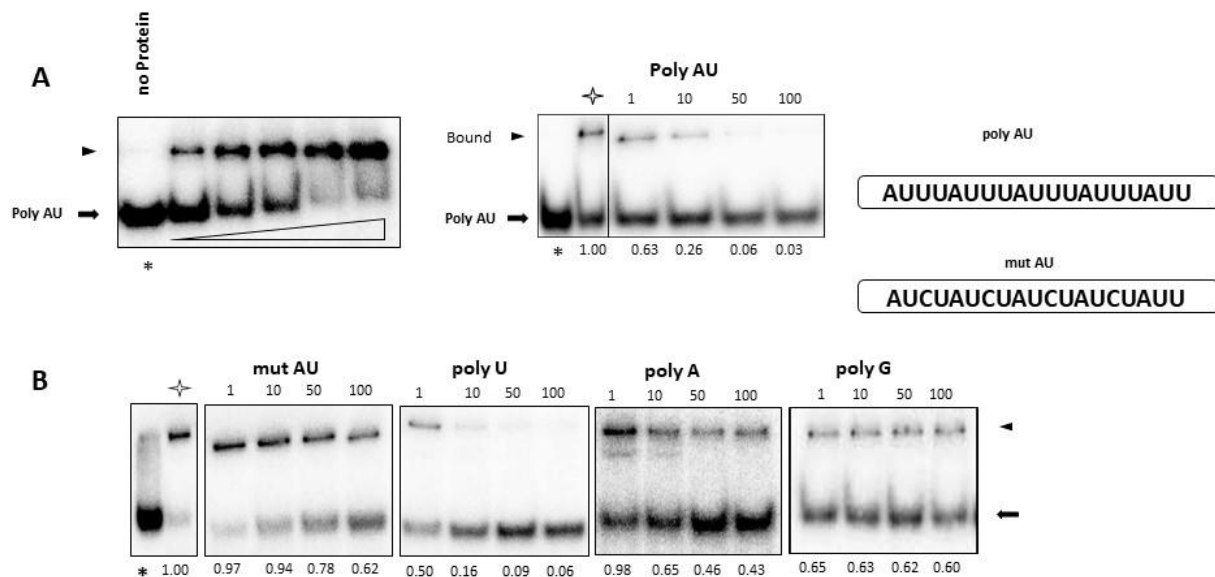


Figure 3.9. Competition assays to determine the affinity binding and specificity of RBP7910 to the labeled poly AU sequence. (A) Titration of RBP7910 protein over the fixed concentration of labeled poly AU RNA. The first lane is the labeled poly AU in the absence of the protein. The protein-RNA bound complexes are shown by a black triangle. Middle panel, RBP7910 RNA binding specificity was checked using unlabeled homologous poly AU competitor in a competition assay. A fixed concentration of RBP7910 was incubated with labeled poly AU in the absence and presence of increasing concentrations of unlabeled competitor. Asterisks indicate the input labeled RNA in the absence of the protein and the white star shows the labeled RNA with protein in the absence of the competitor RNA. Numbers above the panels indicate the fold excess of the unlabeled RNA competitor and numbers below each panel is the % shift in the presence of competitor RNA which normalized to the shift in the absence of a competitor (✧) (B), same as A; except than using different competitors. Competitor RNAs mentioned above each panel.

3.9 Sequence alignment of the predicted ZBDs of RBP7910 with the corresponding $Z\alpha$ and $Z\beta$ domains of ZBPs

Following the experimental establishment of the RNA-binding activity of RBP7910, we were interested in characterizing its mode of function based on sequence and structural alignments. Structural prediction and sequence analysis of RBP7910 identified two potential ZBDs within the N- and C-terminals of RBP7910. The ZBD family belongs to the superclass of WHTH domains, which is largely present in the DNA-binding domain of prokaryotic transcription factors and some eukaryotic transcription factors [208]. This domain specifically recognizes the Z-form of DNA/RNA molecules in a conformation-specific manner. Given that RBP7910 and ZBPs have a similar fold, we examined whether they also share the same nucleotide-binding interface. Multiple sequence alignment of the N- and C-terminal RBP7910 with the $Z\alpha$ and $Z\beta$ of ZBPs, respectively, is shown in **Figure 3.10**

A



B

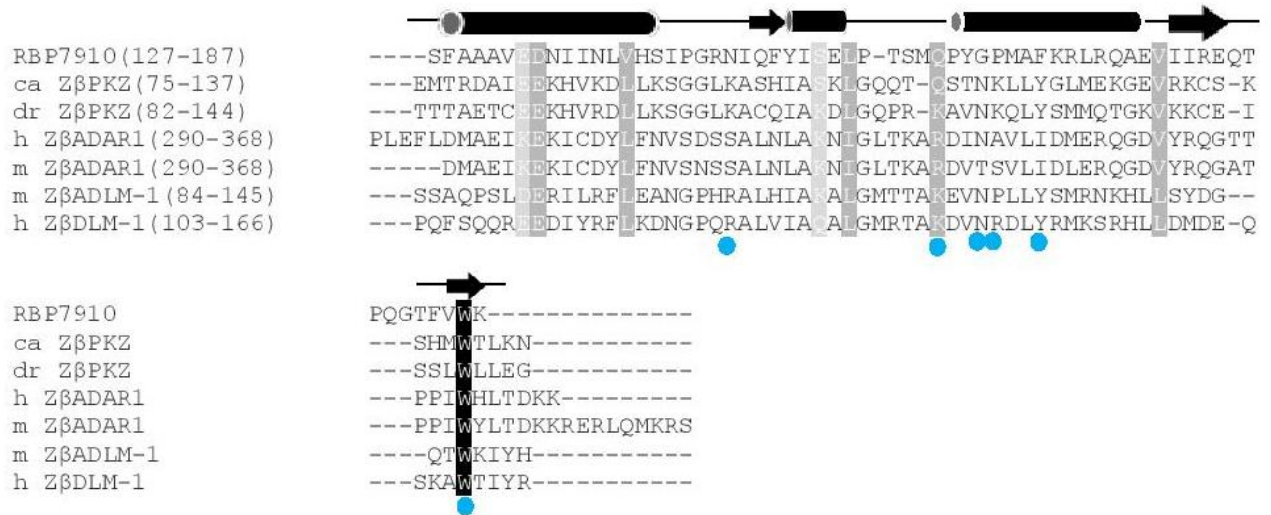


Figure 3.10. Multiple amino acid sequence alignment of predicted N- and C-terminal ZBDs of RBP7910 with $Z\alpha$ and $Z\beta$ domains of ZBPs, respectively. (A) Sequence conservation of the N-terminal ZBD of RBP7910 with $Z\alpha$ of other ZBPs and (B) sequence conservation of the C-terminal ZBD of RBP7910 with $Z\beta$ of other ZBPs. Predicted secondary structure of ZBD is indicated above the sequence of the first and second Z-domains of RBP7910. The α -helices are represented by tubes and β -strands by bold arrows. hZ α ADAR1 and hZ β DLM-1-DNA interactions are marked with green and blue circles, respectively. Shading from black to white corresponds to the degree of the amino acid conservation. Black shaded residues represent a high level of conservation. Numbers in parentheses correspond to the domain boundaries within the respective protein sequence. The sequences are as follows: RBP7910 and for $Z\alpha$ s; DLM-1 from *Homo sapiens* in hZ α DLM-1 and *Mus musculus*, mZ α DLM-1; E3L from orf virus in orfZ α E3L and yabZ α E3L from Yaba-like disease virus; PKZ from goldfish, caZ α PKZ and drZ α PKZ in zebrafish; ADAR1 from *Mus musculus*, mZ α ADAR1, and hZ α ADAR1 in *Homo sapiens*. $Z\beta$ s include goldfish PKZ, caZ β PKZ and zebrafish PKZ, drZ β PKZ; ADAR1 in hZ β ADAR1 from *Homo sapiens* and *Mus musculus*, mZ β ADAR1; DLM-1 in *Mus musculus*, mZ β DLM-1, and hZ β DLM-1 from *Homo sapiens*.

Four families of proteins with one or two tandem ZBDs have been identified: ADAR1, DLM-1 or ZBP1, protein kinase from fish containing ZBD (PKZ) and viral protein E3L [199, 209-211]. ADAR1, DLM-1, and PKZ proteins contain two ZBDs ($Z\alpha$ and $Z\beta$, respectively). E3L only harbours one $Z\alpha$ domain. $Z\alpha$ and $Z\beta$ are structurally homologous domains with a similar arrangement of α helices and β sheets ($\alpha\beta\alpha\beta\beta$), other than the presence of one extra helix ($\alpha4$) in $Z\beta$ ADAR1, which is mostly involved in dimerization of the protein [198]. The crystallography data of ZBPs showed the residues from $\alpha3$ and the $\beta2/\beta3$ wing region as the Z-DNA/RNA binding interfaces [199, 212, 213]. Nucleic acid interfaces in $Z\alpha$ and $Z\beta$ are marked by green and blue circles in **Figure 3.10**, respectively. As it appears in this figure, residues from these regions are highly conserved, especially within the $Z\alpha$ domain of ZBPs. Further, these data also demonstrated the interactions of $Z\alpha$ - and $Z\beta$ with the backbone of Z-DNA to be mediated similarly, via hydrogen bonding, and van der Waals forces (**Fig. 3.11**).

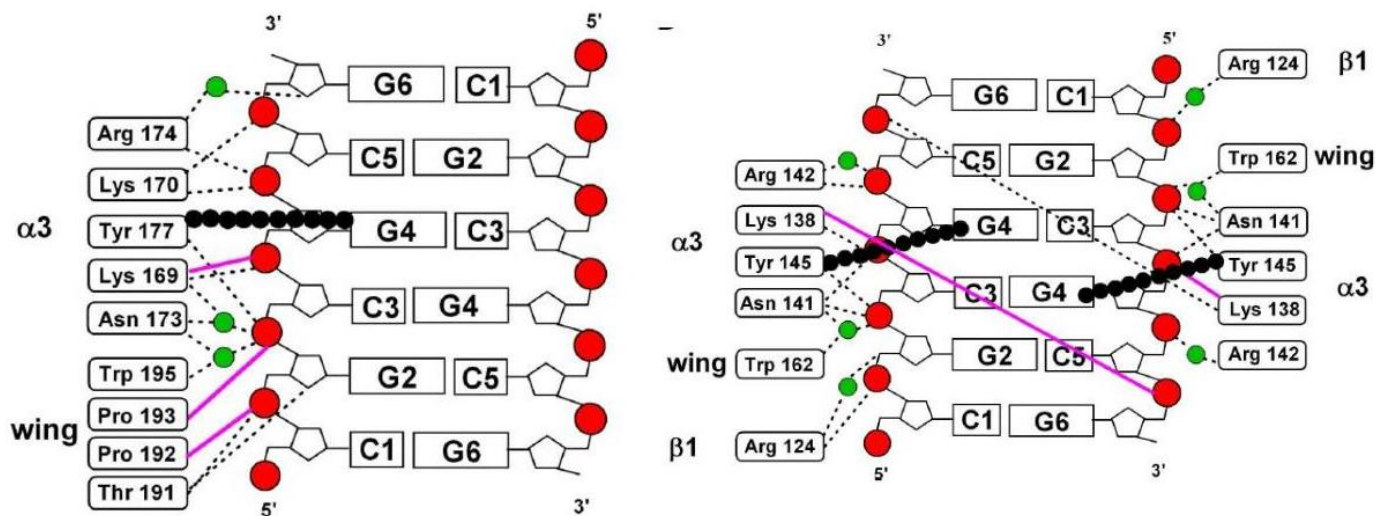


Figure 3.11. Comparison of the protein-DNA interaction in *hZαADAR1* (left) and *hZαDLM-1* (right).

Ha *et al.*, 2008. “Copyright (2008) National Academy of Science”. Hydrogen bonds and van der Waals forces are represented by dashed black lines and pink lines, respectively. The CH- π interaction between the conserved Tyr and the C8 of a *syn*-guanine is indicated by black circles, and water molecules are shown by green circles. The protein-DNA interactions in *hZαADAR1* are identical on both sides of the Z-DNA, thus only one side is shown.

3.10 Functional analysis of RBP7910 RNA-binding activity using structure-based mutagenesis

The RNA-binding function of RBP7910 was probed by replacing the potential RNA-contact residues in the N- and C-terminal domains of RBP7910 with alanine amino acid. Sequence comparison of different ZBPs suggested a presence of a common nucleic acid recognition core, containing hydrophobic and positively charged amino acids in the $\alpha 3$ core and the $\beta 2/\beta 3$ wing [214]. As shown in the **Figure 3.10**, Asn173, Tyr177, and Trp195 of h α ADAR1 are the most conserved core residues in ZBPs [200, 215]. These residues are also conserved in the h β DLM-1/Z-DNA complex [214], although with a different way of hydrogen bonding. Furthermore, ZBPs have one or two proline (P192-P193 of h α ADAR1) residues that contribute to Z α DNA-binding via hydrophobic interactions. These proline residues are usually located adjacent to polar residue such as Thr or Asn, which mediate DNA interactions through water-mediated hydrogen bonds [199, 200, 216]. There is no equivalent residue for Pro or Thr residues of Z α in Z β domains.

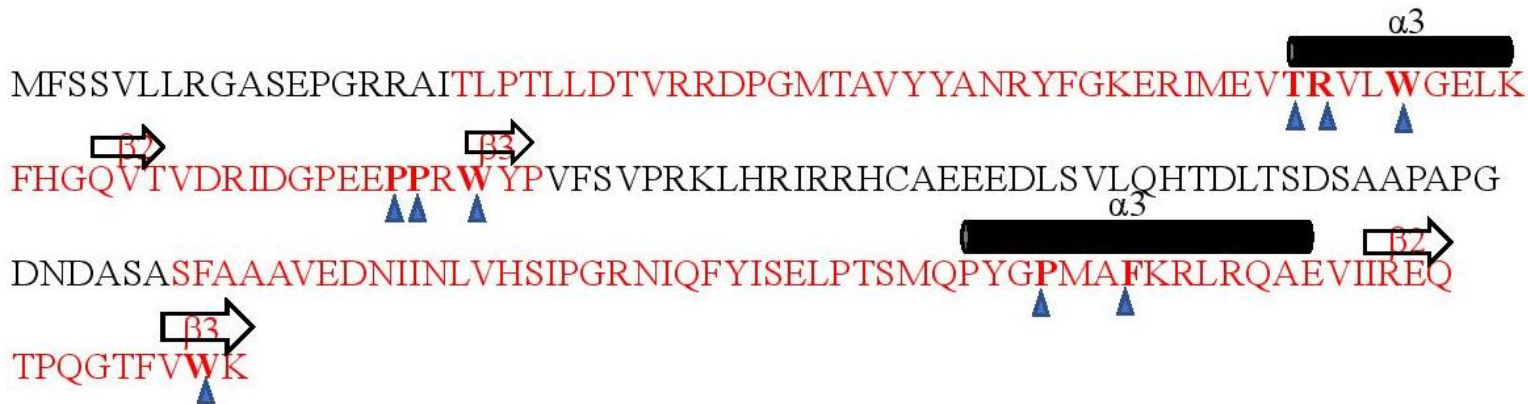
A few mutagenesis studies investigated the Z-DNA/RNA-binding activity of ZBPs. For instance, alanine substitution point mutation of Asn173 and Tyr 177 in h α ADAR1 [215, 217] or corresponding residues in mZ α DLM-1 and mZ β DLM-1 [218], eliminated the DNA-binding ability of each domain without altering protein stability.

The N-terminal domain of RBP7910 showed a high level of conservation for residues in the nucleic acid recognition core of Z α ZBPs (**Fig. 3.10**). While the Thr52 and Trp56 replaced the Asn173 and Tyr177 from h α ADAR1 of the third predicted helix, Arg53, Pro76, Pro77, and Trp79 amino acids are still conserved in the predicted Z α RBP7910 domain. Different amino acids from the N- and C-terminal domains of RBP7910 were selected for mutagenesis studies on

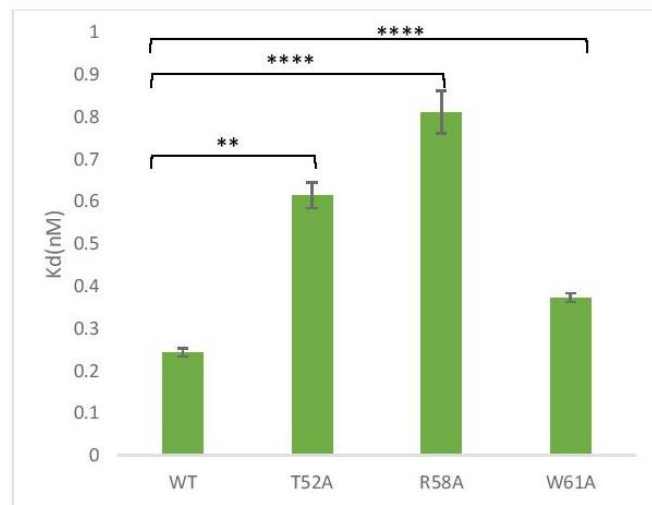
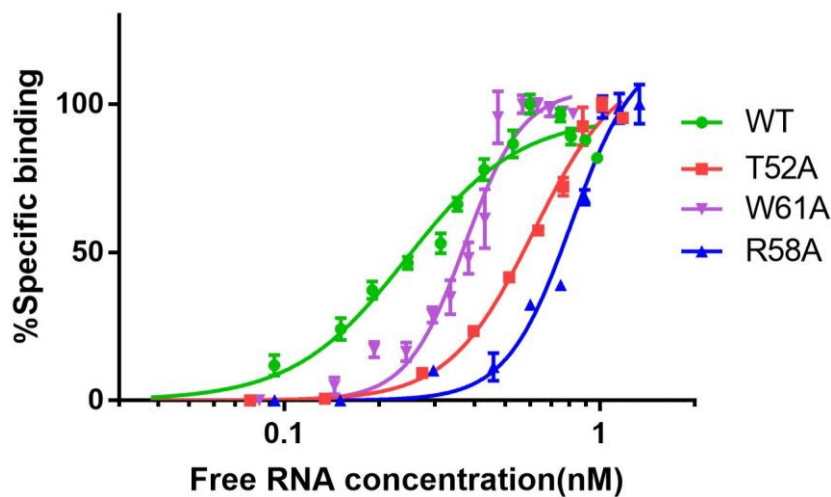
the basis of: (1) conservation of amino acids located in the recognition core of ZBPs; (2) previously reported point mutations affecting nucleic acid-binding activity of ZBPs; and (3) avoiding the previously reported residues that are crucial for the integrity of proteins.

The gel retardation assay was employed to assess the effects of each point mutation on the RNA-binding activity of RBP7910 by using ^{32}P -labeled gA6 RNA. Selected amino acids in the N-terminal domain and the third helix ($\alpha 3$) of RBP7910 were Thr52, Arg53, Trp56 and Pro76, Pro77, Trp79 from the $\beta 2/\beta 3$ wing. Because of the less conservation of Z β domain of ZBPs, we only chose Pro164, Phe167, Trp187 from the Z β recognition core for the mutagenesis analysis of the second predicted ZBD of RBP7910.

RBP7910 point mutations affected the RNA-binding affinity of the protein to varying levels. Of these, T52A, R53A, and W56A mutants demonstrated a less binding affinity for the A6 gRNA compared to the WT, by showing the K_d values of 0.6147 ± 0.03 nM, 0.8112 ± 0.05 nM, and 0.3734 ± 0.01 nM, respectively (**Fig. 3.12-A**). Mutants P76A from the $\beta 2/\beta 3$ wing region of RBP7910 differentially influenced the Z α -binding activity of RBP7910 compared to P192A of hZ α ADAR1 mutants [215]. Previous mutagenesis studies showed the negative effect of P192A on the DNA-binding activity of hZ α ADAR1, while P67A with a K_d value of 0.1827 ± 0.03 nM showed 1.2 times better binding affinity than WT RBP7910 (**Fig. 3.12-B**). However, similar to P193A, P77A with the K_d of 0.3005 ± 0.03 nM exhibited 1.3 times less affinity than WT RBP7910. As expected from the central Z-DNA binding role of conserved tryptophan in the $\beta 3$ of other ZBPs, W79A mutant showed the K_d of 0.3205 ± 0.05 nM, which had 1.5 times less affinity to the WT protein.

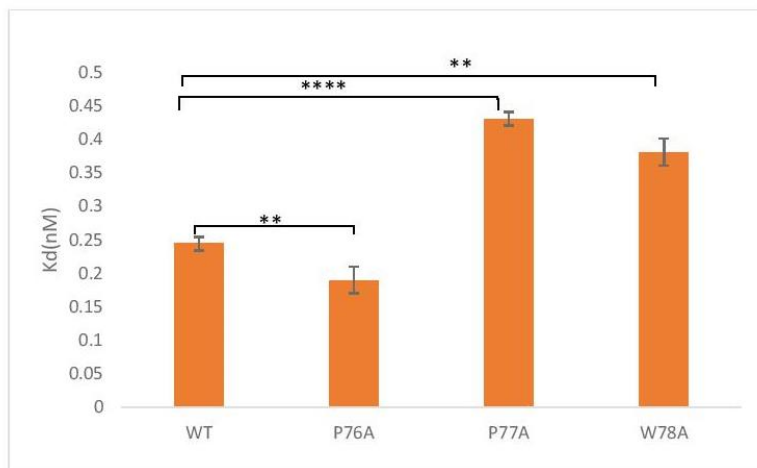
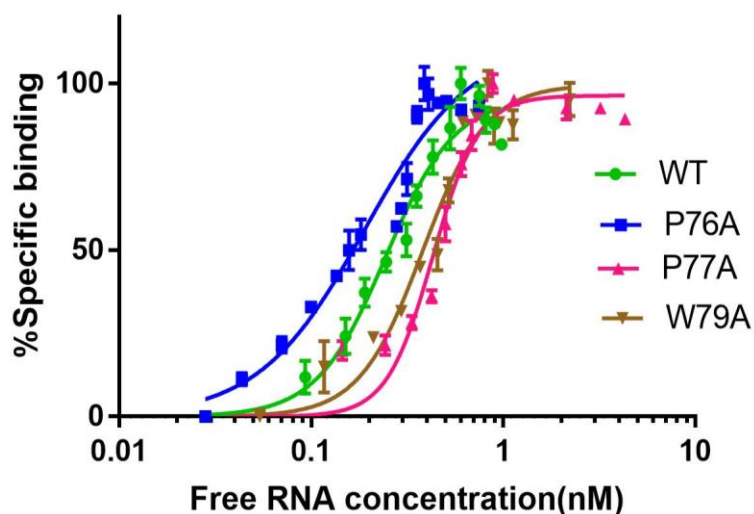


A



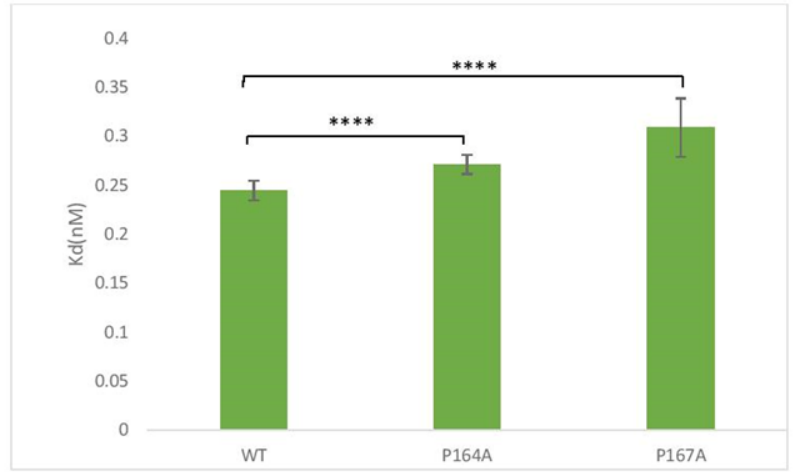
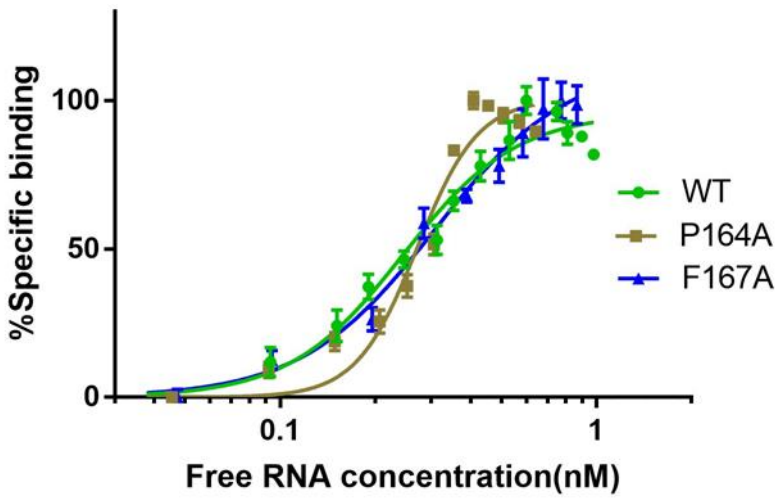
(**P=0.0040, ****P<.0.0001)

B



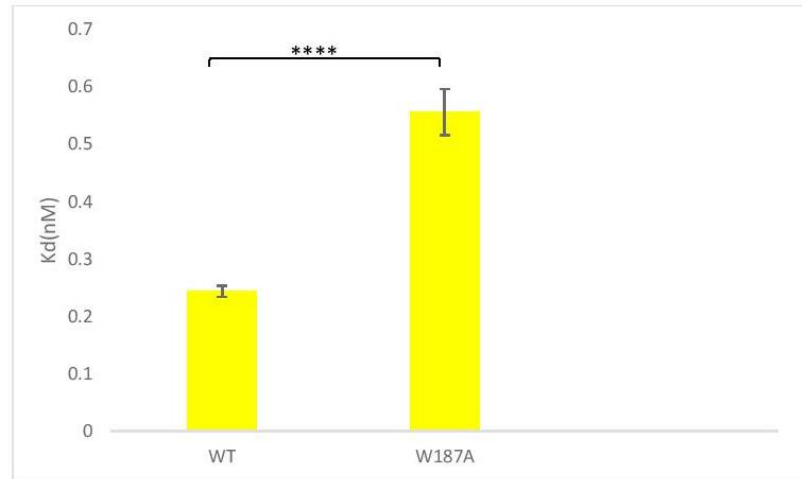
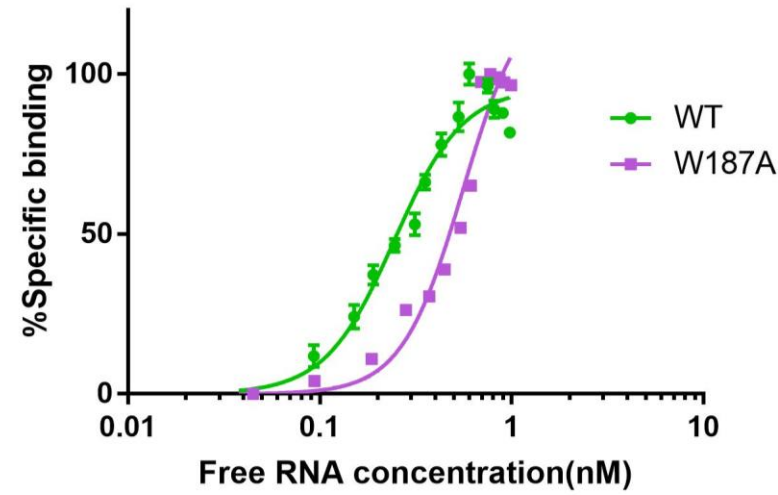
(**P=0.0081, ****P<.0.0001, **P=0.0016)

C



(****P<0.0001)

D



(****P<0.0001)

Figure 3.12. gA6[14] RNA-binding activities of RBP7910 point mutations measured by gel shift mobility analysis. The complete amino acid sequence of RBP7910 is shown with the predicted N- and C-terminal ZBDs in red. The α -helices and β -strands of the predicted RNA recognition core in ZBDs are represented by tubes and by bold arrows, respectively. The point mutations used in this study are marked by blue triangles. (A) Binding activities of point mutations selected from the α 3 and (B) wing region of the predicted Z α RBP7910, and (C) the α 3 and (D) wing region of the predicted Z β RBP7910. Binding activities of mutants from each region were quantified using a nonlinear curve fitting method, as it was done previously for the WT RBP7910. K_d values of each point mutation were calculated and compared to the K_d of WT RBP7910. Data are presented as mean \pm SEM unpaired *t*-test.

The core residues of Z β DLM-1 include N141, Y145, and W162 (**Fig. 3.11**), mediating the interaction in hZ β DLM-1/Z-DNA complex [214]. In addition to these residues, R142 of hZ β DLM-1 seems to play a similar role to R174 of hZ α ADAR1 in Z-DNA recognition. K_d values for P164A, F167A, and W187A mutants from RBP7910 were 0.2712 \pm 0.01 nM, 0.3078 \pm 0.03 nM, and 0.5561 \pm 0.04 nM, respectively, showing 1.2, 1.5, and 2.9 times lower RNA affinity compared to WT RBP7910 (**Fig. 3.12-C, 3.12-D**). Overall, these data support a mode of interaction similar to that of ZBPs, mediated by residues located in the predicted recognition core of RBP7910.

Chapter IV: Discussion.

We systematically studied protein complexes in *T. brucei* to assign hypothetical proteins to the mitochondrial RNA editing process. We combined two complementary biochemical fractionation approaches, GG and IEX, to examine co-fractionation networks of complexes involved in mitochondrial RNA metabolism. Sedimentation patterns of these complexes predicted the physical interaction of some hypothetical and experimentally unannotated proteins with MRB1 and RECC protein complexes. Five of six candidate proteins were essential for growth, and four were needed for proper RNA editing in the parasite PF life stage. Silencing of these proteins had a large effect on various categories of mitochondrial transcripts, raising the question whether these proteins exert their effects on the editing process directly by affecting the activity and integrity of the RECC, or these proteins are needed for proper initiation and/or progression of editing as member of the MRB1 complex.

It should be noted that interactions in the RECC are all protein-protein mediated, and MRB1 is the key factor for RECC RNA recruitment [17, 142]. Interestingly, technical differences between GG and IEX fractionations resulted in clustering of protein groups depending upon the nature of the interaction. RNA-mediated interactions among MRB1 subunits or MRB1 and RECC were captured differently in IEX compared to GG fractionation by the formation of at least three separate groups of the MRB1 complex (**Fig. 3.1**). Also, we confirmed RNA-dependant interactions of three candidate proteins (Tb927.1.1730, Tb927.10.1730 and RBP7910) with members of the TbRGG2 subcomplex. The RNA binding protein TbRGG2 has RNA annealing activity and is essential for the editing of pan-edited transcripts [33]. MRB8170, another component of TbRGG2 subcomplex, is also an RNA-binding protein, functioning by impacting the editing process of pan-edited (A6), minimally-edited (MURF2), and stability of

pre-edited Cox III and ND7 transcripts [152]. Therefore, the TbRGG2 subcomplex has a role in editing by providing proper gRNA/mRNA interactions [34]. RNA-dependent interactions of Tb927.1.1730, Tb927.10.1730, and RBP7910 with the TbRGG2 subcomplex indicate the potential RNA-binding activity for these proteins. However, the question of how these proteins affect different stages of editing or how their effects are coordinated are still unanswered.

Recently, another group reported a new complex called PAMC, which includes four of our candidate proteins (Tb927.1.3010, Tb927.1.1730, Tb927.6.1200, and Tb927.10.1730) [17]. In this study, protein-mediated interactions of PAMC and core MRB1 were shown using pull-down experiments, although non-of the PAMC components had been identified in association with MRB1 before to this study. While this complex does not strongly contact with the KPAP1 complex, GG fractionation patterns also showed separation of these proteins from KPAP1. Ablation of Tb927.1.1730 (PAMC1) suggests a role for this protein in post-transcriptional modification of mitochondrial transcripts by adding long AU-tail to the transcripts since the post-editing AU-tail addition was effectively abolished in PAMC1-deleted cells [17].

This part of our research provides a significant tool for studying protein complexes involved in mitochondrial RNA metabolism of *T. brucei* by integrating results from two different fractionation approaches and refining the interactome by using the results from other experiments (AP or IP). This approach helped remove false positive results from both resources and improve the accuracy of predictions. Multiple groups have tried to identify components of the MRB1 complex by performing LC-MS/MS analysis of different purifications of tagged-MRB1 subunits, which resulted in overlapping and distinct components, making the exact composition of MRB1 unclear [17, 141, 182]. Mass spectrometry-based experiments have limitations in recovering low-abundant proteins, including many regulators, as they become

masked by high-abundant proteins. This issue was partially overcome in the present study by analyzing proteins purified from a mitochondrial preparation, thereby eliminating potential contaminants from the cytosol and other organelles. Moreover, different fractionation methods of the mitochondrial preparation were performed to identify stably interacting proteins that cofractionate together. This proteome study can be used as a useful resource for interpretation of functional studies of proteins that comprise the RNA editing process.

The RNA-mediated interactions of RBP7910 with some members of TbRGG2 subcomplex in IP and IEX fractionation [184] implicated a potential RNA-binding role for this protein in the RNA editing process. The amino acid sequence examination using the HHpred tool revealed two ZBDs with the HTH secondary structure in the sequence of RBP7910. ZBDs recognize the Z-configuration of DNA and RNA molecules by the interaction of ZBDs with the phosphate groups of the nucleic acid backbone in a conformation-specific manner. We probed the *in vitro* RNA-binding activity of the protein using different mitochondrial RNA species; the stem-loop featured gRNAs, pre-edited and edited mRNAs. The result demonstrated a higher affinity of the protein for the gRNA than for the pre-edited and edited mRNAs.

The RNA-binding phenotype of RBP7910 is reminiscent the gRNA binding ability of GAP1/2 [141] by having a better gRNA binding affinity compared to mRNAs, while other RBPs in MRB1 complex, like MRB8170/MRB4160 or TbRGG2 show a higher binding affinity for mRNAs than gRNAs [150, 152]. GAP1/2 in MRB1 core complex stabilizes the gRNAs, and GAP1/2 depleted cells held the lower levels of gRNAs. Capping the total gRNAs from Tet-induced and uninduced RNAi-RBP7910 cells using guanylyl transferase enzyme rejected the possibility of RBP7910 involvement in the stability process of gRNAs during RNA editing in cells, since the levels of gRNAs remained unaffected following RBP7910 knock down.

Although, we cannot rule out a transcript-specific gRNA stability effect of RBP7910 without testing the stabilizing effect of RBP7910 on individual gRNAs.

RBP7910 binding assays pointed out that beside the 3'oligo (U)-tail, the secondary structure of gRNA is also important for the gRNA-binding activity of RBP7910. The secondary structure conformation of purine-pyrimidine repeats in DNA/RNA strands is the main factor in the recognition of these molecules by ZBPs [219]. In contrast to the mitochondrial mRNA, the secondary structure of gRNA is known to have two stem-loop elements and both 5' and 3' ends in a single-stranded conformation [220, 221]. By considering the importance of the secondary structure in the gRNA-binding of RBP7910 and the AU sequence binding activity of this protein, we suggest a crucial role for the secondary structure of the AU-rich sequences in the RBP7910 RNA-binding activity. It will be of interest in the future to determine the secondary structure of gRNA at the binding sites of RBP7910 and whether RBP7910 can stimulate and stabilize a favourable-binding conformation in the gRNA upon recognition of substrate by the protein.

A kinetoplastid ribosomal PPR protein, KRPPR1 RNA-binding protein is essential for the stability of the mitochondrial transcript and their translation in a stage-specific manner [206, 222]. Recognition and/or stabilization of a structural feature within the long AU-tail of the transcripts by KRPPR1 is suggested as a potential mode of action of this protein. Similarly, RBP7910 might stabilize the transcript by recognizing a specific secondary structure of AU sequence in the 3' long AU-tail. To test this hypothesis, the first step would be to investigate the stabilizing effect of RBP7910 on the long AU-tail of transcripts, and if RBP7910 deletion causes any degradation of the AU-tail of any specific transcripts.

Without having a detailed picture, which can define the interaction of RBP7910 in MRB1 complex, any speculations on the role of RBP7910 in the assembly and function of the

MRB1 complex is hindered. Currently, the RBP7910 interaction map in the RNA-editing machinery is not clear. Either direct protein-protein and /or RNA-mediated interactions of MRB7910 with other members of this complex needs to be investigated. Nevertheless, GG and IEX fractionation experiments by our group identified RBP7910 as a protein associated with RECC and MRB1 complex [184]. In addition, another study detected RBP7910 through comprehensive pull-down experiments of the several individual members of the MRB1 complex [17], while the RNA molecule mainly enforced interactions. We partly verified the interactions of RBP7910 in the MRB1 complex by showing the RNA-mediated interactions with the TbRGG2 subcomplex using the IP assay. However, we could not directly identify the interacting partner of RBP7910, since several attempts of protein purification using different protein tagging approaches were failed (data not shown).

Furthermore, RNA-mediated interactions of RBP7910 with the TbRGG2 subcomplex along with its *in vitro* RNA-binding ability implies a role for RBP7910 in the editing process, mostly by recruiting the RNA substrates to the RECC. Silencing of RBP7910 compromised the editing of the minimally-edited CYb transcript, by showing the accumulation of pre-edited mRNA and slight reduction of edited mRNA. Meanwhile, deletion of RBP7910 had a reverse effect on the edited levels of pan-edited COIII and A6 transcripts by increasing the edited transcripts [184]. In contrast to the effects of RBP7910 on the pan-edited transcripts, RNAi of MRB1 proteins have a general downregulation effect on the pan-edited transcripts. For example, the members of the TbRGG2 subcomplex are crucial for the progression of the editing, and deletion of these proteins results in the significant reduction of all pan-edited transcripts [140]. However, similar to RBP7910, there are other RNA-binding proteins, including MRP1/2 [223] and KRPPR1[206] that destabilized the edited level of a few pan-edited mRNAs, such as ND7,

and COIII. These results suggest RBP7910 as an RNA editing factor, which differentially affects the editing of mitochondrial transcripts. Further work is required to clarify the biological role of the RNA-binding function of RBP7910 in the editing process and to characterize its role on stabilizing the CYb edited transcript.

Following the prediction of ZBDs for RBP7910 and showing the RNA binding activity of the protein, we initially determined the percentage identities among the $Z\alpha$ of different ZBPs and then the predicted $Z\alpha$ RBP7910 and the $Z\alpha$ of other ZBPs using Clustal Omega. The percentage identities of hZ α DLM-1 to other $Z\alpha$ ZBPs were; 27% for orfZ α E3L, 24% for PKZ from goldfish (caZ α PKZ), and 31% for hZ α ADAR1. The N-terminal Z-domain of RBP7910 showed limited sequence identity with other $Z\alpha$ domains; 18% for DLM-1 from *H. sapiens* (hZ α DLM-1), 22% for E3L from orf virus (orfZ α E3L), 23% for hZ α ADAR1, and 17% for PKZ from goldfish (caZ α PKZ), respectively. However, residues involved in the nucleic acid recognition are relatively conserved with few exceptions

$Z\alpha$ and a $Z\beta$ domain in ZBPs recognize the Z-form of dsDNA/RNA substrates [199, 212, 213]. Following binding to the nucleic acid substrates, $Z\alpha$ domain promotes B-to-Z or A-to-Z conformation transition in purine-pyrimidine repeats of dsDNA and RNA, respectively [213, 224]. The $Z\alpha$ domain is studied more extensively compared to the $Z\beta$ domain of ZBPs, but from the few studies on $Z\beta$ domain, it is known that hZ β ADAR1 does not bind to the Z-DNA [225]. However, both $Z\alpha$ and $Z\beta$ domains of the DLM-1 bind to Z-DNA [214]. The interaction of $Z\alpha$ to the sugar-phosphate backbone of left handed Z-DNA/RNA has been widely investigated [199, 215], suggesting that $Z\alpha$ binds to the Z-RNA/DNA substrates by using similar binding interfaces [213, 224].

Here, an intriguing question is if RBP7910 uses the similar conserved amino acid as ZBPs to bind to the RNA substrates or if RBP7910 and other known ZBPs have a shared mode for recognition and binding of the nucleic acid substrates.

The alanine mutagenesis experiments of RBP7910 showed that all the mutants (except P76A) had a less RNA-binding affinity compared to the WT RBP7910. In agreement with the previous reports of alanine substitution point mutation of Asn or Arg of $Z\alpha$ ZBPs, our results showed the corresponding Thr52 and Arg53 mutants from the $\alpha 3$ region of $Z\alpha$ RBP7910 as the most disruptive alanine substitution [224]. Mutation in the $Z\beta$ RBP7910 domain did not show a severe effect on RBP7910 RNA-binding activity except mutation of Trp162, which is the most conserved residue in $Z\beta$ ZBPs [198, 214].

Consequently, we were interested in knowing if similar to ZBPs, the secondary structure of the substrate is the driving force in RBP7910-RNA interaction. Unfortunately, data are limited regarding the mutagenesis effects of residues from ZBPs-DNA interface on the Z-DNA binding of ZBPs. The main focus of most structural and biochemical studies conducted on ZBPs is to find the activity of $Z\alpha$ and $Z\beta$ domains of different ZBPs in the induction of B-to-Z transition of the DNA substrates [214, 226, 227]. There is only one study, reporting the affinity (kd value) of h $Z\alpha$ ADAR1 for the Z-DNA-binding affinity in nanomolar concentrations [228], which is close to the result presented here for the RNA binding affinity of RBP7910.

Despite having an overall conserved structure, the functional properties and interaction profiles are quite different in proteins with WHTH conformation. The diversity of interaction properties range from recognition of a sequence-specific dsDNA in transcription factors [229-231] and recognizing the phosphate backbone of Z-DNA/RNA in ZBPs, to the recognition the RNA hairpin [232, 233] or the 3'U-tail of mRNA strands [234]. Nevertheless, in all cases, the

mode of interaction is still conserved by using $\alpha 3$ recognition helix and $\beta 2/\beta 3$ wing. In the case of ZBPs, the Z-conformation of the DNA/RNA is the sole determinant in the nucleic acid recognition and binding activity of these proteins. In addition to the particular physiological condition like high ionic strength, the alternating purine-pyrimidine also favour the Z-DNA/RNA formation *in vivo* [235]. As mentioned earlier, the mitochondrial RNAs by having an AU-rich sequence, are potential elements to form a Z-like step configuration in their structure. The high sequence similarity of the key residues in the nucleic acid recognition core of the predicted Z α RBP7910 and other Z α ZBPs, suggests that RBP7910 also might recognize the secondary structure of the RNA substrates in a similar way of Z α ZBPs. It would be intriguing to test if any specific secondary conformation (like Z-step) forms upon RBP7910 binding to the RNA substrate, or if the RNA secondary structure is different before and after binding to RBP7910 by studying these structures using circular dichroism spectroscopy method. Unfortunately, the low concentration of recombinant RBP7910 prevented us from testing this theory.

In summary, the mutational studies support the RNA-binding function of the recognition core in ZBDs of RBP7910 much the same as ZBPs. Further experiments, such as the construction of RBP7910 Z α and Z β truncations can help to study the contribution of each domain to the RNA-binding activity of the protein. The nucleic acid binding of WHTH domain-containing proteins have different biological implications in cells, such as regulation of the transcription, RNA biogenesis, translation, and immune responses. Similarly, elucidation of the mode of RNA-binding activity in RBP7910 can be an interesting topic for future research to find the possible regulatory role of RBP7910 in the mitochondrial RNA processing of *T. brucei*.

Chapter V: Concluding Remarks & Future Directions

The kinetoplastid pathogens are related parasites responsible for several diseases such as HAT, Chagas disease, and leishmaniasis, which have social and economic impacts on human populations. As the current treatments for these infections are limited, new therapeutic methods are urgently needed. Uridine insertion-deletion RNA editing is a process in kinetoplastids to maintain the metabolism and development of parasites. RNA editing is an essential process required for parasite growth and life cycle; any functional interference causes a severe growth defect compromising the survival of the parasite at both life stages of *T. brucei*. This machinery has two main components; editosome or RECC, which contains several structural proteins and enzymes required for the editing process, and the MRB1 complex, which plays crucial roles in RNA utilization and processivity of the editing. Our current knowledge related to the dynamic assembly of the various complexes during the RNA editing is still limited. Filling knowledge gaps on the functional relationship between different complexes in the RNA editing machinery and understanding the dynamic assembly and the enzymatic functions is key in developing new drugs. Moreover, this important information can contribute to elucidating the mechanism behind the stage-specific RNA editing, whether the assembly and/or the function of multi-protein complexes are different between the BF and PF life stages, or there are other factors responsible for the differential editing process of transcripts. This thesis project was designed to find novel regulatory factor(s), which potentially modulate the activity of the RNA editing during the life cycle of the parasite.

With these goals in mind, the first step in identifying potential RNA-editing regulatory factors was the creation of a protein map by subjecting the whole cell, cytosolic, and mitochondrial extractions of PF parasites into a biochemical fractionation/mass spectrometry

analysis. This approach is a proven proteomics tool in identifying hundreds of protein complexes and predicting their function in a specific cellular context [169]. The combination of two biochemical fractionation methods, GG and IEX, and applying more than one biochemical property i.e.; the shape/density or the overall protein charges was a rational way to investigate the protein complexes [184]. This methodology also created an advantage in examining the co-sedimentation pattern of protein complexes between two methods. The RNA editing machinery is a matrix of complexes with varying type of interactions. While RECC solely relies on relatively stable, direct protein-protein contacts [136], the interactions in the MRB1 complex are a combination of protein-protein and more transient RNA-mediated interactions [17, 142]. These differences were successfully captured by using GG and IEX methods. For example, as RECC remained clustered in both approaches, physical associations among subunits of the MRB1 complex, and between MRB1 complex and RECC came apart through the formation of at least three separate clusters of MRB1 complex proteins at increasing salt concentrations of the IEX method. By using this approach, we were able to identify some uncharacterized proteins, which have physical associations with members of MRB1 complex and RECC.

We considered that any potential factor(s), controlling the PF-specific editing, should be essential for the survival of the parasite and the editing of transcripts that are preferentially edited at this life stage such as CYb. RBP7910 is essential for the normal growth and the RNA editing of PF parasites [184]. IP experiments demonstrated an RNA-dependent interaction of RBP7910 with members of the GRBC. Further, using multiple *in vitro* binding and competition assays, we confirmed the RNA binding activity of this protein. Both RNA-binding activity and RBP7910 interactions with the members of GRBC suggest that RBP7910 is involved in the mitochondrial gene regulation.

The gRNA and mRNA-binding activities of RBP7910 is mediated by both the sequence and the secondary structure of the RNAs, in which the AU sequence of gRNA and mRNAs and the oligo (U)-tail of the gRNA are the main binding determinants. The binding assays suggested the better binding of RBP7910 to the free stretches of poly U of the oligo (U) tail of gRNAs. The 18-nt 3' oligo (U)-tail A6 gRNA demonstrated 100-times better binding than the oligo (U)-tail of gCYb with only 4Us in the oligo(U)-tail. It is currently not known if any specific secondary structure of the poly U can drive the binding of RBP7910 or other gRNA binding proteins, such as RBP16 or KREPA4. However, the competition experiments strongly suggested the importance of the secondary structures in the gRNA-binding activity of RBP7910.

The 3' long poly AU-tail of edited transcripts is a hallmark of translation. The tail sequence composition of very few transcripts is known. However, a few studies have partially determined the tail composition of some transcripts and found developmentally controlled transcript-specific variations [159, 236]. The characteristic tail influences the stability and translation of mitochondrial transcripts, suggesting a regulatory role for the tail of transcripts. The key players involved in this regulation and how the tail composition is defined between life stages are currently unknown. In addition to KPAF1/2 proteins, there are a few numbers of RNA-binding PPR proteins that control the translation of mitochondrial transcripts in a transcript-specific manner. However, the mechanism behind their function is also not clear. One potential regulatory element is the secondary structure of the tail, which can have different configuration between life stages due to the differences in temperature between the BF and PF stages. By considering the specific AU sequence-binding ability of RBP7910 and the importance of the secondary structure in RBP7910-RNA interaction, it is plausible that RBP7910 distinguishes the AU-tailed transcripts in a developmentally-regulated manner. This binding can

indirectly regulate the translation of transcripts via stabilization of a specific secondary structure of the AU-tail and its recognition by mitochondrial ribosomes.

Having described the RNA-binding activity of RBP7910, we next set out to examine the mode of RNA-binding in the protein. Sequence analysis of RBP7910 identified two ZBDs within the N- and C-terminals of the protein. Sequence alignment of these two domains with the $Z\alpha$ and $Z\beta$ ZBPs showed a sequence similarity between RBP7910 and ZBPs of amino acids located in the nucleic acid recognition core. Alanine substitution point mutations were used to explore the importance of those conserved residues in RBP7910-RNA interaction, which showed that RBP7910 and ZBPs shared the same mode of nucleic acid binding using ZBDs. ZBPs interactions with the zigzag structured Z-DNA/RNA have been widely explored using crystallography studies. Our point mutations experiments showed that similar to other WHTH domain-containing proteins, residues from the $\alpha 3$ helix and the wing region contribute to the RNA-binding activity of RBP7910.

One major activity of $Z\alpha$ ZBPs is the induction of the Z-conformation in dsDNA/RNA strands. Certain conditions, such as stretches of alternating purine and pyrimidine residues, favours the adaptation of left-handed Z-conformation in DNA/RNA strands. *In vivo* and *in vitro* experiments confirmed the recognition and induction of Z-conformation in 4-7 stretches of alternating purines and pyrimidines at the base of the stem region of rRNAs in small and large ribosomal subunits by $Z\alpha$ ADAR1 [237]. Alternatively, the recombinant RBP7910 binds stably to the synthetic A6gRNA and Cyb-edited mRNA substrates with a stretch of six alternating purines and pyrimidines nucleotides (**Fig. 3.7-A**). Therefore, we suggested that recognition of mitochondrial RNA substrates by RBP7910 can be due to the recognition of Z-like RNA features of the mitochondrial substrates.

By utilizing proteomics and RNAi studies, this thesis project successfully identified a novel RBP involved in the RNA-editing machinery of PF *T. brucei*. We also characterized its RNA-binding activity using *in vitro* binding assays, and the basis of this activity using point mutation studies. However, the function of RBP7910 is still unknown. The gRNA- and mRNA-binding activity of RBP7910, the protein identification in the pulldown of the multiple members of RESC (mainly in RNA-dependent manner), and its impact on the editing of mitochondrial transcripts suggested that the RBP7910 RNA binding function during the RNA editing. Considering the binding affinity of RBP7910 to the pre-edited and edited Cyb mRNAs (**Fig. 3.2**), and the stable secondary structure of pre-edited Cyb mRNA [238], we proposed a role for the RBP7910 in processing of the RNA editing substrates during the RNA editing, possibly by; (1) relaxing the stable stem-loop structure of pre-edited Cyb mRNA prior binding to the gRNA, (2) stabilizing the edited Cyb mRNA and increasing its translation rate. Future *in vivo* cross-linking immunoprecipitation from RBP7910 expressed and repressed cells and high-throughput sequencing of RNA transcripts (RNA-Seq) experiments, may elucidate the mechanism of protein's function in the cell by demonstrating the *in vivo* RNA targets and the position at which RBP7910 binds to the RNAs. Regarding the preferential AU-sequence binding of RBP7910, it would be interesting to measure the activity of RBP7910 on the formation and stability of different AU-tailed transcripts, such as Cyb mRNA, and evaluate its role on the translation of the mitochondrial transcripts.

Considering the importance of stem-loop structures in the RBP7910-RNA interaction, it would be helpful to examine the secondary structure of the mitochondrial substrate RNA such as gA6RNA or edited Cyb mRNA before and after binding to the WT RBP7910 using circular dichroism spectroscopy. This experiment can support our earlier hypothesis on RBP7910

recognition ability of Z-like structures in alternating purines and pyrimidines nucleotides of the RNA substrates. To follow up on structure-function analysis on ZBDs of RBP7910, we suggest to create a comparative homology-based model for the RBP7910/Z-DNA interaction using a public webserver called I-TASSER [239, 240]. This can be used as a complementary approach to the sequence-alignment study to gain a better visualization of ZBDs-RNA mode of interaction in RBP7910 and its similarity to the ZBP family.

Chapter VI: Contribution to Knowledge

RNA editing in the mitochondria of kinetoplastid protists is a post-transcriptional modification which includes uridine insertion/deletion. The enzymatic mechanisms behind the editing process were investigated through extensive structure-function studies, which identified the RECC as the main catalytic core. The discovery of the MRB1 complex and its importance in processing and stabilization of editing substrates suggested that this machinery is more complicated than the basic enzymatic reactions that occur in RECC. There is still a lack of knowledge on how life stage-specific editing is achieved, or how MRB1 subunits are essential to the editing and what function they play in the regulation of editing. To answer these questions, we investigated the composition of the RNA-editing machinery in PF parasites, which led to identification of a novel protein. In turn, we showed that these proteins have physical associations with RECC and the MRB1 complex.

In summary, this thesis contributed to new knowledge through:

1. Presentation of a high-resolution protein map of the RNA-editing machinery at PF life stage of *T. brucei*, using two complementary biochemical approaches. This data provided a new view on the protein complexes involved in the RNA editing and mRNA 3' end maturation while identifying novel RNA editing-related proteins.
2. Identification of a new mitochondrial protein (Tb927.10.7910) essential for the optimal growth of PF parasites. This protein is also associated with the mitochondrial RNA-editing pathway by having RNA-mediated interactions with a member of the GRBC.

3. Identification of gRNA- and mRNA-binding properties of RBP7910 suggested a mode of RNA-binding for the protein, mediated by the AU sequence and the secondary structure of the gRNA and mRNA, and the 3' oligo (U)-tail of gRNA.
4. Prediction of two WTH structured-ZBDs in RBP7910, contributing to its RNA-binding activity and presented the first report of the basis of this RNA-binding activity via ZBDs in *T. brucei*.
5. Determination of $\alpha 3$ and the wing regions of predicted ZBDs as the protein-RNA interfaces of RBP7910 similar to other WTH domain-containing proteins.

Chapter VII: References

1. Brun, R., J. Blum, F. Chappuis, and C. Burri. Human african trypanosomiasis. *Lancet*, 2010. **375**(9709): p. 148-159.
2. Ribeiro, A.L., M.P. Nunes, M.M. Teixeira, and M.O. Rocha. Diagnosis and management of Chagas disease and cardiomyopathy. *Nature Reviews Cardiology*, 2012. **9**(10): p. 576.
3. Kaye, P. and P. Scott. Leishmaniasis: complexity at the host–pathogen interface. *Nature Reviews Microbiology*, 2011. **9**(8): p. 604.
4. WHO. Investing to overcome the global impact of Neglected Tropical Diseases: Third WHO Report on Neglected Tropical Diseases Vol. 3. 2015: WHO.
5. McCall, L.-I. and J.H. McKerrow. Determinants of disease phenotype in trypanosomatid parasites. *Trends in Parasitology*, 2014. **30**(7): p. 342-349.
6. Sundar, S. and J. Chakravarty. An update on pharmacotherapy for leishmaniasis. *Expert opinion on Pharmacotherapy*, 2015. **16**(2): p. 237-252.
7. Jones, A.J. and V.M. Avery. Future treatment options for human African trypanosomiasis. 2015, Taylor & Francis.
8. Bermudez, J., C. Davies, A. Simonazzi, J.P. Real, and S. Palma. Current drug therapy and pharmaceutical challenges for Chagas disease. *Acta Tropica*, 2016. **156**: p. 1-16.
9. Keating, J., J.O. Yukich, C.S. Sutherland, G. Woods, and F. Tediosi. Human African trypanosomiasis prevention, treatment and control costs: a systematic review. *Acta tropica*, 2015. **150**: p. 4-13.
10. Alvar, J., I.D. Velez, C. Bern, M. Herrero, P. Desjeux, J. Cano, J. Jannin, M. den Boer, and W.L.C. Team. Leishmaniasis worldwide and global estimates of its incidence. *PloS ONE*, 2012. **7**(5): p. e35671.
11. Bonney, K.M. and D.M. Engman. Autoimmune pathogenesis of Chagas heart disease: looking back, looking ahead. *American journal of Pathology*, 2015. **185**(6): p. 1537-1547.

12. Barros-Alvarez, X., M. Gualdron-Lopez, H. Acosta, A.J. Caceres, M.A.S. Graminha, P.A. Michels, J.L. Concepcion, and W. Quiñones. Glycosomal targets for anti-trypanosomatid drug discovery. *Current Medicinal Chemistry*, 2014. **21**(15): p. 1679-1706.
13. Durrant, J.D., L. Hall, R.V. Swift, M. Landon, A. Schnauffer, and R.E. Amaro. Novel naphthalene-based inhibitors of *Trypanosoma brucei* RNA editing ligase 1. *PLoS Neglected Tropical Diseases*, 2010. **4**(8): p. e803.
14. Salavati, R., H. Moshiri, S. Kala, and H.S. Najafabadi. Inhibitors of RNA editing as potential chemotherapeutics against trypanosomatid pathogens. *International Journal for Parasitology: Drugs and Drug Resistance*, 2012. **2**: p. 36-46.
15. Moshiri, H., S. Acoca, S. Kala, H.S. Najafabadi, H. Hogues, E. Purisima, and R. Salavati. Naphthalene-based RNA editing inhibitor blocks RNA editing activities and editosome assembly in *Trypanosoma brucei*. *Journal of Biological Chemistry*, 2011. **286**(16): p. 14178-89.
16. Read, L.K., J. Lukeš, and H. Hashimi. Trypanosome RNA editing: the complexity of getting U in and taking U out. *Wiley Interdisciplinary Reviews: RNA*, 2016. **7**(1): p. 33-51.
17. Aphasizheva, I., L. Zhang, X. Wang, R.M. Kaake, L. Huang, S. Monti, and R. Aphasizhev. RNA binding and core complexes constitute the U-insertion/deletion editosome. *Molecular and Cellular Biology*, 2014. **34**(23): p. 4329-42.
18. Stuart, K.D., A. Schnauffer, N.L. Ernst, and A.K. Panigrahi. Complex management: RNA editing in trypanosomes. *Trends in biochemical sciences*, 2005. **30**(2): p. 97-105.
19. Simpson, L., R. Aphasizhev, J. Lukeš, and J.C. Reyes. Guide to the nomenclature of kinetoplastid RNA editing: a proposal. *Protist*, 2010. **161**(1): p. 2.
20. Carnes, J., J.R. Trotter, A. Peltan, M. Fleck, and K. Stuart. RNA editing in *Trypanosoma brucei* requires three different editosomes. *Molecular and Cellular Biology*, 2008. **28**(1): p. 122.
21. Stuart, K., A. Panigrahi, A. Schnauffer, M. Drozd, C. Clayton, and R. Salavati. Composition of the editing complex of *Trypanosoma brucei*. *Philosophical Transactions-Royal society of London series Biological Sciences* 2002. **357**: p. 71-80.
22. Schnauffer, A., A.K. Panigrahi, B. Panicucci, R.P. Igo Jr, R. Salavati, and K. Stuart. An RNA ligase essential for RNA editing and survival of the bloodstream form of *Trypanosoma brucei*. *Science*, 2001. **291**(5511): p. 2159-2162.

23. Gao, G. and L. Simpson. Is the *Trypanosoma brucei* REL1 RNA ligase specific for U-deletion RNA editing, and is the REL2 RNA ligase specific for U-insertion editing? *Journal of Biological Chemistry*, 2003. **278**(30): p. 27570-27574.
24. Besteiro, S., M.P. Barrett, L. Rivière, and F. Bringaud. Energy generation in insect stages of *Trypanosoma brucei*: metabolism in flux. *Trends in Parasitology*, 2005. **21**(4): p. 185-191.
25. Zíková, A., A. Schnauffer, R.A. Dalley, A.K. Panigrahi, and K.D. Stuart. The F₀F₁-ATP synthase complex contains novel subunits and is essential for procyclic *Trypanosoma brucei*. *PLoS Pathogens*, 2009. **5**(5): p. e1000436.
26. Hannaert, V., F. Bringaud, F.R. Opperdoes, and P.A. Michels. Evolution of energy metabolism and its compartmentation in Kinetoplastida. *Kinetoplastid Biology and Disease*, 2003. **2**(1): p. 11.
27. Hashimi, H., V. Benkovičová, P. Čermáková, D.-H. Lai, A. Horváth, and J. Lukeš. The assembly of F₁F₀-ATP synthase is disrupted upon interference of RNA editing in *Trypanosoma brucei*. *International Journal for Parasitology*, 2010. **40**(1): p. 45-54.
28. Schnauffer, A., G.D. Clark-Walker, A.G. Steinberg, and K. Stuart. The F₁-ATP synthase complex in bloodstream stage trypanosomes has an unusual and essential function. *EMBO Journal*, 2005. **24**(23): p. 4029-4040.
29. Panigrahi, A.K., A. Zíková, R.A. Dalley, N. Acestor, Y. Ogata, A. Anupama, P.J. Myler, and K.D. Stuart. Mitochondrial complexes in *Trypanosoma brucei* a novel complex and a unique oxidoreductase complex. *Molecular & Cellular Proteomics*, 2008. **7**(3): p. 534-545.
30. Aphasizhev, R. and I. Aphasizheva. Mitochondrial RNA editing in trypanosomes: small RNAs in control. *Biochimie*, 2014. **100**: p. 125-31.
31. Aphasizheva, I., D. Maslov, X. Wang, L. Huang, and R. Aphasizhev. Pentatricopeptide repeat proteins stimulate mRNA adenylation/uridylation to activate mitochondrial translation in trypanosomes. *Molecular Cell*, 2011. **42**(1): p. 106-17.
32. Ammerman, M.L., H. Hashimi, L. Novotná, Z. Čičová, S.M. McEvoy, J. Lukeš, and L.K. Read. MRB3010 is a core component of the MRB1 complex that facilitates an early step of the kinetoplastid RNA editing process. *RNA*, 2011. **17**(5): p. 865-877.
33. Ammerman, M.L., V. Presnyak, J.C. Fisk, B.M. Foda, and L.K. Read. TbRGG2 facilitates kinetoplastid RNA editing initiation and progression past intrinsic pause sites. *RNA*, 2010. **16**(11): p. 2239-2251.

34. Ammerman, M.L., D.L. Tomasello, D. Faktorová, L. Kafková, H. Hashimi, J. Lukeš, and L.K. Read. A core MRB1 complex component is indispensable for RNA editing in insect and human infective stages of *Trypanosoma brucei*. PLoS ONE, 2013. **8**(10): p. e78015.
35. Riley, G.R., P.J. Myler, and K. Stuart. Quantitation of RNA editing substrates, products and potential intermediates: implications for developmental regulation. Nucleic acids research, 1995. **23**(4): p. 708-712.
36. Koslowsky, D.J., G.J. Bhat, A.L. Perrollaz, J.E. Feagin, and K. Stuart. The MURF3 gene of *T. brucei* contains multiple domains of extensive editing and is homologous to a subunit of NADH dehydrogenase. Cell, 1990. **62**(5): p. 901-911.
37. Feagin, J. and K. Stuart. Developmental aspects of uridine addition within mitochondrial transcripts of *Trypanosoma brucei*. Molecular and Cellular Biology, 1988. **8**(3): p. 1259-1265.
38. Feagin, J.E., D.P. Jasmer, and K. Stuart. Developmentally regulated addition of nucleotides within apocytochrome b transcripts in *Trypanosoma brucei*. Cell, 1987. **49**(3): p. 337-345.
39. Benne, R., J. Van Den Burg, J.P. Brakenhoff, P. Sloof, J.H. Van Boom, and M.C. Tromp. Major transcript of the frameshifted coxII gene from trypanosome mitochondria contains four nucleotides that are not encoded in the DNA. Cell, 1986. **46**(6): p. 819-826.
40. Bhat, G.J., A.E. Souza, J.E. Feagin, and K. Stuart. Transcript-specific developmental regulation of polyadenylation in *Trypanosoma brucei* mitochondria. Molecular and Biochemical Parasitology, 1992. **52**(2): p. 231-240.
41. Souza, A.E., H.-H. Shu, L.K. Read, P.J. Myler, and K.D. Stuart. Extensive editing of CR2 maxicircle transcripts of *Trypanosoma brucei* predicts a protein with homology to a subunit of NADH dehydrogenase. Molecular and Cellular Biology, 1993. **13**(11): p. 6832-6840.
42. Koslowsky, D.J., G.R. Riley, J.E. Feagin, and K. Stuart. Guide RNAs for transcripts with developmentally regulated RNA editing are present in both life cycle stages of *Trypanosoma brucei*. Molecular and cellular biology, 1992. **12**(5): p. 2043-2049.
43. Madina, B.R., V. Kumar, R. Metz, B.H. Mooers, R. Bundschuh, and J. Cruz-Reyes. Native mitochondrial RNA-binding complexes in kinetoplastid RNA editing differ in guide RNA composition. RNA, 2014. **20**(7): p. 1142-1152.
44. Carnes, J., C.Z. Soares, C. Wickham, and K. Stuart. Endonuclease associations with three distinct editosomes in *Trypanosoma brucei*. Journal of Biological Chemistry, 2011: p. jbc. M111. 228965.

45. McDermott, S.M., X. Guo, J. Carnes, and K. Stuart. Differential editosome protein function between life cycle stages of *Trypanosoma brucei*. *Journal of Biological Chemistry*, 2015. **290**(41): p. 24914-24931.
46. WHO. First WHO report on neglected tropical diseases: working to overcome the global impact of neglected tropical diseases, in *First WHO report on neglected tropical diseases: Working to overcome the global impact of neglected tropical diseases*. 2010, WHO.
47. Liese, B., M. Rosenberg, and A. Schratz. Programmes, partnerships, and governance for elimination and control of neglected tropical diseases. *Lancet*, 2010. **375**(9708): p. 67-76.
48. Molyneux, D.H. Neglected tropical diseases—beyond the tipping point? *Lancet*, 2010. **375**(9708): p. 3-4.
49. Hotez, P.J., A. Fenwick, L. Savioli, and D.H. Molyneux. Rescuing the bottom billion through control of neglected tropical diseases. *Lancet*, 2009. **373**(9674): p. 1570-1575.
50. Baker, M., E. Mathieu, F. Fleming, M. Deming, J. King, A. Garba, J. Koroma, M. Bockarie, A. Kabore, and D. Sankara. Mapping, monitoring, and surveillance of neglected tropical diseases: towards a policy framework. *Lancet*, 2010. **375**(9710): p. 231-238.
51. Molyneux, D.H., L. Savioli, and D. Engels. Neglected tropical diseases: progress towards addressing the chronic pandemic. *The Lancet*, 2017. **389**(10066): p. 312-325.
52. WHO. Sustaining the drive to overcome the global impact of neglected tropical diseases: second WHO report on neglected tropical diseases: summary. 2013.
53. Conteh, L., T. Engels, and D.H. Molyneux. Socioeconomic aspects of neglected tropical diseases. *Lancet*, 2010. **375**(9710): p. 239-247.
54. Breiman, R.F., C.A. Van Beneden, and E.C. Farnon. Surveillance for respiratory infections in low- and middle-income countries: experience from the Centers for Disease Control and Prevention's Global Disease Detection International Emerging Infections Program. *Journal of Infectious Diseases*, 2013. **208**(suppl_3): p. S167-S172.
55. Hotez, P.J. NTDs V. 2.0: “blue marble health”—neglected tropical disease control and elimination in a shifting health policy landscape. *PLoS Neglected Tropical Diseases*, 2013. **7**(11): p. e2570.
56. WHO. Working to overcome the global impact of neglected tropical diseases. 2010.

57. Mackey, T.K. and B. Liang. Threats from emerging and re-emerging neglected tropical diseases (NTDs). *Infection Ecology & Epidemiology*, 2012. **2**(1): p. 18667.
58. Stuart, K., R. Brun, S. Croft, A. Fairlamb, R.E. Gürtler, J. McKerrow, S. Reed, and R. Tarleton. Kinetoplastids: related protozoan pathogens, different diseases. *Journal of clinical investigation*, 2008. **118**(4): p. 1301-1310.
59. MacLean, L., E. Myburgh, J. Rodgers, and H. Price. Imaging African trypanosomes. *Parasite Immunology*, 2013. **35**(9-10): p. 283-294.
60. Lutje, V., J. Seixas, and A. Kennedy. Chemotherapy for second-stage Human African trypanosomiasis. *Cochrane Database of Systematic Reviews*, 2010. **8**.
61. Fevre, E.M., B.v. Wissmann, S.C. Welburn, and P. Lutumba. The burden of human African trypanosomiasis. *PLoS Neglected Tropical Diseases*, 2008. **2**(12): p. e333.
62. Ndeledje, N., J. Bouyer, F. Stachurski, P. Grimaud, A.M.G. Belem, F.M. Mbaïndingtoloum, Z. Bengaly, I.O. Alfaroukh, G. Cecchi, and R. Lancelot. Treating cattle to protect people? Impact of footbath insecticide treatment on tsetse density in Chad. *PLoS ONE*, 2013. **8**(6): p. e67580.
63. Malvy, D. and F. Chappuis. Sleeping sickness. *Clinical Microbiology and Infection*, 2011. **17**(7): p. 986-995.
64. Boatin, B., G. Wyatt, F. Wurapa, and M. Bulsara. Use of symptoms and signs for diagnosis of *Trypanosoma brucei rhodesiense* trypanosomiasis by rural health personnel. *Bulletin of the World Health Organization*, 1986. **64**(3): p. 389.
65. MacLean, L.M., M. Odiit, J.E. Chisi, P.G. Kennedy, and J.M. Sternberg. Focus-specific clinical profiles in human African trypanosomiasis caused by *Trypanosoma brucei rhodesiense*. *PLoS Neglected Tropical Diseases*, 2010. **4**(12): p. e906.
66. Lutje, V., J. Seixas, and A. Kennedy. Chemotherapy for second-stage Human African trypanosomiasis. *The Cochrane Library*, 2013.
67. Fairlamb, A.H. Chemotherapy of human African trypanosomiasis: current and future prospects. *Trends in Parasitology*, 2003. **19**(11): p. 488-494.
68. Stich, A., A. Ponte-Sucre, and U. Holzgrabe. Do we need new drugs against human African trypanosomiasis? *Lancet Infectious Diseases*, 2013. **13**(9): p. 733-734.

69. Stein, J., S. Mogk, C. Mudogo, B. Sommer, M. Scholze, A. Meiwes, M. Huber, A. Gray, and M. Duszenko. Drug development against sleeping sickness: old wine in new bottles? *Current Medicinal Chemistry*, 2014. **21**(15): p. 1713-1727.
70. Babokhov, P., A.O. Sanyaolu, W.A. Oyibo, A.F. Fagbenro-Beyioku, and N.C. Iriemenam. A current analysis of chemotherapy strategies for the treatment of human African trypanosomiasis. *Pathogens and Global Health*, 2013. **107**(5): p. 242-252.
71. Ferrins, L., R. Rahmani, and J.B. Baell. Drug discovery and human African trypanosomiasis: a disease less neglected? *Future Medicinal Discovery*, 2013. **5**(15): p. 1801-1841.
72. Mesu, V.K.B.K., W.M. Kalonji, C. Bardonneau, O.V. Mordt, S. Blesson, F. Simon, S. Delhomme, S. Bernhard, W. Kuziena, and J.-P.F. Lubaki. Oral fexinidazole for late-stage African *Trypanosoma brucei* gambiense trypanosomiasis: a pivotal multicentre, randomised, non-inferiority trial. *Lancet*, 2018. **391**(10116): p. 144-154.
73. Pollastri, M.P. Fexinidazole: A New Drug for African Sleeping Sickness on the Horizon. *Trends in parasitology*, 2017.
74. Rassi, A. and J.M. de Rezende. American trypanosomiasis (Chagas disease). *Infectious Disease Clinics of North America*, 2012. **26**(2): p. 275-291.
75. Rassi, A. and J.A. Marin-Neto. Chagas disease. *Lancet*, 2010. **375**(9723): p. 1388-1402.
76. Manne-Goehler, J., C.A. Umeh, S.P. Montgomery, and V.J. Wirtz. Estimating the burden of Chagas disease in the United States. *PLoS Neglected Tropical Diseases*, 2016. **10**(11): p. e0005033.
77. Forsyth, C.J., S. Hernandez, W. Olmedo, A. Abuhamidah, M.I. Traina, D.R. Sanchez, J. Soverow, and S.K. Meymandi. Safety profile of nifurtimox for treatment of chagas disease in the United States. *Clinical Infectious Diseases*, 2016. **63**(8): p. 1056-1062.
78. Jackson, Y., E. Alirol, L. Getaz, H. Wolff, C. Combescure, and F. Chappuis. Tolerance and safety of nifurtimox in patients with chronic chagas disease. *Clinical Infectious Diseases*, 2010. **51**(10): p. e69-e75.
79. Le Loup, G., G. Pialoux, and F.X. Lescure. Update in treatment of Chagas disease. *Current Opinion in Infectious Diseases*, 2011. **24**(5): p. 428-434.

80. Bustamante, J.M., J.M. Craft, B.D. Crowe, S.A. Ketchie, and R.L. Tarleton. New, combined, and reduced dosing treatment protocols cure *Trypanosoma cruzi* infection in mice. *Journal of Infectious Diseases*, 2013. **209**(1): p. 150-162.
81. Francisco, A.F., M.D. Lewis, S. Jayawardhana, M.C. Taylor, E. Chatelain, and J.M. Kelly. The limited ability of posaconazole to cure both acute and chronic *Trypanosoma cruzi* infections revealed by highly sensitive in vivo imaging. *Antimicrobial Agents and Chemotherapy*, 2015: p. AAC. 00520-15.
82. Pigott, D.M., S. Bhatt, N. Golding, K.A. Duda, K.E. Battle, O.J. Brady, J.P. Messina, Y. Balard, P. Bastien, and F. Pratlong. Global distribution maps of the leishmaniasis. *Elife*, 2014. **3**: p. e02851.
83. WHO. World Health Organization. Leishmaniasis. World Health Org Fact Sheet. . 2016.
84. Steverding, D. The history of leishmaniasis. *Parasites & Vectors*, 2017. **10**(1): p. 82.
85. Eiras, D.P., L.A. Kirkman, and H.W. Murray. Cutaneous leishmaniasis: current treatment practices in the USA for returning travelers. *Current Treatment Options in Infectious Diseases*, 2015. **7**(1): p. 52-62.
86. Freitas-Junior, L.H., E. Chatelain, H.A. Kim, and J.L. Siqueira-Neto. Visceral leishmaniasis treatment: what do we have, what do we need and how to deliver it? *International Journal for Parasitology: Drugs and Drug Resistance*, 2012. **2**: p. 11-19.
87. Fenn, K. and K.R. Matthews. The cell biology of *Trypanosoma brucei* differentiation. *Current Opinion in Microbiology*, 2007. **10**(6): p. 539-546.
88. Matthews, K.R. The developmental cell biology of *Trypanosoma brucei*. *Journal of Cell Science*, 2005. **118**(2): p. 283-290.
89. Roditi, I. and M. Liniger. Dressed for success: the surface coats of insect-borne protozoan parasites. *Trends in Microbiology*, 2002. **10**(3): p. 128-134.
90. Rodríguez, J.A., M.A. Lopez, M.C. Thayer, Y. Zhao, M. Oberholzer, D.D. Chang, N.K. Kisalu, M.L. Penichet, G. Helguera, and R. Bruinsma. Propulsion of African trypanosomes is driven by bihelical waves with alternating chirality separated by kinks. *Proceedings of the National Academy of Sciences of the United States of America*, 2009. **106**(46): p. 19322-19327.
91. Vaughan, S. and K. Gull. The trypanosome flagellum. *Journal of Cell Science*, 2003. **116**(5): p. 757-759.

92. Ogbadoyi, E.O., D.R. Robinson, and K. Gull. A high-order trans-membrane structural linkage is responsible for mitochondrial genome positioning and segregation by flagellar basal bodies in trypanosomes. *Molecular Biology of the Cell*, 2003. **14**(5): p. 1769-1779.
93. Kakkar, P. and B. Singh. Mitochondria: a hub of redox activities and cellular distress control. *Molecular and Cellular Biochemistry*, 2007. **305**(1-2): p. 235-253.
94. Schägger, H. Respiratory chain supercomplexes. *IUBMB life*, 2001. **52**(3-5): p. 119-128.
95. Bringaud, F., L. Rivière, and V. Coustou. Energy metabolism of trypanosomatids: adaptation to available carbon sources. *Molecular and Biochemical Parasitology*, 2006. **149**(1): p. 1-9.
96. Timms, M.W., F.J. van Deursen, E.F. Hendriks, and K.R. Matthews. Mitochondrial development during life cycle differentiation of African trypanosomes: evidence for a kinetoplast-dependent differentiation control point. *Molecular Biology of the Cell*, 2002. **13**(10): p. 3747-3759.
97. Osinga, K.A., B.W. Swinkels, W.C. Gibson, P. Borst, G.H. Veeneman, J.H. Van Boom, P. Michels, and F. Opperdoes. Topogenesis of microbody enzymes: a sequence comparison of the genes for the glycosomal (microbody) and cytosolic phosphoglycerate kinases of *Trypanosoma brucei*. *EMBO Journal*, 1985. **4**(13B): p. 3811.
98. Lamour, N., L. Rivière, V. Coustou, G.H. Coombs, M.P. Barrett, and F. Bringaud. Proline metabolism in procyclic *Trypanosoma brucei* is down-regulated in the presence of glucose. *Journal of Biological Chemistry*, 2005.
99. Besteiro, S., M. Biran, N. Biteau, V. Coustou, T. Baltz, P. Canioni, and F. Bringaud. Succinate secreted by *Trypanosoma brucei* is produced by a novel and unique glycosomal enzyme, NADH-dependent fumarate reductase. *Journal of Biological Chemistry*, 2002. **277**(41): p. 38001-38012.
100. Coustou, V., S. Besteiro, L. Rivière, M. Biran, N. Biteau, J.-M. Franconi, M. Boshart, T. Baltz, and F. Bringaud. A mitochondrial NADH-dependent fumarate reductase involved in the production of succinate excreted by procyclic *Trypanosoma brucei*. *Journal of Biological Chemistry*, 2005. **280**(17): p. 16559-16570.
101. Allmann, S., P. Morand, C. Ebikeme, L. Gales, M. Biran, J. Hubert, A. Brennand, M. Mazet, J.-M. Franconi, and P.A. Michels. Cytosolic NADPH homeostasis in glucose-starved procyclic *Trypanosoma brucei* relies on malic enzyme and the pentose phosphate pathway fed by gluconeogenic flux. *Journal of Biological Chemistry*, 2013: p. jbc. M113. 462978.
102. Van Hellemond, J.J., F.R. Opperdoes, and A.G. Tielens. Trypanosomatidae produce acetate via a mitochondrial acetate: succinate CoA transferase. *Proceedings of the National Academy of Sciences of the United States of America*, 1998. **95**(6): p. 3036-3041.

103. Rivière, L., S.W. van Weelden, P. Glass, P. Vegh, V. Coustou, M. Biran, J.J. van Hellemond, F. Bringaud, A.G. Tielens, and M. Boshart. Acetyl: succinate CoA-transferase in procyclic *Trypanosoma brucei* Gene identification and role in carbohydrate metabolism. *Journal of Biological Chemistry*, 2004. **279**(44): p. 45337-45346.
104. Michels, P.A., F. Bringaud, M. Herman, and V. Hannaert. Metabolic functions of glycosomes in trypanosomatids. *Biochimica et Biophysica Acta -Molecular Cell Research*, 2006. **1763**(12): p. 1463-1477.
105. Simpson, L. The mitochondrial genome of kinetoplastid protozoa: genomic organization, transcription, replication, and evolution. *Annual Reviews in Microbiology*, 1987. **41**(1): p. 363-380.
106. LeBowitz, J., H. Smith, L. Rusche, and S. Beverley. Coupling of poly (A) site selection and trans-splicing in *Leishmania*. *Genes & Development*, 1993. **7**(6): p. 996.
107. Martinez-Calvillo, S., J.C. Vizuet-de-Rueda, L.E. Florencio-Martinez, R.G. Manning-Cela, and E.E. Figueroa-Angulo. Gene expression in trypanosomatid parasites. *Journal of Biomedicine and Biotechnology* 2010: p. 1-15.
108. Campbell, D.A., S. Thomas, and N.R. Sturm. Transcription in kinetoplastid protozoa: why be normal? *Microbes and Infection*, 2003. **5**(13): p. 1231-1240.
109. Benz, C., D. Nilsson, B. Andersson, C. Clayton, and D.L. Guilbride. Messenger RNA processing sites in *Trypanosoma brucei*. *Molecular and Biochemical Parasitology*, 2005. **143**(2): p. 125-134.
110. Xu, C. and D.S. Ray. Isolation of proteins associated with kinetoplast DNA networks in vivo. *Proceedings of the National Academy of Sciences of the United States of America*, 1993. **90**(5): p. 1786-1789.
111. Machado Motta, M.C. Kinetoplast as a potential chemotherapeutic target of trypanosomatids. *Current Pharmaceutical Design*, 2008. **14**(9): p. 847-854.
112. Shapiro, T.A. and P.T. Englund. The structure and replication of kinetoplast DNA. *Annual Reviews in Microbiology*, 1995. **49**(1): p. 117-143.
113. Randau, L., B.J. Stanley, A. Kohlway, S. Mechta, Y. Xiong, and D. Söll. A cytidine deaminase edits C to U in transfer RNAs in Archaea. *Science*, 2009. **324**(5927): p. 657-659.
114. Gray, M.W. Evolutionary origin of RNA editing. *Biochemistry*, 2012. **51**(26): p. 5235-5242.

115. Alfonzo, J.D., V. Blanc, A.M. Estévez, M.A.T. Rubio, and L. Simpson. C to U editing of the anticodon of imported mitochondrial tRNA^{Trp} allows decoding of the UGA stop codon in *Leishmania tarentolae*. *EMBO Journal*, 1999. **18**(24): p. 7056-7062.
116. Blum, B., N. Bakalara, and L. Simpson. A model for RNA editing in kinetoplastid mitochondria: RNA molecules transcribed from maxicircle DNA provide the edited information. *Cell*, 1990. **60**(2): p. 189-198.
117. Blum, B. and L. Simpson. Guide RNAs in kinetoplastid mitochondria have a nonencoded 3' oligo (U) tail involved in recognition of the preedited region. *Cell*, 1990. **62**(2): p. 391-397.
118. Bakalara, N., A.M. Simpson, and L. Simpson. The *Leishmania* kinetoplast-mitochondrion contains terminal uridylyltransferase and RNA ligase activities. *Journal of Biological Chemistry*, 1989. **264**(31): p. 18679-18686.
119. Seiwert, S.D., S. Heidmann, and K. Stuart. Direct visualization of uridylyate deletion in vitro suggests a mechanism for kinetoplastid RNA editing. *Cell*, 1996. **84**(6): p. 831-841.
120. Cruz-Reyes, J. and B. Sollner-Webb. Trypanosome U-deletional RNA editing involves guide RNA-directed endonuclease cleavage, terminal U exonuclease, and RNA ligase activities. *Proceedings of the National Academy of Sciences of the United States of America*, 1996. **93**(17): p. 8901-8906.
121. Panigrahi, A.K., S.P. Gygi, N.L. Ernst, R.P. Igo, S.S. Palazzo, A. Schnauffer, D.S. Weston, N. Carmean, R. Salavati, and R. Aebersold. Association of two novel proteins, TbMP52 and TbMP48, with the *Trypanosoma brucei* RNA editing complex. *Molecular and Cellular Biology*, 2001. **21**(2): p. 380-389.
122. Rusché, L.N., C.E. Huang, K.J. Piller, M. Hemann, E. Wirtz, and B. Sollner-Webb. The two RNA ligases of the *Trypanosoma brucei* RNA editing complex: cloning the essential band IV gene and identifying the band V gene. *Molecular and Cellular Biology*, 2001. **21**(4): p. 979-989.
123. Panigrahi, A.K., N.L. Ernst, G.J. Domingo, M. Fleck, R. Salavati, and K.D. Stuart. Compositionally and functionally distinct editosomes in *Trypanosoma brucei*. *RNA*, 2006. **12**(6): p. 1038-1049.
124. Panigrahi, A.K., A. Schnauffer, N. Carmean, R.P. Igo, S.P. Gygi, N.L. Ernst, S.S. Palazzo, D.S. Weston, R. Aebersold, and R. Salavati. Four related proteins of the *Trypanosoma brucei* RNA editing complex. *Molecular and Cellular Biology*, 2001. **21**(20): p. 6833-6840.

125. Panigrahi, A.K., A. Schnauffer, N.L. Ernst, B. Wang, N. Carmean, R. Salavati, and K. Stuart. Identification of novel components of *Trypanosoma brucei* editosomes. *RNA*, 2003. **9**(4): p. 484-492.
126. Aphasizhev, R., I. Aphasizheva, R.E. Nelson, G. Gao, A.M. Simpson, X. Kang, A.M. Falick, S. Sbicego, and L. Simpson. Isolation of a U-insertion/deletion editing complex from *Leishmania tarentolae* mitochondria. *EMBO Journal*, 2003. **22**(4): p. 913-24.
127. Rusché, L.N., J. Cruz-Reyes, K.J. Piller, and B. Sollner-Webb. Purification of a functional enzymatic editing complex from *Trypanosoma brucei* mitochondria. *EMBO Journal*, 1997. **16**(13): p. 4069-4081.
128. Aphasizhev, R., I. Aphasizheva, and L. Simpson. A tale of two TUTases. *Proceedings of the National Academy of Sciences of the United States of America*, 2003. **100**(19): p. 10617.
129. Ernst, N.L., B. Panicucci, R.P. Igo Jr, A.K. Panigrahi, R. Salavati, and K. Stuart. TbMP57 is a 3'terminal uridylyl transferase (TUTase) of the *Trypanosoma brucei* editosome. *Molecular cell*, 2003. **11**(6): p. 1525-1536.
130. Mcmanus, M.T., M. Shimamura, J. Grams, and S.L. Hajduk. Identification of candidate mitochondrial RNA editing ligases from *Trypanosoma brucei*. *RNA*, 2001. **7**(2): p. 167-175.
131. Sabatini, R. and S.L. Hajduk. RNA Ligase and its involvement in guide RNA/mRNA chimera formation evidence for a cleavage-ligation mechanism of *Trypanosoma brucei* mRNA editing. *Journal of Biological Chemistry*, 1995. **270**(13): p. 7233-7240.
132. Schnauffer, A., N.L. Ernst, S.S. Palazzo, J. O'Rear, R. Salavati, and K. Stuart. Separate insertion and deletion subcomplexes of the *Trypanosoma brucei* RNA editing complex. *Molecular Cell*, 2003. **12**(2): p. 307-319.
133. Ernst, N.L., B. Panicucci, J. Carnes, and K. Stuart. Differential functions of two editosome exoUases in *Trypanosoma brucei*. *RNA*, 2009. **15**(5): p. 947-957.
134. Park, Y.-J., T. Budiarto, M. Wu, E. Pardon, J. Steyaert, and W.G. Hol. The structure of the C-terminal domain of the largest editosome interaction protein and its role in promoting RNA binding by RNA-editing ligase L2. *Nucleic Acids Research*, 2012. **40**(14): p. 6966-6977.
135. Gao, G., K. Rogers, F. Li, Q. Guo, D. Osato, S.X. Zhou, A.M. Falick, and L. Simpson. Uridine insertion/deletion RNA editing in trypanosomatids: specific stimulation in vitro of *Leishmania tarentolae* REL1 RNA ligase activity by the MP63 zinc finger protein. *Protist*, 2010. **161**(3): p. 489-496.

136. Schnauffer, A., M. Wu, Y. Park, T. Nakai, J. Deng, R. Proff, W.G.J. Hol, and K.D. Stuart. A protein-protein interaction map of trypanosome~ 20S editosomes. *Journal of Biological Chemistry*, 2010. **285**(8): p. 5282.
137. Guo, X., J. Carnes, N.L. Ernst, M. Winkler, and K. Stuart. KREPB6, KREPB7, and KREPB8 are important for editing endonuclease function in *Trypanosoma brucei*. *RNA*, 2012. **18**(2): p. 308-320.
138. Seiwert, S.D. and K. Stuart. RNA editing: transfer of genetic information from gRNA to precursor mRNA in vitro. *Science*, 1994. **266**(5182): p. 114-117.
139. Hashimi, H., S.L. Zimmer, M.L. Ammerman, L.K. Read, and J. Lukeš. Dual core processing: MRB1 is an emerging kinetoplast RNA editing complex. *Trends in parasitology*, 2013. **29**(2): p. 91-99.
140. Simpson, R.M., A.E. Bruno, R. Chen, K. Lott, B.L. Tylec, J.E. Bard, Y. Sun, M.J. Buck, and L.K. Read. Trypanosome RNA Editing Mediator Complex proteins have distinct functions in gRNA utilization. *Nucleic Acids Research*, 2017. **45**(13): p. 7965-7983.
141. Weng, J., I. Aphasizheva, R.D. Etheridge, L. Huang, X. Wang, A.M. Falick, and R. Aphasizhev. Guide RNA-binding complex from mitochondria of trypanosomatids. *Molecular Cell*, 2008. **32**(2): p. 198-209.
142. Ammerman, M.L., K.M. Downey, H. Hashimi, J.C. Fisk, D.L. Tomasello, D. Faktorová, L. Kafková, T. King, J. Lukeš, and L.K. Read. Architecture of the trypanosome RNA editing accessory complex, MRB1. *Nucleic Acids Research*, 2012. **40**(12): p. 5637-5650.
143. Hashimi, H., A. Zíková, A.K. Panigrahi, K.D. Stuart, and J. Lukeš. TbRGG1, an essential protein involved in kinetoplastid RNA metabolism that is associated with a novel multiprotein complex. *RNA*, 2008. **14**(5): p. 970-980.
144. Vanhamme, L., D. Perez-Morga, C. Marchal, D. Speijer, L. Lambert, M. Geuskens, S. Alexandre, N. Ismaïli, U. Göringer, and R. Benne. *Trypanosoma brucei* TBRGG1, a mitochondrial oligo (U)-binding protein that co-localizes with an in vitro RNA editing activity. *Journal of Biological Chemistry*, 1998. **273**(34): p. 21825-21833.
145. Hashimi, H., Z. Čičová, L. Novotná, Y.Z. Wen, and J. Lukeš. Kinetoplastid guide RNA biogenesis is dependent on subunits of the mitochondrial RNA binding complex 1 and mitochondrial RNA polymerase. *RNA*, 2009. **15**(4): p. 588-599.
146. Aphasizheva, I. and R. Aphasizhev. RET1-catalyzed uridylylation shapes the mitochondrial transcriptome in *Trypanosoma brucei*. *Molecular and Cellular Biology*, 2010. **30**(6): p. 1555-67.

147. Madina, B.R., V. Kumar, B.H. Mooers, and J. Cruz-Reyes. Native variants of the MRB1 complex exhibit specialized functions in kinetoplastid RNA editing. *PLoS ONE*, 2015. **10**(4): p. e0123441.
148. Acestor, N., A.K. Panigrahi, J. Carnes, A. Zíková, and K.D. Stuart. The MRB1 complex functions in kinetoplastid RNA processing. *RNA*, 2009. **15**(2): p. 277-286.
149. Huang, Z., D. Faktorová, A. Křížová, L. Kafková, J. Lukeš, and H. Hashimi. Integrity of the core mitochondrial RNA-binding complex 1 is vital for trypanosome RNA editing. *RNA*, 2015. **21**(12): p. 2088-2102.
150. Fisk, J.C., M.L. Ammerman, V. Presnyak, and L.K. Read. TbRGG2, an essential RNA editing accessory factor in two *Trypanosoma brucei* life cycle stages. *Journal of Biological Chemistry*, 2008. **283**(34): p. 23016-23025.
151. Foda, B.M., K.M. Downey, J.C. Fisk, and L.K. Read. Multifunctional G-rich and RRM-containing domains of TbRGG2 perform separate yet essential functions in trypanosome RNA editing. *Eukaryotic Cell*, 2012. **11**(9): p. 1119-1131.
152. Kafková, L., M.L. Ammerman, D. Faktorová, J.C. Fisk, S.L. Zimmer, R. Sobotka, J. Lukeš, and H. Hashimi. Functional characterization of two paralogs that are novel RNA binding proteins influencing mitochondrial transcripts of *Trypanosoma brucei*. *RNA*, 2012. **18**(10): p. 1846-1861.
153. McAdams, N.M., R.M. Simpson, R. Chen, and Y. Sun. MRB7260 is essential for productive protein-RNA interactions within the RNA Editing Substrate Binding Complex during trypanosome RNA editing. *RNA*, 2018. **24**(4): p. 065169.117.
154. Carnes, J., M. Lerch, I. Kurtz, and K. Stuart. Bloodstream form *Trypanosoma brucei* do not require mRPN1 for gRNA processing. *RNA*, 2015. **21**(1): p. 28-35.
155. Madina, B.R., G. Kuppan, A.A. Vashisht, Y.-H. Liang, K.M. Downey, J.A. Wohlschlegel, X. Ji, S.-H. Sze, J.C. Sacchettini, and J. Cruz-Reyes. Guide RNA biogenesis involves a novel RNase III family endoribonuclease in *Trypanosoma brucei*. *RNA*, 2011. **17**(10): p. 1821-1830.
156. Panigrahi, A.K., T.E. Allen, K. Stuart, P.A. Haynes, and S.P. Gygi. Mass spectrometric analysis of the editosome and other multiprotein complexes in *Trypanosoma brucei*. *Journal of the American Society for Mass Spectrometry*, 2003. **14**(7): p. 728-735.
157. Adler, B.K., M.E. Harris, K.I. Bertrand, and S.L. Hajduk. Modification of *Trypanosoma brucei* mitochondrial rRNA by posttranscriptional 3' polyuridine tail formation. *Molecular and cellular biology*, 1991. **11**(12): p. 5878-5884.

158. Etheridge, R.D., I. Aphasizheva, P.D. Gershon, and R. Aphasizhev. 3' adenylation determines mRNA abundance and monitors completion of RNA editing in *T. brucei* mitochondria. *EMBO Journal*, 2008. **27**(11): p. 1596-608.
159. Zimmer, S.L., S.M. McEvoy, S. Menon, and L.K. Read. Additive and transcript-specific effects of KPAP1 and TbRND activities on 3' non-encoded tail characteristics and mRNA stability in *Trypanosoma brucei*. *PLoS ONE*, 2012. **7**(5): p. e37639.
160. Zhang, L., F.M. Sement, T. Suematsu, T. Yu, S. Monti, L. Huang, R. Aphasizhev, and I. Aphasizheva. PPR polyadenylation factor defines mitochondrial mRNA identity and stability in trypanosomes. *EMBO J*, 2017. **36**(16): p. 2435-2454.
161. Read, L.K., P.J. Myler, and K. Stuart. Extensive editing of both processed and preprocessed maxicircle CR6 transcripts in *Trypanosoma brucei*. *Journal of Biological Chemistry*, 1992. **267**(2): p. 1123-1128.
162. Souza, A., P. Myler, and K. Stuart. Maxicircle CR1 transcripts of *Trypanosoma brucei* are edited and developmentally regulated and encode a putative iron-sulfur protein homologous to an NADH dehydrogenase subunit. *Molecular and Cellular Biology*, 1992. **12**(5): p. 2100-2107.
163. Halbig, K., M. DE NOVA-OCAMPO, and J. Cruz-Reyes. Complete cycles of bloodstream trypanosome RNA editing in vitro. *RNA*, 2004. **10**(6): p. 914-920.
164. Sharan, R., I. Ulitsky, and R. Shamir. Network-based prediction of protein function. *Molecular Systems Biology*, 2007. **3**(1): p. 88.
165. De Las Rivas, J. and C. Fontanillo. Protein–protein interactions essentials: key concepts to building and analyzing interactome networks. *PLoS Computational Biology*, 2010. **6**(6): p. e1000807.
166. Ito, T., T. Chiba, R. Ozawa, M. Yoshida, M. Hattori, and Y. Sakaki. A comprehensive two-hybrid analysis to explore the yeast protein interactome. *Proceedings of the National Academy of Sciences of the United States of America*, 2001. **98**(8): p. 4569-4574.
167. Stelzl, U., U. Worm, M. Lalowski, C. Haenig, F.H. Brembeck, H. Goehler, M. Stroedicke, M. Zenkner, A. Schoenherr, and S. Koeppen. A human protein-protein interaction network: a resource for annotating the proteome. *Cell*, 2005. **122**(6): p. 957-968.
168. Malovannaya, A., R.B. Lanz, S.Y. Jung, Y. Bulynko, N.T. Le, D.W. Chan, C. Ding, Y. Shi, N. Yucer, and G. Krenciute. Analysis of the human endogenous coregulator complexome. *Cell*, 2011. **145**(5): p. 787-799.

169. Havugimana, P.C., G.T. Hart, T. Nepusz, H. Yang, A.L. Turinsky, Z. Li, P.I. Wang, D.R. Boutz, V. Fong, and S. Phanse. A census of human soluble protein complexes. *Cell*, 2012. **150**(5): p. 1068-1081.
170. Kirkwood, K.J., Y. Ahmad, M. Larance, and A.I. Lamond. Characterization of native protein complexes and protein isoform variation using size-fractionation-based quantitative proteomics. *Molecular & Cellular Proteomics*, 2013. **12**(12): p. 3851-3873.
171. Wan, C., B. Borgeson, S. Phanse, F. Tu, K. Drew, G. Clark, X. Xiong, O. Kagan, J. Kwan, and A. Bezginov. Panorama of ancient metazoan macromolecular complexes. *Nature*, 2015. **525**(7569): p. 339-344.
172. Guruharsha, K., J.-F. Rual, B. Zhai, J. Mintseris, P. Vaidya, N. Vaidya, C. Beekman, C. Wong, D.Y. Rhee, and O. Cenaj. A protein complex network of *Drosophila melanogaster*. *Cell*, 2011. **147**(3): p. 690-703.
173. Krogan, N.J., G. Cagney, H. Yu, G. Zhong, X. Guo, A. Ignatchenko, J. Li, S. Pu, N. Datta, and A.P. Tikuisis. Global landscape of protein complexes in the yeast *Saccharomyces cerevisiae*. *Nature*, 2006. **440**(7084): p. 637.
174. Gavin, A.-C., M. Bösch, R. Krause, P. Grandi, M. Marzioch, A. Bauer, J. Schultz, J.M. Rick, A.-M. Michon, and C.-M. Cruciat. Functional organization of the yeast proteome by systematic analysis of protein complexes. *Nature*, 2002. **415**(6868): p. 141.
175. Stuart, J.M., E. Segal, D. Koller, and S.K. Kim. A gene-coexpression network for global discovery of conserved genetic modules. *Science*, 2003. **302**(5643): p. 249-255.
176. Zhang, L.V., O.D. King, S.L. Wong, D.S. Goldberg, A.H. Tong, G. Lesage, B. Andrews, H. Bussey, C. Boone, and F.P. Roth. Motifs, themes and thematic maps of an integrated *Saccharomyces cerevisiae* interaction network. *Journal of Biology*, 2005. **4**(2): p. 6.
177. McDermott, S.M., J. Luo, J. Carnes, J.A. Ranish, and K. Stuart. The architecture of *Trypanosoma brucei* editosomes. *Proceedings of the National Academy of Sciences of the United States of America*, 2016. **113**(42): p. E6476-E6485.
178. Yu, H., P. Braun, M.A. Yildirim, I. Lemmens, K. Venkatesan, J. Sahalie, T. Hirozane-Kishikawa, F. Gebreab, N. Li, and N. Simonis. High-quality binary protein interaction map of the yeast interactome network. *Science*, 2008. **322**(5898): p. 104-110.
179. Stelzl, U. *E. coli* network upgrade. *Nature Biotechnology*, 2014. **32**(3): p. 241.

180. Schneider, A., F. Charrière, M. Pusnik, and E.K. Horn. Isolation of mitochondria from procyclic *Trypanosoma brucei*. *Mitochondria: Practical Protocols*, 2007: p. 67-80.
181. Estévez, A.M., T. Kempf, and C. Clayton. The exosome of *Trypanosoma brucei*. *EMBO Journal*, 2001. **20**(14): p. 3831-3839.
182. Panigrahi, A.K., Y. Ogata, A. Zíková, A. Anupama, R.A. Dalley, N. Acestor, P.J. Myler, and K.D. Stuart. A comprehensive analysis of *Trypanosoma brucei* mitochondrial proteome. *Proteomics*, 2009. **9**(2): p. 434-450.
183. Havugimana, P.C., P. Wong, and A. Emili. Improved proteomic discovery by sample pre-fractionation using dual-column ion-exchange high performance liquid chromatography. *Journal of Chromatography B*, 2007. **847**(1): p. 54-61.
184. Gazestani, V.H., N. Nikpour, V. Mehta, H.S. Najafabadi, H. Moshiri, A. Jardim, and R. Salavati. A protein complex map of *Trypanosoma brucei*. *PLoS Neglected Tropical Diseases*, 2016. **10**(3): p. e0004533.
185. Wickstead, B., K. Ersfeld, and K. Gull. Targeting of a tetracycline-inducible expression system to the transcriptionally silent minichromosomes of *Trypanosoma brucei*. *Molecular and Biochemical Parasitology*, 2002. **125**(1): p. 211-216.
186. Carnes, J. and K.D. Stuart. Uridine insertion/deletion editing activities. *Methods in Enzymology*, 2007. **424**: p. 25-54.
187. Carnes, J., J.R. Trotter, N.L. Ernst, A. Steinberg, and K. Stuart. An essential RNase III insertion editing endonuclease in *Trypanosoma brucei*. *Proceedings of the National Academy of Sciences of the United States of America*, 2005. **102**(46): p. 16614-16619.
188. Ingham, D.J., S. Beer, S. Money, and G. Hansen. Quantitative real-time PCR assay for determining transgene copy number in transformed plants. *Biotechniques*, 2001. **31**(1): p. 132-141.
189. Colasante, C., V.P. Alibu, S. Kirchberger, J. Tjaden, C. Clayton, and F. Voncken. Characterization and developmentally regulated localization of the mitochondrial carrier protein homologue MCP6 from *Trypanosoma brucei*. *Eukaryotic Cell*, 2006. **5**(8): p. 1194-1205.
190. Alibu, V.P., L. Storm, S. Haile, C. Clayton, and D. Horn. A doubly inducible system for RNA interference and rapid RNAi plasmid construction in *Trypanosoma brucei*. *Molecular and Biochemical Parasitology*, 2005. **139**(1): p. 75-82.

191. Nielsen, H., J. Engelbrecht, S. Brunak, and G. von Heijne. Identification of prokaryotic and eukaryotic signal peptides and prediction of their cleavage sites. *Protein Engineering*, 1997. **10**(1): p. 1-6.
192. Kala, S. and R. Salavati. OB-fold domain of KREPA4 mediates high-affinity interaction with guide RNA and possesses annealing activity. *RNA*, 2010. **16**(10): p. 1951-1967.
193. Koslowsky, D.J., S.M. Kutas, and K. Stuart. Distinct differences in the requirements for ribonucleoprotein complex formation on differentially regulated pre-edited mRNAs in *Trypanosoma brucei*. *Molecular and biochemical parasitology*, 1996. **80**(1): p. 1-14.
194. Setzer, D.R. Measuring equilibrium and kinetic constants using gel retardation assays, in *RNA-Protein Interaction Protocols*. 1999, Springer. p. 115-128.
195. Zimmermann, L., A. Stephens, S.-Z. Nam, D. Rau, J. Kübler, M. Lozajic, F. Gabler, J. Söding, A.N. Lupas, and V. Alva. A Completely Reimplemented MPI Bioinformatics Toolkit with a New HHpred Server at its Core. *Journal of molecular biology*, 2017.
196. Sievers, F., A. Wilm, D. Dineen, T.J. Gibson, K. Karplus, W. Li, R. Lopez, H. McWilliam, M. Remmert, and J. Söding. Fast, scalable generation of high-quality protein multiple sequence alignments using Clustal Omega. *Molecular systems biology*, 2011. **7**(1): p. 539.
197. McWilliam, H., W. Li, M. Uludag, S. Squizzato, Y.M. Park, N. Buso, A.P. Cowley, and R. Lopez. Analysis tool web services from the EMBL-EBI. *Nucleic acids research*, 2013. **41**(W1): p. W597-W600.
198. Athanasiadis, A., D. Placido, S. Maas, B.A. Brown, K. Lowenhaupt, and A. Rich. The crystal structure of the Z β domain of the RNA-editing enzyme ADAR1 reveals distinct conserved surfaces among Z-domains. *Journal of molecular biology*, 2005. **351**(3): p. 496-507.
199. Schwartz, T., J. Behlke, K. Lowenhaupt, U. Heinemann, and A. Rich. Structure of the DLM-1-Z-DNA complex reveals a conserved family of Z-DNA-binding proteins. *Nature Structural & Molecular Biology*, 2001. **8**(9): p. 761-765.
200. Schwartz, T., M.A. Rould, K. Lowenhaupt, A. Herbert, and A. Rich. Crystal structure of the Z α domain of the human editing enzyme ADAR1 bound to left-handed Z-DNA. *Science*, 1999. **284**(5421): p. 1841-1845.
201. Miller, M.M., K. Halbig, and J. Cruz-Reyes. RBP16 stimulates trypanosome RNA editing in vitro at an early step in the editing reaction. *Rna*, 2006. **12**(7): p. 1292-1303.

202. Igo, R.P., S.D. Lawson, and K. Stuart. RNA sequence and base pairing effects on insertion editing in *Trypanosoma brucei*. *Molecular and cellular biology*, 2002. **22**(5): p. 1567-1576.
203. Salavati, R., A.K. Panigrahi, B.A. Morach, S.S. Palazzo, R.P. Igo, and K. Stuart. Endoribonuclease activities of *Trypanosoma brucei* mitochondria. *Molecular and biochemical parasitology*, 2002. **120**(1): p. 23-31.
204. Brown, L.M., B.J. Burbach, B.A. McKenzie, and G.J. Connell. A cis-acting AU sequence element induces kinetoplastid U-insertions. *Journal of Biological Chemistry*, 1999. **274**(10): p. 6295-6304.
205. Oppegard, L.M., A.L. Kabb, and G.J. Connell. Activation of Guide RNA-directed Editing of a *Cytochrome b* mRNA. *Journal of Biological Chemistry*, 2000. **275**(43): p. 33911-33919.
206. Aphasizheva, I., D.A. Maslov, Y. Qian, L. Huang, Q. Wang, C.E. Costello, and R. Aphasizhev. Ribosome-associated pentatricopeptide repeat proteins function as translational activators in mitochondria of trypanosomes. *Molecular Microbiology*, 2016. **99**(6): p. 1043-1058.
207. Najafabadi, H.S., Z. Lu, C. MacPherson, V. Mehta, V. Adoue, T. Pastinen, and R. Salavati. Global identification of conserved post-transcriptional regulatory programs in trypanosomatids. *Nucleic acids research*, 2013. **41**(18): p. 8591-8600.
208. Aravind, L., V. Anantharaman, S. Balaji, M.M. Babu, and L.M. Iyer. The many faces of the helix-turn-helix domain: transcription regulation and beyond. *FEMS microbiology reviews*, 2005. **29**(2): p. 231-262.
209. Herbert, A., K. Lowenhaupt, J. Spitzner, and A. Rich. Chicken double-stranded RNA adenosine deaminase has apparent specificity for Z-DNA. *Proceedings of the National Academy of Sciences*, 1995. **92**(16): p. 7550-7554.
210. Kim, Y.-G., M. Muralinath, T. Brandt, M. Percy, K. Hauns, K. Lowenhaupt, B.L. Jacobs, and A. Rich. A role for Z-DNA binding in vaccinia virus pathogenesis. *Proceedings of the National Academy of Sciences*, 2003. **100**(12): p. 6974-6979.
211. Rothenburg, S., N. Deigendesch, K. Dittmar, F. Koch-Nolte, F. Haag, K. Lowenhaupt, and A. Rich. A PKR-like eukaryotic initiation factor 2 α kinase from zebrafish contains Z-DNA binding domains instead of dsRNA binding domains. *Proceedings of the National Academy of Sciences*, 2005. **102**(5): p. 1602-1607.
212. Brown, B.A., K. Lowenhaupt, C.M. Wilbert, E.B. Hanlon, and A. Rich. The Z α domain of the editing enzyme dsRNA adenosine deaminase binds left-handed Z-RNA as well as Z-DNA. *Proceedings of the National Academy of Sciences*, 2000. **97**(25): p. 13532-13536.

213. Placido, D., B.A. Brown, K. Lowenhaupt, A. Rich, and A. Athanasiadis. A left-handed RNA double helix bound by the α domain of the RNA-editing enzyme ADAR1. *Structure*, 2007. **15**(4): p. 395-404.
214. Ha, S.C., D. Kim, H.-Y. Hwang, A. Rich, Y.-G. Kim, and K.K. Kim. The crystal structure of the second Z-DNA binding domain of human DAI (ZBP1) in complex with Z-DNA reveals an unusual binding mode to Z-DNA. *Proceedings of the National Academy of Sciences*, 2008. **105**(52): p. 20671-20676.
215. Schade, M., C.J. Turner, K. Lowenhaupt, A. Rich, and A. Herbert. Structure–function analysis of the Z-DNA-binding domain α of dsRNA adenosine deaminase type I reveals similarity to the (α + β) family of helix–turn–helix proteins. *EMBO Journal*, 1999. **18**(2): p. 470-479.
216. Ha, S.C., N.K. Lokanath, D. Van Quyen, C.A. Wu, K. Lowenhaupt, A. Rich, Y.-G. Kim, and K.K. Kim. A poxvirus protein forms a complex with left-handed Z-DNA: crystal structure of a Yatapoxvirus α bound to DNA. *Proceedings of the National Academy of Sciences of the United States of America*, 2004. **101**(40): p. 14367-14372.
217. Li, H., J. Xiao, J. Li, L. Lu, S. Feng, and P. Dröge. Human genomic Z-DNA segments probed by the α domain of ADAR1. *Nucleic acids research*, 2009. **37**(8): p. 2737-2746.
218. Maelfait, J., L. Liverpool, A. Bridgeman, K.B. Ragan, J.W. Upton, and J. Rehwinkel. Sensing of viral and endogenous RNA by ZBP1/DAI induces necroptosis. *EMBO journal*, 2017. **36**(17): p. 2529-2543.
219. D'Ascenzo, L., F. Leonarski, Q. Vicens, and P. Auffinger. 'Z-DNA like' fragments in RNA: a recurring structural motif with implications for folding, RNA/protein recognition and immune response. *Nucleic acids research*, 2016. **44**(12): p. 5944-5956.
220. Hermann, T., B. Schmid, H. Heumann, and H.U. Göringer. A three-dimensional working model for a guide RNA from *Trypanosoma brucei*. *Nucleic acids research*, 1997. **25**(12): p. 2311-2318.
221. Schumacher, M.A., E. Karamooz, A. Zíková, L. Trantírek, and J. Lukeš. Crystal structures of *T. brucei* MRP1/MRP2 guide-RNA binding complex reveal RNA matchmaking mechanism. *Cell*, 2006. **126**(4): p. 701-711.
222. Pusnik, M., I. Small, L.K. Read, T. Fabbro, and A. Schneider. Pentatricopeptide repeat proteins in *Trypanosoma brucei* function in mitochondrial ribosomes. *Molecular and cellular biology*, 2007. **27**(19): p. 6876-6888.

223. Vondrušková, E., J. Van Den Burg, A. Zíková, N.L. Ernst, K. Stuart, R. Benne, and J. Lukeš. RNA interference analyses suggest a transcript-specific regulatory role for mitochondrial RNA-binding proteins MRP1 and MRP2 in RNA editing and other RNA processing in *Trypanosoma brucei*. *Journal of Biological Chemistry*, 2005. **280**(4): p. 2429-2438.
224. Kim, D., J. Hur, K. Park, S. Bae, D. Shin, S.C. Ha, H.-Y. Hwang, S. Hohng, J.-H. Lee, and S. Lee. Distinct Z-DNA binding mode of a PKR-like protein kinase containing a Z-DNA binding domain (PKZ). *Nucleic acids research*, 2014: p. gku189.
225. Kim, Y.-G., K. Lowenhaupt, D.-B. Oh, K.K. Kim, and A. Rich. Evidence that vaccinia virulence factor E3L binds to Z-DNA in vivo: Implications for development of a therapy for poxvirus infection. *Proceedings of the National Academy of Sciences of the United States of America*, 2004. **101**(6): p. 1514-1518.
226. Lee, A.-R., C.-J. Park, H.-K. Cheong, K.-S. Ryu, J.-W. Park, M.-Y. Kwon, J. Lee, K.K. Kim, B.-S. Choi, and J.-H. Lee. Solution structure of the Z-DNA binding domain of PKR-like protein kinase from *Carassius auratus* and quantitative analyses of the intermediate complex during B–Z transition. *Nucleic acids research*, 2016. **44**(6): p. 2936-2948.
227. Subramani, V.K., D. Kim, K. Yun, and K.K. Kim. Structural and functional studies of a large winged Z-DNA-binding domain of *Danio rerio* protein kinase PKZ. *FEBS Letters*, 2016. **590**(14): p. 2275-2285.
228. Herbert, A., J. Alfken, Y.-G. Kim, I.S. Mian, K. Nishikura, and A. Rich. A Z-DNA binding domain present in the human editing enzyme, double-stranded RNA adenosine deaminase. *Proceedings of the National Academy of Sciences*, 1997. **94**(16): p. 8421-8426.
229. Clark, K.L., E.D. Halay, E. Lai, and S.K. Burley. Co-crystal structure of the HNF-3/fork head DNA-recognition motif resembles histone H5. *Nature*, 1993. **364**(6436): p. 412.
230. Passner, J. and T. Steitz. The structure of a CAP–DNA complex having two cAMP molecules bound to each monomer. *Proceedings of the National Academy of Sciences*, 1997. **94**(7): p. 2843-2847.
231. Benayoun, B.A., S. Caburet, and R.A. Veitia. Forkhead transcription factors: key players in health and disease. *Trends in Genetics*, 2011. **27**(6): p. 224-232.
232. Yoshizawa, S., L. Rasubala, T. Ose, D. Kohda, D. Fourmy, and K. Maenaka. Structural basis for mRNA recognition by elongation factor SelB. *Nature Structural and Molecular Biology*, 2005. **12**(2): p. 198.

233. Soler, N., D. Fourmy, and S. Yoshizawa. Structural insight into a molecular switch in tandem winged-helix motifs from elongation factor SelB. *Journal of molecular biology*, 2007. **370**(4): p. 728-741.
234. Wolin, S.L. and T. Cedervall. The Ia protein. *Annual review of biochemistry*, 2002. **71**(1): p. 375-403.
235. Johnston, B.H. [7] Generation and detection of Z-DNA, in *Methods in enzymology*. 1992, Elsevier. p. 127-158.
236. Gazestani, V.H., M. Hampton, A.K. Shaw, R. Salavati, and S.L. Zimmer. Tail characteristics of *Trypanosoma brucei* mitochondrial transcripts are developmentally altered in a transcript-specific manner. *International Journal for Parasitology*, 2018. **48**(2): p. 179-189.
237. Feng, S., H. Li, J. Zhao, K. Pervushin, K. Lowenhaupt, T.U. Schwartz, and P. Dröge. Alternate rRNA secondary structures as regulators of translation. *Nature structural & molecular biology*, 2011. **18**(2): p. 169-176.
238. Reifur, L., E.Y. Laura, J. Cruz-Reyes, and D.J. Koslowsky. The impact of mRNA structure on guide RNA targeting in kinetoplastid RNA editing. *PloS ONE*, 2010. **5**(8): p. e12235.
239. Roy, A., A. Kucukural, and Y. Zhang. I-TASSER: a unified platform for automated protein structure and function prediction. *Nature protocols*, 2010. **5**(4): p. 725.
240. Yang, J., R. Yan, A. Roy, D. Xu, J. Poisson, and Y. Zhang. The I-TASSER Suite: protein structure and function prediction. *Nature methods*, 2015. **12**(1): p. 7.

Appendix

S2.1 Table. Oligonucleotides used in this study.

qRT-PCR primers

Name	5' primer	3' primer
COIII pre	GAAACCAGATGAGATTGTTTGCA	TTCATTCCAACCTAAACCCTTTCC
COIII edit	TTGTGTTTTATTACGTTGTATCCAGTATTG	CGAAAGCAAACCTCACAAACACAAA
CYb pre	ATATAAAAGCGGAGAAAAAGAAAG	CCCATATATTCTATATAAAACAACCTGACA
CYb edit	AAATATGTTTTCGTTGTAGATTTTTATTATTT	CCCATATATTCTATATAAAACAACCTGACA
A6 pre	TTGCCTTTGCCAAACTTTTAGAAG	ATTCTATAACTCCAAAATCACAACTTTCC
A6 edit	GATTTATTTGGTTGCGTTTGTTATTATG	CAAACCAACAAACAAATACAAATCAAAC
CoII pre	ATTACAGTGTAACCATGTATTGACATT	TTCATTACACCTACCAGGTTCTCT
CoII edit	ATTACAGTGTAACCATGTATTGACATT	ATTTTCATTACACCTACCAGGTATACAA
Murf2 pre	GATTTTAAGATTGGCTTTGATTGA	AATATAAAATCTAGATCAAACCATCACA
Murf2 edit	GATTTTAATGTTTGGTTGTTTTAATTTAG	AATATAAAATCTAGATCAAACCATCACA
RPS12 pre	CGACGGAGAGCTTCTTTTGAATA	CCCCCACCCAAATCTTT
RPS12 edit	CGTATGTGATTTTTGTATGGTTGTTG	ACACGTCGGTTACCGGAACT
CoI	CCCGATATGGTATTTCCCTCGTATAAA	CCCCCATAACCCTCTTCAGTCA
ND4	CAATCTGACCATTCCATGTGTGA	TTTCAGCACAACTACTTGCTAATAAAAACA
A6-Cyb precursor	TCCGCCCAAATTCCTCTTT	CCAATATGAATGGAATTACAATACTGAGT
9S/ND8 precursor	AAAAGGTATTGTTGCCACCAA	CAACCAAACCTTAAAATTATTAATTGATTC
RPS12/ND5	GGGAACCCTTTGTTTTGGTTAAAG	TTCCTACCAAACATAAATGAACCTGAT
18SrRNA	CGGAATGGCACCACAAGAC	TGGTAAAGTTCCCCGTGTTGA
Tb927.1.1730	GCCTCCTCTGCACGTCTTG	CCACCGCAGACACAAACG
Tb927.10.1730	GGTCGCAGGACGATATTGTTTT	ATCGCCGCCCAATG
Tb927.10.7910	GCTTAGTCTTGCGGGTCTTG	CGCAGTAATACGCTGGAAAACAT
Tb927.6.1200	GCCGTGGCTGCAAAATTT	CGGATAGTCGCCCAAGTCTTT
Tb927.10.5830	AGTGCCGACACGTGAATGC	CTTCACCTCCCCACACGATT
Tb927.1.3010	CGTTCCTGGCACCGACTT	GACGGGAGATTTGGCAAAAA

Radiolabeled RNA binding assays. Underlined sequences represent T7 promoter sequence.

Uridylated nonguide RNA; 49-nt	AAAAAAAAAAAAAAAAATAGTGATATCGAATTCCTTAGTATGTATCTGGTA <u>CCCTATAGTGACTCTATTA</u>
CYb edited RNA	TAAAAAGACAACATAAATTTCTAAATAATAAAAAAAAAATAACAAAAATCTAACACGAAAAACATA TT <u>CCCTATAGTGAGTCGTATTA</u>

Plasmid Construction primers

P2T7-177 plasmids. Underlined sequences represent restriction site sequence.

Name	5' primer	3' primer
Tb927.1.1730	TAATCTCT <u>AGAG</u> GAGCAATTGGATCCTTTCCA	TAATCCTCGAGCGGCGAACTGCATTATTA
Tb927.10.1730	TAATCGGATCCTCAGATGCACTCAACCTTGC	TAATTCTCGAGCGAAGTCGGTATAAACGGGA
Tb927.10.7910	TAATCGGATCCATGACGGCCGTTTATTATGC	TAATCCTCGAGATGATTACCTCAGCTTGCCG
Tb927.6.1200	TTAATCGGATCCGCGAGTTTGTACCCGATGAT	TAATACTCGAGGTGATCGCTCAGCAAGCATA
Tb927.10.5830	TAATCGGATCCAAAAAGCAGCGAGTTTTGGA	TAATCCTCGAGAACACGGCAATTAAGCACC
Tb927.1.3010	TAATCGGATCCCTTCAACGTCATTTTCGGGTT	TAATTCTCGAGCACGCTCTCCTCCCTCATAG

c-Myc plasmids

Name	5' primer	3' primer
Tb927.1.1730	ATATA <u>AAGCTT</u> ATGTTGCGCTACACCA	ATATGTTAACAGCTGGAGCTCCTACTTTAT
Tb927.10.1730	ATATA <u>AAGCTT</u> ATGTGGCGTTGCTCTACTC	ATATGGATCCACTTTTCCCCACAGTT
Tb927.10.7910	ATTA <u>AAGCTT</u> ATGTTTTCCAGCGTATTACT	ATATGGATCCCTTCCATACAACCGTTCCC

Figure S2.1. SDS-PAGE analysis of WT RBP7910 and point mutants. Purified, recombinant his-tagged proteins were analyzed by 12% SDS-PAGE. The molecular weight marker is shown on left side.

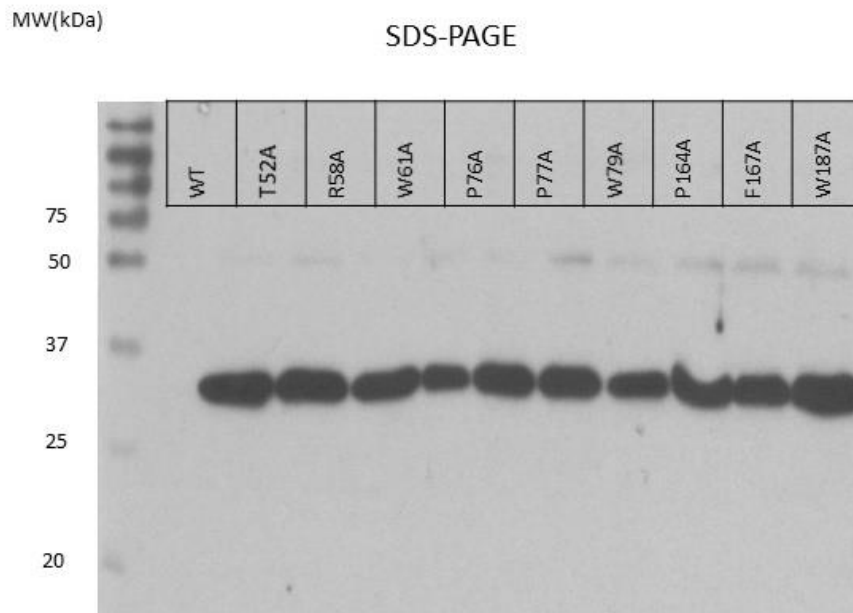


Table 3.1. List of the 50 proteins predicted to be associated with the RNA editing machinery

TritrypDB#	Name	Alias	Complex or Sub-complex
Tb11.02.5390	GAP1	GRB2	Core MRB1
Tb927.1.1690	KREN1	None	RECC
Tb927.1.1730	hypothetical protein conserved	None	Unknown
Tb927.1.3010	mRNA processing protein, putative	None	Unknown
Tb927.1.3030	KREL2	None	RECC
Tb927.10.10130	MRB10130	REMC1	Unknown
Tb927.10.10830	TbRGG2	None	TbRGG2
Tb927.10.11870	MRB11870	GRBC5	Core MRB1
Tb927.10.1730	hypothetical protein conserved	None	Unknown
Tb927.10.3570	KREX2	None	RECC
Tb927.10.5110	KREPA4	None	RECC
Tb927.10.5120	KREPA6	None	RECC
Tb927.10.5440	KREN2	None	RECC
Tb927.10.5830	hypothetical protein conserved	None	Unknown
Tb927.10.7910	hypothetical protein conserved	None	Unknown
Tb927.10.8210	KREPA2	None	RECC
Tb927.11.13280	MRP2	GBP25	Unknown
Tb927.11.15640	MERS1	None	Unknown
Tb927.11.16860	MRB8620	GRBC3	Core MRB1
Tb927.11.1710	MRP1	GBP21	Unknown
Tb927.11.2990	KREPB4	None	RECC
Tb927.11.7960	KPAP1	None	KPAP1 complex
Tb927.11.9140	MRB0880	GRBC7	Core MRB1
Tb927.11.940	KREPB5	None	RECC
Tb927.2.1860	MRB1860	REMC2	TbRGG2
Tb927.2.2470	KREPA1	None	RECC
Tb927.2.3800	GAP1	GRBC2	Core MRB1

Tb927.2.6070	MRB6070	None	MRB1
Tb927.3.1590	MRB1590	None	MRB1
Tb927.3.1820	MRB1820	None	MRB1
Tb927.3.3990	KREPB6	None	RECC
Tb927.4.1500	REH2	None	Unknown
Tb927.4.4150	MRB4150	None	Unknown
Tb927.4.4160	MRB4160	REMC5	TbRGG2
Tb927.5.3010	MRB3010	GRBC6	Core MRB1
Tb927.6.1200	hypothetical protein conserved	None	Unknown
Tb927.6.1680	MRB 1680	None	Unknown
Tb927.6.2140	hypothetical protein conserved	None	Unknown
Tb927.6.2230	TbRGG1	None	Unknown
Tb927.7.1070	KREX1	None	RECC
Tb927.7.1550	KRET2	None	RECC
Tb927.7.2570	GAP2	GRBC1	Core MRB1
Tb927.7.800	MRB800	REMC3	TbRGG2
Tb927.8.5690	KREPB8	None	RECC
Tb927.8.620	KREPA3	None	RECC
Tb927.8.680	KREPA5	None	RECC
Tb927.8.8170	MRB8170	REMC5A	TbRGG2
Tb927.8.8180	MRB8180	REMC4	TbRGG2
Tb927.9.4360	KREL1	None	RECC
Tb927.9.7260	PhyH	None	TbRGG2